Pollution externalities and emissions' consequences of the U.S. electricity sector

Submitted in partial fulfillment of the requirements for

the degree of

Doctor of Philosophy

in

Engineering & Public Policy

Xiaodi Sun

B.S., Chemical Engineering, Washington University in St. Louis

Carnegie Mellon University
Pittsburgh, Pennsylvania

May 2019

Acknowledgements

I am grateful for the funding sources that made this thesis possible. This work was funded by the U.S. Department of Energy under award number DE-FE0024008 and the National Science Foundation under award number CBET-1554117. This work was funded, in part, by the Center for Climate and Energy Decision Making (Awards SES-0949710 and SES-1463492), through a cooperative agreement between the National Science Foundation and Carnegie Mellon University. Lastly, I acknowledge support from the Liang Ji-Dian Graduate Fellowship. The views expressed in this document are solely those of the author and do not necessarily reflect those of the funding sources.

I am grateful for the many mentors, friends, and family who have contributed to my academic and personal growth over the years. Thank you to my thesis advisor and my committee chair, Inês Azevedo. I am grateful for all the support and advice I have received over these past four years. It is difficult for me to imagine myself in this position without your guidance. I also want to thank Michael Griffin for helping me see the big picture and guiding me through a project I knew little about when I started. I would like to thank my remaining committee members – Denise Mauzerall and Costa Samaras – for challenging my research and exposing me to ideas that give me the opportunity to grow. I also thank Meagan Mauter and Daniel Gingerich for their help, guidance, and mentorship.

The EPP staff has done a tremendous job keeping everything in order so that my life as a Ph.D. student can proceed as smoothly as possible. Thank you to Adam Loucks, Debbie Kuntz, Deb Scappatura, Diana Rotando, Elisabeth Udyawar, Kim Martin, Patti Steranchak, Sam Cryster, Vicki Finney and anyone else who helps keep the ship upright.

I would like to acknowledge my fellow EPP students who have kept me company over the years. A special shout-out to Rachel Steratore, Sneha Shanbhag, and Tobi “Tbi” Adekanye.

I think next of my college friends who help me learn more about myself and the activist community whose day-to-day bravery and resistance of the status quo inspire me to dream bigger and push harder. I thank these friends: Ana, Hana, Jake, Joao, Johanne, Jordan, Krystle, Madhana, Nancy, Nikita, and Seth and my mentors: Judy Suh, Randall Taylor, and the rest of Penn Plaza Support and Action. We will make the future brighter.

Lastly, I owe my deepest gratitude to my parents and my brother who are the fixtures of my life. Thank you for supporting me throughout my entire life. A lifetime is a lot of support and it is the type of support that can rarely be defined with words. I am very grateful. I promise that I’ll stop being in school soon!

Abstract

The electricity sector generates externalities due to pollution that can have damaging impacts on human health, environment, ecology, and climate. This thesis focuses on three problems related to health, environmental and/or climate change externalities associated with the operation of the power sector.

In Chapter 1, I estimate the trace elements mass flow rates from U.S. coal-fired power plants, a negative externality that is not well monitored at the plant level, except for gas phase emissions of Hg. I create a generalizable model for stochastically estimating trace element mass flow rates, specifically Hg, Se, As, and Cl, to solid, liquid, and gas phase waste streams of coal-fired power plants and evaluate the accuracy against available data. When compared with measured and reported data on trace element mass flow rates, I find that my model generally overestimates trace element concentrations in coal, leading to overestimation of trace element mass flow rates to the waste streams. The partitioning estimates are consistent for Se, As, and Cl removal from flue gas, but tend to underestimate Hg removal. Model performance would improve with access to more recent measurements of trace element concentrations in the coal blend, where data quality is the weakest.

In Chapter 2, I focus on the issue of understanding the emissions of SO_2, NO_x and CO_2 that would result from policies that would lead to an increased usage of coal. I also study the emissions consequences of turning off some of the currently installed air pollution technologies at U.S. coal power plants. While a coal resurgence is unlikely due to other market forces, an increase in coal electricity will cause increases in SO_2, NO_x and CO_2, which have significant human health, environment, and climate consequences. I explore the potential consequences of an increase in coal generation under two bounding scenarios: 1) I assume that environmental regulations are weakened so that coal plants turn off their wet flue gas desulfurization and selective catalytic reduction devices and 2) I assume coal electricity becomes cheaper to operate than natural gas and displaces natural gas electricity. Turning off wet flue gas desulfurization and selective catalytic reactor devices leads to SO_2 and NO_x that would be twice to three times the emissions observed in 2017. These emissions levels were last observed about 7-10 years ago. A resurgence of coal that would displace natural gas would increase SO_2, NO_x, and CO_2 emissions by 41%, 45%, and 21% compared to 2017 levels.

In Chapter 3, I study the potential of deep decarbonization of the Pennsylvania electricity sector, which is an energy policy goal which would push coal out of the fuel mix. The Pennsylvania Department of Environmental Protection aims to reduce greenhouse gas emissions from Pennsylvania to 20% of 2005 levels by 2050. While deep decarbonization is crucial for mitigating the effects of climate change, the infrastructure required to implement deep decarbonization can create significant land and forest impacts

that may negatively impact ecology. I model pathways to deep decarbonize Pennsylvania's electricity sector, quantify the land and forest land use from these pathways, and estimate potential ecological impacts using fragmentation indices. Even if all the coal plants retire, the emissions from current natural gas plants exceed the carbonization goals, suggesting that natural gas cannot be a bridge fuel. If only wind is built, the total land use is 13,300 km^2 (Pennsylvania is 119,000 km^2), with direct land use and forest land use impacts of 520 km^2 and 370 km^2, respectively. Solar farms are constructed across Pennsylvania, as there is insufficient land in the southeast where resources are highest, impacting 2400 km^2 of forested land. As such, solar contributes to a greater loss of landscape than wind, but wind requires significantly more land allocated to deep decarbonize the Pennsylvania electricity sector.

Through these three chapters, I find that energy policy needs to be assessed on a holistic basis by considering all possible cost and benefits of a potential policy. While policy goals, such as decarbonization of the electricity grid, will create obvious net benefits, energy interventions still need to be carefully planned out by decision makers to avoid and minimize other downstream problems. Other policy interventions, such as promoting more coal for the sake of grid reliability, may introduce such significant costs that they should be scrapped entirely.

Table of Contents

List of Tables

List of Figures

Glossary

APCD	Air pollution control device
As	Arsenic
CAIR	Clean Air Interstate Rule
CCS	Carbon capture sequestration
CEMS	Continuous emissions monitoring system
CFPP	Coal-fired power plant
COALQUAL	Coal quality database
Cl	Chloride
CO_2	Carbon dioxide
CSAPR	Cross-state air pollution rule
eGRID	Emissions & Generation Resource Integrated Database
EIA	U.S. Energy Information Administration
EIA-860	EIA's annual electric generator data
EIA-923	EIA's annual electric utility data
ELGs	Effluent Limitation Guidelines
EPA	U.S. Environmental Protection Agency
FERC	Federal Energy Regulatory Commission
GHG	Greenhouse gas
GIS	Geographical information systems
Hg	Mercury
ICR	Information collection request
MATS	Mercury air toxics standards
MROW	Midwest reliability organization – west
MWh	Megawatthour
NCP	Number of core patches
NGCC	Natural gas combined cycle
NO_x	Nitrogen oxides
PA	Pennsylvania
PISCES	Power plant integrated systems: chemical emissions studies
PLAND	Percent of habitat available in the landscape
PM	Particulate matter
$PM_{2.5}$	Particulate matter smaller than 2.5 microns in diameter
RFCE	Reliability first corporation – east
SCR	Selective catalytic reactor
Se	Selenium
SO_2	Sulfur dioxide
VOCs	Volatile organic compounds
wFGD	Wet flue gas desulfurizer

Introduction

The U.S. electricity sector is a large contributor of emissions that affect human health, environment, and climate. Estimates from the literature suggest that in 2005, the electricity power generation operations are associated with more than 52,000 premature mortalities by exposing people to particulate matter.[1] The Hidden Cost of Energy report suggests that in 2010, the damages from emissions from coal-fired power plants alone could be nearly $62 billion.[2] Coal plants are a large contributor of those damages because they emit a significant amount of nitrogen oxides (NO_x) and the largest share of sulfur dioxide (SO_2) in the electricity mix, which are precursors to secondary particulate matter (PM).

Since 2005, the Environmental Protection Agency (EPA) has promulgated numerous regulations under the Clean Air Act to curb emissions from coal plants in the past decade. The Cross State Air Pollution Rule, implemented in 2015 and the successor to the Clean Air Interstate Rule in 2009, allows states to allocate SO_2 and NO_x budgets to electrical generating units to meet the National Ambient Air Quality Standards.[3] The 2011 Mercury Air Toxics Standards requires coal and oil-fired power plants to reduce emissions of toxic pollutants and $PM_{2.5}$ (PM less than 2.5 microns in diameter), including $PM_{2.5}$ precursors such as SO_2 and NO_x, to meet the National Emissions Standards for Hazardous Air Pollutants.[4]

Though solid, liquid, and gas phase discharges from coal plants have decreased over time,[5–8] setting these regulatory standards in an efficient manner requires an understanding of how pollution control technologies will affect the partitioning of non-targeted pollutants. For example, the adoption of wet flue gas desulfurization technologies reduces SO_2 emissions by >90%, but also generates an aqueous waste stream containing mercury, arsenic, selenium, lead, chlorine, bromine, and other trace elements.[9] Though these trace elements are less harmful than the precursors of $PM_{2.5}$, they still pose problems to human health and environment by causing morbidity to humans and wildlife and creating biomagnification effects down the food chain.[9]

Therefore, in Chapter 1 I study the gas, liquid, and solid mass flow rates of these non-targeted pollutants from coal-fired power plants at the plant level. By studying four trace elements with different partitioning properties, Hg, Se, As, and Cl, Chapter 1 creates a model that can be used by researchers to generalize the behavior of trace elements in coal plant processes and by decision-makers to understand current mass flow rates despite an absence of well-resolved monitoring data and predict the shift in trace element mass flow rates if further regulation were to promulgate. Though the Effluent Limitation Guidelines,[9] promulgated by the EPA, requires coal plants to treat trace elements in post-wet flue gas desulfurization waste streams, coal ash remains a concern in the U.S. where spills and accidental discharge of trace

elements into water bodies are problematic for human health and environment.[10,11] Therefore, it is worthwhile to track coal plants that could have the largest potential solid and liquid discharge to the environment.

While Chapter 1 leans on negative consequences caused by regulating coal plants, in Chapter 2 I examine the potential negative consequences of coal if the federal government successfully props coal. Namely, current federal policy has supported coal electricity by rolling back environmental and climate protections, such as repealing the Stream Protection Rule and the Clean Power Plan and looking to vacate the Mercury Air Toxic Standards,[12] and pushing for market structures that favor coal electricity with the "Grid Resiliency Pricing Rule," which would allow "for the recovery of costs of fuel-secure generation units" by directing the Federal Energy Regulatory Commission (FERC) to "develop and implement market rules that accurately price generation resources necessary to maintain reliability and resiliency."[13] Shawhan and Picciano argue that if the Grid Resiliency Pricing Rule was enacted, then approximately 25 GW of coal capacity may delay retirement causing about 27,000 premature deaths in the U.S. over 25 years due to the increase of criteria air pollutants emissions such as SO_2, NO_x, and $PM_{2.5}$.[14] While FERC has voted down the Grid Resiliency Pricing Rule,[15] the Department of Energy continues to look for ways to increase the longevity and generation of coal plants in the U.S.[16] Although it is unlikely for coal to make a strong resurgence even with federal policy, it is worthwhile to examine the potential consequences of an increase in coal generation since an increase in coal could displace the use of natural gas and increase health, environmental and climate change damages.[14] I model SO_2, NO_x, and CO_2 emissions from coal-fired power plants and natural gas plants under the assumption that coal plants can operate without key environmental controls or coal displaces natural gas electricity. These assumptions mimic coal-favored policies that have been suggested by the federal government. I recognize that more coal electricity will create air pollution and set out to explore how significant a resurgence in coal could be as a warning of what could happen.

In Chapter 3 I examine the future of the electricity sector in Pennsylvania, where deep decarbonization policies will promote energy transitions that will likely phase out coal electricity. Globally, deep decarbonization policies will be necessary to limit the global temperature below 2°C above pre-industrial levels and avoid the serious impacts of climate change.[17–20] Various U.S. institutions, such as the Environmental Protection Agency under the Obama Administration and the current Pennsylvania Department of Environmental Protection, have pushed policy goals that attempt to deep decarbonize (80% reduction of 2005 levels) by 2050.[21,22] Reaching a deeply decarbonized energy system will require drastic transformations to the electricity sector, such as decreasing the carbon intensity of electricity and

the electrification of end uses.[21,23,24] Projections of future deep decarbonization scenarios highlight that fossil fuels make up less than 20% of the fuel mix.[25–30] However, the current U.S. fuel mix is still 27% coal and 35% natural gas.[31] Therefore, to meet deep decarbonization goals in time, fossil fuels will need to be rapidly phased out and significant renewables infrastructure will be required. However, deep decarbonization will create significant land use change because of the amount of infrastructure needed to build new renewable capacity, transmission for new electricity production, and pipelines for carbon capture and sequestration.[32–37] This land use change associated with new renewables capacity may then create adverse effects on wildlife by fragmenting forests and disrupting habitats.[32,34,38–40] Chapter 3 examines this problem for the state of Pennsylvania, where climate change impacts are less extreme than in other parts of the country, and climate-based ecological impacts are a more significant component of total impacts.[41] Thus, in Chapter 3, I model the land and forested land use impacts from deep decarbonizing the Pennsylvania electricity sector. While mitigating the effects of climate change is an important task and one that every state is likely to undertake, Pennsylvania can also damage its forests and habitats if the infrastructure needed for deep decarbonization is sited haphazardly. I examine how Pennsylvania's ecology could be affected by the buildout of infrastructure for renewables capacity and transmission under a few deep decarbonization bounding scenarios.

In the Conclusions, I summarize key findings and policy implications.

1 Trace element mass flow rates from U.S. coal fired power plants

Abstract: Trace elements exit coal-fired power plants (CFPPs) via solid, liquid, and gaseous waste streams. Estimating the trace element concentrations of these waste streams is essential to selecting pollution control technologies and estimating the benefits of emission reduction. This work introduces a generalizable model for estimating trace element mass flow rates in the waste streams of CFPPs and evaluates the accuracy of this model for the US coal fleet given current data constraints. We stochastically estimate the 2015 mass flow rates of Hg, Se, As, and Cl to solid, liquid, and gas phase waste streams at the plant-level by combining publicly available data for trace element concentrations in combusted coal with estimates of trace element partitioning within installed air pollution control processes. When compared with measured and reported data on trace element mass flow rates, this model generally overestimates trace element concentrations in coal, leading to overestimation of trace element mass flow rates to the waste streams. The partitioning estimates are consistent for Se, As, and Cl removal from flue gas, but tend to underestimate Hg removal. Model performance would improve with access to more recent measurements of trace element concentrations in the coal blend, where data quality is the weakest.

A version of this chapter is currently under revised and resubmit in Environmental Science and Technology as: **Sun, X., Gingerich, D. B., Azevedo, I. L., & Mauter, M. S. "Trace element mass flow rates from U.S. coal fired power plants"**.

Notation used in this Chapter:

Symbols:
c: Concentration [g/kg]
$\hat{c}$: Plant-average concentration [g/kg]
E: Mass of trace element exiting APCD [g/yr]
G: Electricity generation [MWh]
I: Generation normalized trace element mass flow rate [g/MWh]
$\dot{M}$: Mass of trace element entering plant or APCD [g/yr]
$\dot{m}$: Mass of coal combusted [kg/month] or [kg/yr]
x: Partitioning fraction [-]
Subscripts:
i: Coal-fired power plant
l: County
j: Trace element
k: Boiler
m: Month
PM: Particulate matter control
r: Rank
SO_2: Flue gas desulfurization system
φ: Phase

1.1 Introduction

Coal-fired power plants (CFPPs) are a significant source of trace element emissions[4] impacting human health[42–47] and the environment.[48–53] Though U.S. regulations have curtailed solid, liquid, and gas phase discharges from CFPPs,[5–8] as exemplified by a 61% reduction between 1990 and 2014 of Hg emissions to the atmosphere driven by regulations and reductions in coal generation,[54] setting these regulatory standards in an efficient manner requires an understanding of how pollution control technologies will affect the partitioning of non-targeted pollutants. For example, the adoption of wet flue gas desulfurization technologies reduces SO_2 emissions by >90%, but also generates an aqueous waste stream containing mercury, arsenic, selenium, lead, chlorine, bromine, and other trace elements.[9] Without a detailed understanding of trace element partitioning across plant processes, it is difficult to estimate the implications of regulations on the fate of trace elements in the environment.

A second challenge associated with setting regulatory standards is an inability to easily quantify trace element emissions across the entire U.S. coal fleet. Because each coal plant has different coal sources, combinations of installed air pollution control technologies, generation efficiencies, and capacity factors, accurately performing a national assessment of the cumulative benefits of regulation requires boiler or plant level modeling of trace element emissions across the solid, liquid, and gas phases.

Current models for estimating trace element mass flow rates at CFPPs either provide estimates of trace element emissions to a single phase or a single plant, but none are specifically developed for capturing the fleet-level variation described above. For instance, several models estimate the behavior of trace element partitioning within select air pollution control devices, but none provides comprehensive coverage of the common post-combustion controls deployed at U.S. CFPPs.[55–65] Other models have been developed to estimate trace element mass flow rates to the gas phase from Kosovan[66] and Chinese[67–70] coal fleets or for mass flows of any trace element to waste water.[71,72] Most of these studies use a mass-balance approach similar to the framework we will use in this paper, termed by Zhang L. et al.[69] the "probabilistic technology-based emission factor" approach that consists of multiplying the probability distribution functions of coal concentration, coal cleaning, and removal in APCDs to predict mass flow rates to the gas phase. These models, unfortunately, focus on only one phase at a time despite the sequestration of trace elements like mercury into multiple phases such as fly ash, bottom ash, FGD wastewater, and gypsum having long been of interest.[73–76] To date, the most comprehensive plant-level model for simulating trace element mass flow rates is the Power Plant Integrated Systems: Chemical Emissions Studies (PISCES) model. Most recently updated in 2016,[77] PISCES combines user inputs for installed air

pollution control devices and trace element concentrations in the coal blend to estimate the concentration of dozens of trace elements in the solid, liquid, and gas phase waste streams of CFPPs.[78–81] Rubin applied the PISCES model to estimate trace element emissions from three CFPPs intended to represent the entire U.S. CFPP fleet on the basis of size, rank of coal combusted, and installed air pollution control devices. These representative plants were then used to perform "back of the envelope" calculations on the total trace element mass flow rate from all U.S. CFPPs in 1996.[81] While suitable for a zeroth-order analysis, accurately describing trace element mass flow rates at CFPPs requires a model that accounts for the wide variation in the trace element concentrations of combusted coal and in installed post-combustion air pollution control devices at U.S. CFPPs. Such a model could be used to inform selection of pollution control technologies, as well as provide fleet-level estimates that form the basis for policy assessment.

The other significant drawback of these earlier modeling studies is inadequate model validation and assessment, largely due to an absence of robust monitoring data. The handful of analyses that perform model validation compare national-level estimates[69,82] or province-level estimates[70] to previous studies rather than plant-level emission inventories. Only one study[70] compares plant-level estimates to actual observations, comparing predicted ambient mercury concentrations to observed ambient mercury concentrations at a single observation station. Therefore, there is a significant gap in validating the results of models that are structured similarly to our own.

Fortunately, recent efforts by the U.S. Environmental Protection Agency (EPA) to collect data on trace element emissions at the plant-level can be used to validate these approaches. Data collected by the U.S. Environmental Protection Agency (EPA) as part of the Mercury and Air Toxics Standards Information Collection Request (MATS ICR) on trace element concentrations in coal purchased and gaseous trace element emissions by CFPPs facilitate comparisons between predicted and actual coal quality and trace element partitioning fractions. Recently implemented stack-level monitoring and reporting of mercury emissions at large CFPPs via the EPA's Continuous Emissions Monitoring System (CEMS) enables the first assessment of model fidelity for Hg emissions in the gas phase. Similarly, several recent plant-level monitoring studies conducted during rule development for the EPA's recently updated Effluent Limitation Guidelines for the Steam Electric Power Generating Category (ELGs) enable validation of aqueous phase concentrations of several trace elements of relevance to human health and the environment.

This work estimates the mass flow rates of trace elements in solid, liquid, and gas waste streams at the boiler, plant, and fleet levels. We construct the first stochastic mass balance model that combines the estimates of trace element concentration in combusted coal with estimates of trace element partitioning by post-combustion air pollution control devices. We apply this model to estimate Hg, Se, As, and Cl mass

flow rates in the solid, liquid and gas phases, focusing on these trace elements because of their relevance to human or environmental health[9] and their diverse partitioning behavior in installed air pollution control processes.[83] We compare model results with empirical data reported by the EPA in establishing the Mercury Air Toxics Standards[84], updating the Effluent Limitation Guidelines[9] and implementing the Continuous Emissions Monitoring Systems program.[85]

1.2 Data and Methods

Figure 1.1 provides an overview of our model formulation. In brief, the model takes coal concentration data from COALQUAL and coal purchase data from U.S. EIA to estimate the mass of arsenic, chlorine, mercury, and selenium entering each coal-fired boiler. We then model trace element partitioning in air pollution control devices based on partitioning coefficients in the reported literature and for each reportedly installed air pollution control device. This allows us to calculate the mass flow rates to the gas phase (air emissions from the CFPP), liquid phase (input into the FGD wastewater treatment process), and solid phase (bottom ash, fly ash, or gypsum waste streams that are retained on-site in an ash pond, landfilled, or sold to market). We then apply this model to each of the 626 boilers we have information for at U.S. CFPPs. Altogether, these boilers are responsible for 89% of total electricity generation in 2015 to calculate total gas, solid, and liquid phases for US plants. The model does not consider partitioning between the solid and liquid phases during wet sluicing of solids, as wet sluicing practices are being phased out under the ELGs,[6] or trace element removal in FGD wastewater treatment processes. The model is available on GitHub to encourage and facilitate extensions of our study (Appendix A provides repository link).

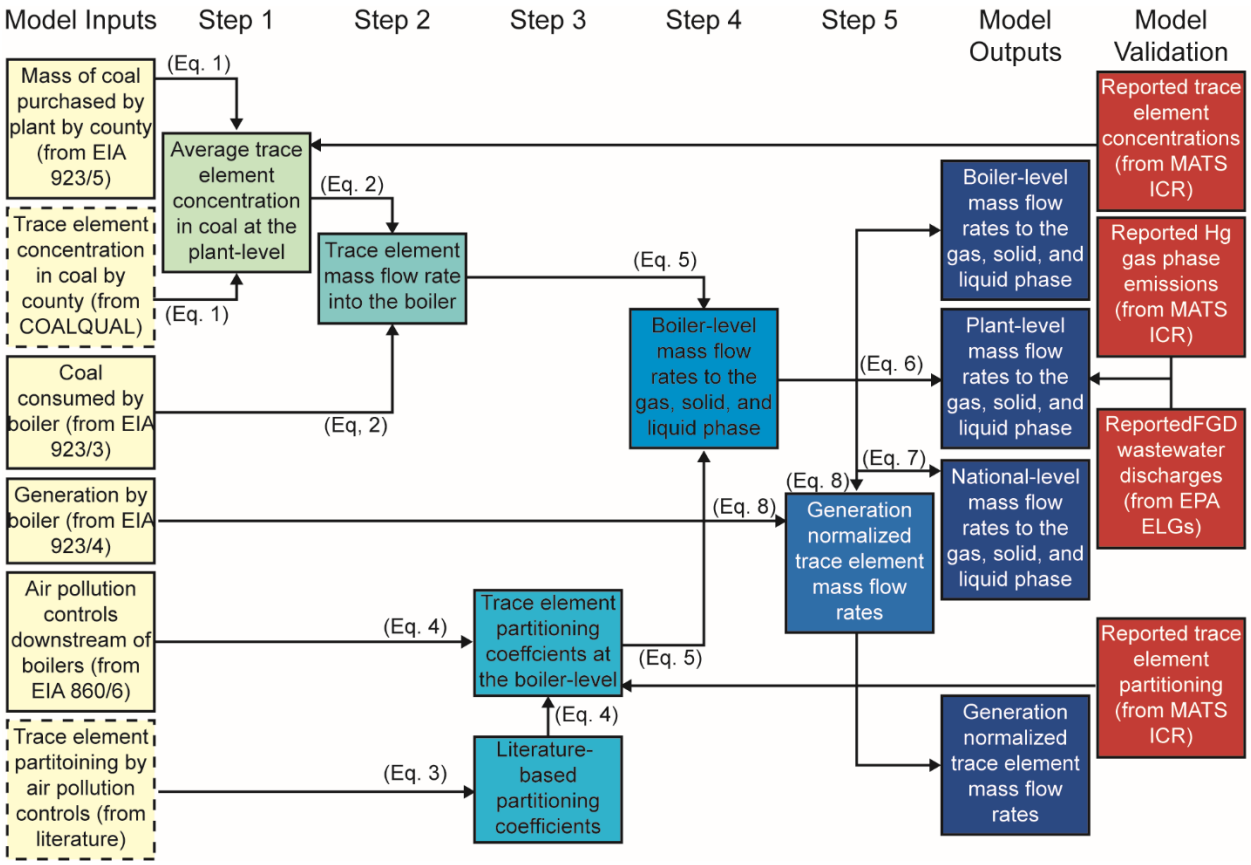

Figure 1.1: Overview of the data and methods used in estimating and validating the trace element mass flow rate model. We begin by estimating the trace element content of coal entering each U.S. CFPP by matching county-level coal purchase data to county-level trace element concentration data. We then multiply the concentration of trace elements in coal fed to U.S. boilers by the quantity consumed at those boilers to estimate the mass flow rate of trace elements at the boiler level. Next, we estimate trace element partitioning coefficients for each air pollution control technology by assessing the fraction of each trace element exiting and entering the air pollution control device in each phase. This data is derived from 17 peer-reviewed studies on trace element partitioning at U.S. CFPPs. Then, we combine these estimates of trace element mass inputs and partitioning coefficients to estimate trace element mass flow rates in the solid, liquid, and gaseous waste streams for the year 2015. Finally, we normalize trace element mass flow rates to the solid, liquid, gaseous waste streams by electricity generation. We explicitly treat variability and uncertainty in our datasets by performing a bootstrapping analysis with replacement, rather than producing point estimates of trace element mass flow rates. We randomly draw 10,000 trials with replacement for the following variables: the concentration of trace elements in coal by county and rank and the partitioning of trace elements by air pollution controls. Yellow boxes represent inputs, dark blue boxes represent outputs, and red boxes represent comparison analyses. Dashed yellow boxes represent stochastic inputs and solid yellow boxes are deterministic inputs. CEMS is the Continuous Emissions Monitoring System.[85] COALQUAL is the U.S. Geological Survey COAL QUALity database.[86] EIA A/B is the Energy Information Administration, form number A, schedule number B.[87,88] EPA ELGs is the Environmental Protection Agency's Effluent Limitation Guidelines.[9] MATS ICR is the Mercury Air Toxic Standards Information Collection Request.[84]

1.2.1 Model Input Data: A total of 443 U.S CFPPs report boiler and generator level data through the U.S. Energy Information Administration (EIA) Form 923 (EIA-923) and EIA Form 860 (EIA-860) for 1,135 boilers and 1,036 generators.[87,88] We exclude 302 boiler-generator pairs because they do not report all necessary data for the analysis or have multiple connections to other generators and boilers (see Table A2 and Table A1 for further detail). Our final dataset includes 277 coal plants, consisting of 626 boiler-generator pairs, and covers 89% of total electricity generated from coal in 2015. We use boiler level data reported to the EIA, including boiler capacity from EIA-860/3, installed air pollution controls from EIA-860/6, coal consumption at the boiler level from EIA-923/3, annual boiler generation from EIA-923/4, and coal rank and county of origin from EIA-923/5.

1.2.2 Trace element mass flow rates to the gas, solid, and liquid phase:

Trace element content in the coal combusted in each U.S. boiler: Coal trace element concentration by rank and county is drawn from the U.S. Geological Survey (USGS) COAL QUALity database V3 (COALQUAL). COALQUAL was originally assembled in the 1970s-80s by the USGS and includes over 6,500 run-of-mill coal samples covering over 60 trace elements across 36 states and 328 counties.[86] The number of samples for a given county in COALQUAL varies widely from county to county (min = 1; max = 427). In Table A3, Figure A1, we plot the variability of trace element concentrations for several counties with representative levels of variability. We treat the variability in the concentration of the coal sample *c* for a given coal rank *r* and county *l* by assuming each sample is a discrete observation with a uniform probability from which we perform a random draw in a bootstrapping analysis. We use the concentrations of all four trace elements from a single COALQUAL coal sample in a draw to account for potential correlations of trace element concentrations in coal. If a sample is missing data for a trace element, we use the median trace element concentration for all samples of the same rank at the county level. Similarly, we use basin-level data if there are no samples reporting at the state-level.

Thus, for each U.S. CFPP *i*, we will have 10,000 observations for the average concentration of a trace element *j*, $\widehat{c_{i,j}}$ [g/kg] entering the power plant that results from using each of those samples one at a time and by multiplying the concentration by the proportion of coal that the plant has purchased from county *l* in 2015 (Equation 1.1).

$$\widehat{c_{i,j}} = \sum_l \sum_r c_{l,r,j} \times \frac{\dot{m}_{i,l,r}}{\sum_l \sum_r \dot{m}_{i,l,r}} \qquad (1.1)$$

The concentration of trace elements in coal blends combusted at the plant level, Emissions and Generation Resource Integrated Database (eGRID) sub-region level (See Table A4, Figure A2, and Table A2 for sub-region definitions), and fleet-level are plotted in Table A5, Figures S3 and S4. In Table A5,

Figure A5, we also compare differences in concentration estimates when bootstrapping COALQUAL samples versus using the median of the COALQUAL samples.

We calculate the total mass of trace element *j*, $\dot{M_{j,k}}$ [g/yr] entering a power plant boiler by multiplying the concentration of trace element *j*, $\widehat{c_{i,j}}$, by the mass of coal combusted in boiler *k* in month *m,* $\dot{m_{k,m}}$ [kg/month] (Equation 1.2).

$$\dot{M_{j,k}} = \sum_m \widehat{c_{i,j}} \times \dot{m_{k,m}} \qquad (1.2)$$

As we do not know if counties of origin for coal combusted at the boiler-level, we assume that each boiler at a plant burns coal with the plant-level average concentration.

One limitation of the COALQUAL dataset is that numerous coal samples are below the detection limit. In such cases, the USGS assigned a value of 70% of the lower detection limit. This issue occurs for approximately 4%, 3%, 1%, and 21% of Hg, Se, As, and Cl samples, respectively. In Table A6 and Figure A6, we explore differences in Cl concentrations in coal blends when samples below the detection limit are assumed to have concentration equal to 0% or 100% of the lower detection limit.

This analysis does not account for coal preparation and cleaning, because we find that coal purchased from coal preparation plants accounts for less than 6% of total coal purchases in 2015 (See Table A7 and Figures A7 and A8 for additional detail).[88] Furthermore, previous work has estimated that less than 1% of trace metals are removed by pulverization at the plant site prior to combustion.[89,90]

Trace element partitioning in post-combustion air pollution control devices: The second step of the model is to calculate the partitioning fraction of trace elements at the boiler-level. In Table A3 of Table A8, we provide a summary of studies that have estimated, measured, or reported the partitioning of trace elements to solid, liquid, and gaseous phases at U.S. CFPPs for different post-combustion air pollution control devices and combinations of those devices. We do not include studies that sampled plants from other countries, as the technology and operation of the air pollution control devices may have been specifically adapted to comply with different emissions standards.[91]

Most existing partitioning studies provide data on the mass of a trace element entering and the mass of that trace element exiting each stream of the coal plant, which may include bottom ash, fly ash, gypsum, the chloride purge, and/or the stack. We estimate the partitioning fraction *x* into phase ϕ for each air pollution control technology as:

$$x_\phi = \frac{E_\phi}{\dot{M}} \qquad (1.3)$$

where E_ϕ is the mass of a trace element exiting an air pollution control device in phase ϕ [g] and $\dot{M}$ is the mass of trace element entering the air pollution control device [g]. We assume all trace elements exiting with the bottom ash, fly ash, and gypsum are in the solid phase, all trace elements exiting in the chloride purge are in the liquid phase, and all trace elements exiting the stack are in the gaseous phase.

In Figure 1.2, we show the partitioning coefficients to solid, liquid, and gas phase for each study included in the model for different combinations of air pollution controls (Table A8 reviews the literature on trace element partitioning, Table A3 provides numerical values for Figure 1.2). There is a large body of information on the capture and fate of mercury at coal-fired power plants; much of which is summarized in several publications.[73,74] Because of this focus on mercury removal, we have 29 different studies from which we draw partitioning coefficients, compared to 12 for selenium, 11 for arsenic, and 8 for chloride.

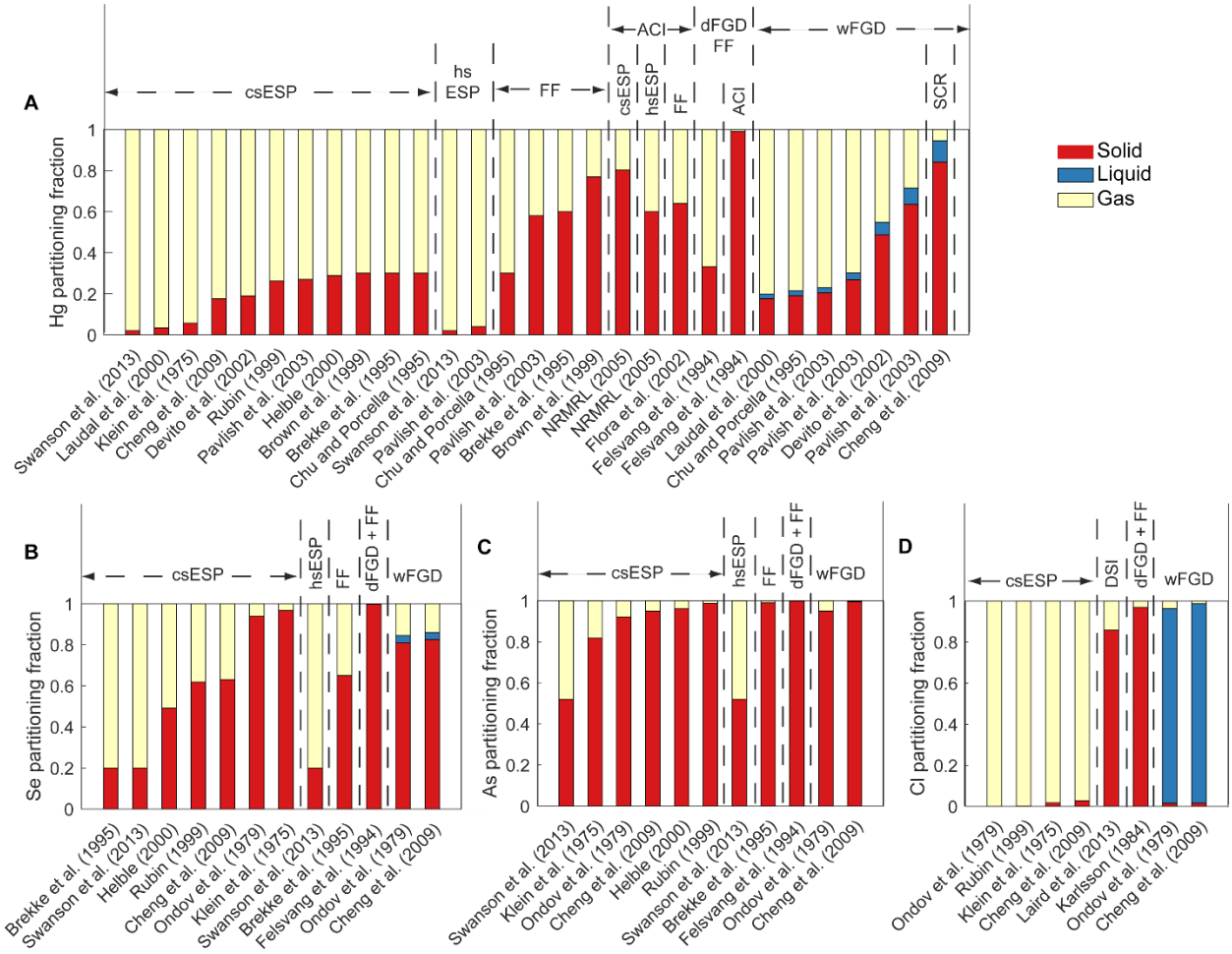

Figure 1.2: Solid, liquid, and gas phase trace element partitioning fractions for (A) mercury; (B) selenium; (C) arsenic and (D) chloride. The partitioning factors are either directly reported or estimated using the information reported in the studies. The air pollution control technologies listed are: ACI = activated carbon injection; csESP = cold side electrostatic precipitator; dFGD = dry flue gas desulfurizer,

DSI = dry sorbent injection; FF = fabric filter; hsESP = hot side electrostatic precipitator; SCR = selective catalytic reactor; wFGD = wet flue gas desulfurizer. *Samples from Swanson et al. are a mixture of csESP and hsESP fly ash.

We account for the variability observed in trace element partitioning across phases (Figure 1.2) by performing a bootstrapping analysis. We assume discrete distributions with uniform probabilities and develop a distribution of partitioning fractions for each air pollution control device by sampling 10,000 $x_{\phi,}$ with replacement, from all studies containing the same air pollution control device.

Using partitioning data for each air pollution control device, we create a distribution of partitioning fractions for the combination of air pollution control devices associated with each boiler. First, we perform a bootstrapping analysis at the boiler level on the partitioning fractions for each air pollution control device (Table A9, Figure A9). Then, we use Equation 1.4 to assess the partitioning fraction of trace elements across the entire boiler treatment train to the solid, liquid or gas phase.

$$x_{i,\phi,j} = x_{PM,\phi,j} + (x_{PM,\phi=gas,k} \times x_{SO_2,\phi,j}) \qquad (1.4)$$

Here, $x_{i,\phi}$ is the overall partitioning fraction for boiler *i* and its downstream air pollution controls for a phase ϕ and a trace element *j*; $x_{PM,\phi,TE}$ is the partitioning fraction at the particulate matter control, activated carbon injection, dry flue gas desulfurization and dry sorbent injection; and $x_{SO_2,\phi,j}$ is the partitioning fraction at the sulfur dioxide control and the selective catalytic reactor. Equation 3 assumes that partitioning of trace elements by air pollution controls are independent of the controls downstream or upstream, which we test in Table A10, Figure A10. Table A11, Table A4, quantifies the TWh of U.S. coal generation treated by each air pollution control technology.

Of our 17 peer-reviewed studies, only five studies report partitioning to bottom ash in addition to partitioning to fly ash (Table A8, Table A3 reports the five studies). For those five studies, we combine trace element mass flow rate in the bottom ash waste stream and the particulate matter control device waste stream. In these cases, the fraction of trace elements partitioning to the solid phase in the particulate matter control equals the sum of the fraction of trace elements in bottom ash plus the fraction of trace elements in the fly ash.

Boiler-, plant-, and national-level trace element mass flow rates to each waste stream: In the third step, we calculate the annual boiler-level trace element mass flow rates to the gas, solid, and liquid phases,

$\dot{M}_{k,\varphi,J}$ [g/yr], by multiplying the total mass of trace element *j* entering a power plant boiler, $\dot{M}_{J,k}$ [g/yr], and the overall boiler partitioning fraction, $x_{i,\varphi,j}$, (Equation 1.5).

$$\dot{M}_{k,\varphi,J} = \dot{M}_{J,k} x_{i,\varphi,j} \qquad (1.5)$$

We then aggregate the boiler-level trace element mass flow rates at both the plant-level and national-level. We calculate the annual plant-level trace element mass flow rates for a given plant *i* and phase φ, $\dot{M}_{J,\varphi,J}$ [g/yr] by summing boiler-level trace element mass flow rates, as shown in Equation 1.6.

$$\dot{M}_{J,\varphi,J} = \sum_{k \in [boilers\ at\ plant\ i]} \dot{M}_{k,\varphi,J} \qquad (1.6)$$

Finally, we calculate the national-level trace element mass flow rates for each phase, $\dot{M}_{\varphi,J}$ [g/yr] by summing over all boilers included in our analysis (Equation 1.7).

$$\dot{M}_{\varphi,J} = \sum_{i} \dot{M}_{\iota,\varphi,J} \qquad (1.7)$$

Generation normalized trace element mass flow rates in the solid, liquid, and gaseous phases at each U.S. CFPP : Finally, using Equation 1.8 we estimate the generation normalized trace element mass flow rate $I_{i,\phi,j}$ [g/MWh] to solid, liquid, and gaseous waste streams at each U.S. CFPP by dividing the plant-level trace element mass flow rate for plant *i* to phase *φ,* $\dot{M}_{\iota,\varphi,J}$ [g/yr] by net annual generation for plant i, G_i [MWh/yr], i.e.,

$$I_{i,\phi,j} = \frac{\dot{M}_{\iota,\varphi,J}}{G_i} \qquad (1.8)$$

***1.2.3 Model Validation*:** We compare our model estimates against sampled data in four ways:

(i) We validate trace element concentrations in coal blends by comparing the trace element concentration in coal blends estimated in this study to those reported in the MATS ICR. To enable comparison to the 2010 MATS ICR data, we re-run our analysis using 2010 coal purchase data from EIA.

(ii) We validate partitioning fraction estimates by comparing the median partitioning fractions estimated in this study to experimentally determined partitioning fractions reported in the MATS ICR. Details of this analysis and its results are provided in the Table A12 and Figure A11.

(iii) We validate gas phase Hg mass flow rates by comparing our estimates of gas phase Hg emissions in 2015 against Hg measurements from the Continuous Emissions Monitoring System (CEMS) in 2015. CEMS includes stack level measurements of Hg emissions, but not other trace elements.

(iv) We validate liquid phase trace element mass flow rates by comparing our estimates to the average trace element concentration in FGD wastewater reported in the Environmental Assessment of the ELGs in

2015.[9] The Environmental Assessment estimated the average annual trace element mass discharge of Hg, Se, As, Cl, and several other species across 88 CFPPs. While the data was sampled across a six-year window, we compare it to data in 2015. Although we are unable to make a plant-by-plant comparison, we can compare our fleet-level estimates of trace element mass flow rates to flue gas desulfurization wastewater against data sampled at these 88 plants.

1.3 Results

2015 annual mass flow rate of trace elements to solid, liquid, and gas waste streams: In Table 1.1, we provide 25th, 50th, and 75th percentile estimates of 2015 annual trace element waste stream mass flow rates from the coal fleet modeled in our dataset. We find significant variability in total pollutant mass flow rates as the 25th and 75th percentile flow rates estimates vary from 200% - 600%, depending on the trace element and phase. The variability is partially caused by the variability in trace element concentrations in coal at the plant-level, which is shown in Figure A3E-H. This large variation in trace element concentrations between plants underscores the importance of performing plant-level analyses when performing policy analysis. It is also useful in explaining some of the discrepancy between our model results and the average plant emissions data from sampling campaigns, as discussed below.

Additional variability stems from differences in trace element partitioning between installed air pollution control technologies. While Hg, Se, and As predominantly partition to the solid phase, Cl exits plants in the solid phase waste stream if dry sorbent injection or dry FGD technologies are installed, the liquid phase waste stream if wet FGD technology is installed, or the gas phase waste stream if there are no sulfur dioxide controls installed downstream of the boiler.

Despite this variability, our results are consistent with the physical-chemical properties of the trace elements. Less volatile trace elements, such as Se and As, are more likely to be discharged as solid waste than more volatile metals, such as Hg, where a higher proportion is discharged as a gaseous waste.[92,93]

Table 1.1: Estimates of total 2015 trace element mass flow rates from the CFPP fleet in our dataset, which represents 89% of 2015 U.S. coal generation. Results are shown using 25th, 50th, and 75th percentile estimates from our bootstrap analysis.

Trace element	Solid (metric ton/year)			Liquid (metric ton/year)			Air (metric ton/year)			All phases (metric tons/year)		
	25th	50th	75th	25th	50th	75th	25th	50th	75th	25th	50th	75th
Hg	35	51	70	1.4	1.9	3.0	10	16	24	51	71	93
Se	790	990	1300	4.6	11	18	54	150	240	950	1200	1500
As	2300	3400	5600	0.14	0.23	0.51	28	72	180	2400	3500	5800
Cl	24,000	28,000	32,000	93,000	110,000	130,000	22,000	25,000	30,000	140,000	160,000	190,000

Generation normalized mass flow rate to each phase at each U.S. coal-fired power plant: In Figure 1.3, normalize the annual mass flow rate at each U.S. CFPP by the plant's annual generation to determine a distribution of median generation normalized mass flow rates (in g/MWh) across the fleet of CFPPs (see Table A13, Figure A12 for a boiler level analysis). Median generation normalized mass flow rates vary by up to 5 orders of magnitude across plants. Table A13 provides data and a permanent link to the MATLAB code that allows the reader to generate similar distributions for each eGRID sub-region. We caution the reader that plant-level CFPP coverage in these sub-regions varies between 45-89%.

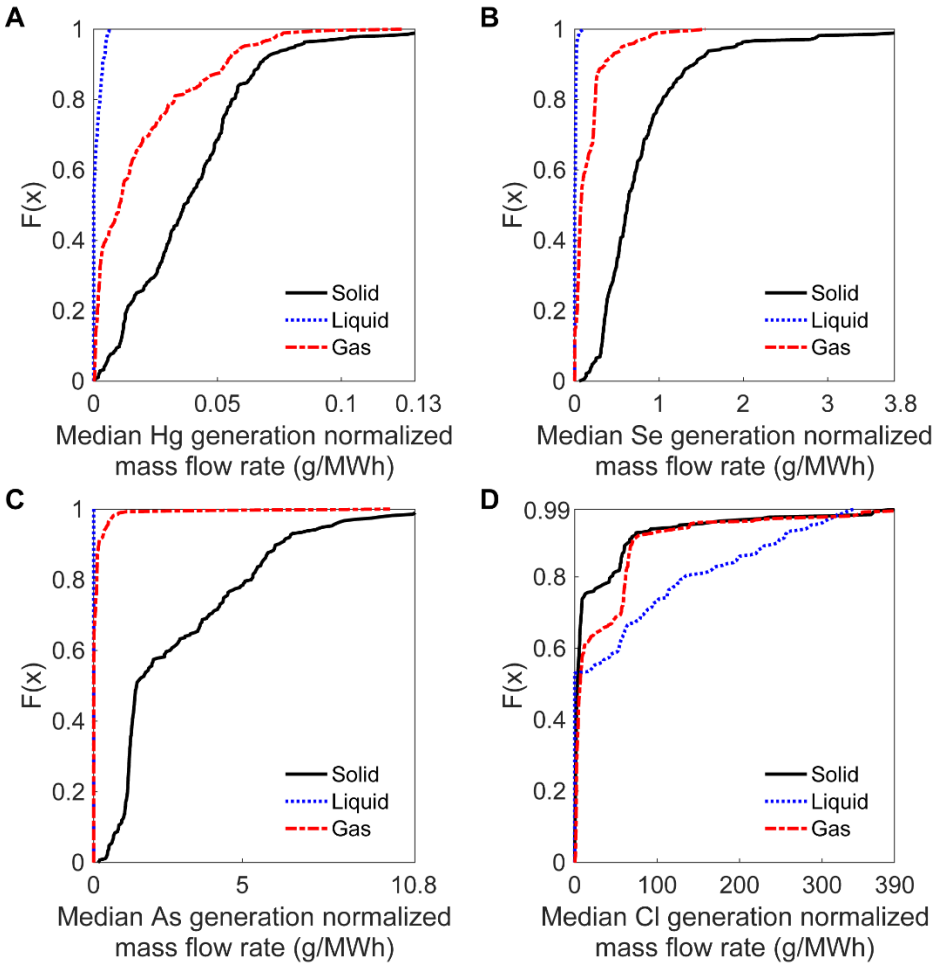

Figure 1.3: Cumulative distribution functions of plant-level median trace element generation normalized mass flow rates (g/MWh) across the U.S. CFPP fleet to the solid, liquid, and gas phases. Distribution is derived from bootstrapping coal concentrations in coal at each plant and the solid, liquid, and gas partitioning of trace elements by air pollution controls at each boiler across the coal fleet for A) Hg, B) Se, C) As, and D) Cl. The x-axis on all figures is cut-off at the 99th percentile (0.18 g/MWh for Hg, 4.9 g/MWh for Se, 10.8 g/MWh for As, and 358 g/MWh for Cl) for readability.

1.4 Assessment of Model Validity using Empirical Data from U.S. CFPPs

1.4.1 Model Validation Against Available Empirical Data

We compare our results for trace element mass flow rates in the solid, liquid, and gas phases against empirical data from the 2010 MATS ICR dataset,[84] 2015 CEMS,[85] and the 2015 EPA ELGs,[9] as explained in the methods section. We summarize the comparisons made in this section in Figure 1.4. Overall, we find that our estimates differ from empirical data for both the coal concentrations and waste stream concentrations. Our partitioning estimates for Se, As, and Cl agree with empirical data reported in the datasets referenced above, while our estimates for Hg are poorly matched.

Validation of trace element concentrations in coal blends using MATS ICR coal quality data: The MATS ICR is a publicly available dataset reporting trace element concentrations of coal, the fuel content, and the emissions to air for 1,000 boiler-level coal samples from 210 U.S. CFPPs collected between February and August 2010.[84] The limited sampling period may have constrained the range of coal qualities combusted at each plant, as we observe significant temporal variability in the concentration of trace elements in the coal blend over the course of a year (Table A14, Figure A13). The number of plants in this analysis reduced from 210 plants to 122 plants after removing 1) CFPPs with boilers connected to multiple generators and vice-versa and 2) CFPPs without complete coal purchase and consumption data in EIA (Table A2 reports the complete set of inclusion and exclusion criteria).

For these 122 plants, the median concentrations of coal entering the plants in the MATS ICR dataset are 0.08 ppm for Hg, 1.0 ppm for Se, 2.0 ppm for As, and 142 ppm for Cl. Using 2010 coal purchase data, our model estimates concentrations of 0.12 ppm for Hg, 1.3 for Se, 2.8 ppm for As, and 120 ppm for Cl. We plot median percent differences for each trace element in Figure 1.4A. Additional details are reported in Table A15 and Figure A14.

We attribute the differences between our estimates and the value reported in MATS ICR to two factors. First, COALQUAL reports trace element concentrations at the coal mine, whereas the MATS ICR reports them at the plant. While the expected change in trace element concentration between the mine and the plant is very small, there may be significant differences in concentration as a result of uneven spatial or temporal coal blending. This is especially likely because the MATS ICR data collection occurred for only half of a year.

Second, COALQUAL data was collected 30 years before the MATS ICR data, when the detection limit and accuracy of analytical methods for trace element detection were inferior. Indeed, 4%, 3%, 1%, and 21% of COALQUAL samples do not detect the presence of Hg, Se, As, and Cl, respectively. Instead, COALQUAL reports a trace element concentration equal to 0.7 times the detection limit. While this could lead to overestimation of the actual concentration in the coal blend, we find that COALQUAL lower

detection limit assumptions are only likely to affect Cl concentrations (Table A6). Additional details comparing our estimates of trace element concentrations entering the plant with measurements from the MATS ICR for those plants that are common to both datasets in more detail.

Validation of partitioning fraction model using MATS ICR partitioning fractions: The median boiler surveyed by the MATS ICR has a gas phase partitioning fraction of 0.11 for Hg, 0.03 for Se, 0.003 for As, and 0.02 for Cl. In contrast, the median of the bootstrapped fraction emitted to the gas phase from our partitioning model for these same boilers is 0.52 for Hg, 0.12 for Se, 0.01 for As, and 0.03 for Cl. The median difference in boiler-level trace element partitioning to the gas phase between our model estimates and data reported in MATS ICR is plotted in Figure 1.4B.

While there is reasonable agreement in partitioning fractions for Se, As, and Cl, we significantly overestimate Hg partitioning to gas phase. We attribute this difference to the inability of our model to account for unreported methods plants may use to reduce mercury emissions, such as fuel blending, addition of oxidizing chemicals, and increasing unburned carbon in the fly ash.[94] Boiler-level results from CFPPs in our dataset are reported in Table A9, Figure A9.

Validation of boiler level Hg gas phase mass flow rate using CEMS emissions measurements: We compare our estimated median boiler-level gas phase Hg emissions to 224 of the 276 boilers reporting to CEMS in 2015. Excluded boilers are those excluded in our dataset for the reasons stated in Table A2. These boilers operated at 113 CFPPs and generated 527 TWh of electricity or 40% of coal electricity in 2015.

The histogram of the CEMS boiler level median gas phase Hg emissions intensity (median of 2.0 mg Hg/MWh across all boilers) is plotted with the histogram of modeled emissions for those same boilers (median of 2.8 mg Hg/MWh) in Figure 1.4C. The regulated mercury emission limit for low-rank coal units is 18.1 mgHg /MWh and for high-rank coal units is 5.9 mg Hg/MWh. Our model estimates 72 boilers, or about a third of the boilers, exceed 5.9 mg Hg/MWh.[8]

We attribute the model's overestimation of gas phase Hg emissions to overestimation in both the estimated Hg concentrations in the coal blend (see Table A6, Figure A4e for plant-level Hg concentrations produced by bootstrapping) and overestimation of Hg partitioning to the gas phase discussed above. In Figure A15 of Table A16, we repeat our analysis using the minimum Hg concentration and gas-phase Hg partitioning coefficient to test this explanation. We find that model overestimation of our model falls from 58% to 15% when using these minimum model inputs.

Comparison of fleet level aqueous phase mass flow rates to the reported FGD wastewater mass flow rates at 88 plants sampled during ELG rule making: The Environmental Assessment of the ELGs estimates liquid phase trace element mass flow rates in FGD wastewater from 88 coal plants.[9] The identity of these 88 coal plants have been restricted as confidential business information. As such, we compare our median fleet level liquid phase FGD wastewater trace element mass flow rate to the average value for these 88 plants.

The ELGs report the trace element mass flow rates to FGD wastewater at the average plant as 2.5 kg Hg/yr, 641 kg Se/yr, 4.3 kg As/yr and 4.6 million kg Cl/yr.[9]. In our dataset, we average Hg, Se, As, and Cl mass flow rates to FGD wastewater for 129 plants. Based on the 25th and 75th percentile annual mass flow rates reported in Table 1.1, we estimate the average plant FGD wastewater discharge to be 11 – 23 kg Hg/yr, 36 – 139 kg Se/yr, 1.1 – 4.0 kg As/yr, and 0.7 – 1.0 million kg Cl/yr.

For the four trace elements, only EPA's average As wastewater discharge is contained within our uncertainty bounds. As shown in Figure 1.4D, we overestimate average Hg mass flow rates to flue gas desulfurization wastewater by 500% and underestimate Se, As, and Cl by 86%, 58%, and 82% respectively. Consistent with the CEMS comparison, we overestimate Hg emissions, suggesting that we overestimate Hg content in coal and underestimate the removal of Hg by particulate matter controls. We underestimate Se, As, and Cl mass flow rates to wastewater, despite overestimating trace element concentrations in coal, and showing agreement with removal estimates from MATS ICR. Because the trace element removal analysis compares combined solid and liquid removal, we are likely underestimating the partitioning of trace elements to the liquid phase within the wet FGD.

Comparison of gas phase mass flow rates against other model results: Additionally, we compare our estimates of mass flow rates to the gas phase for arsenic, selenium, and chloride to modeled results from a 2018 Electric Power Research Institute study.[95] We do this comparison in order to benchmark our model against previous modeling efforts, and find that we have reasonable agreement (+/- 30%) for the majority of plants common to our data sets for arsenic and selenium mass flows. Details of this analysis, including methods and results, can be found in Table A17 and Figures S16 and S17.

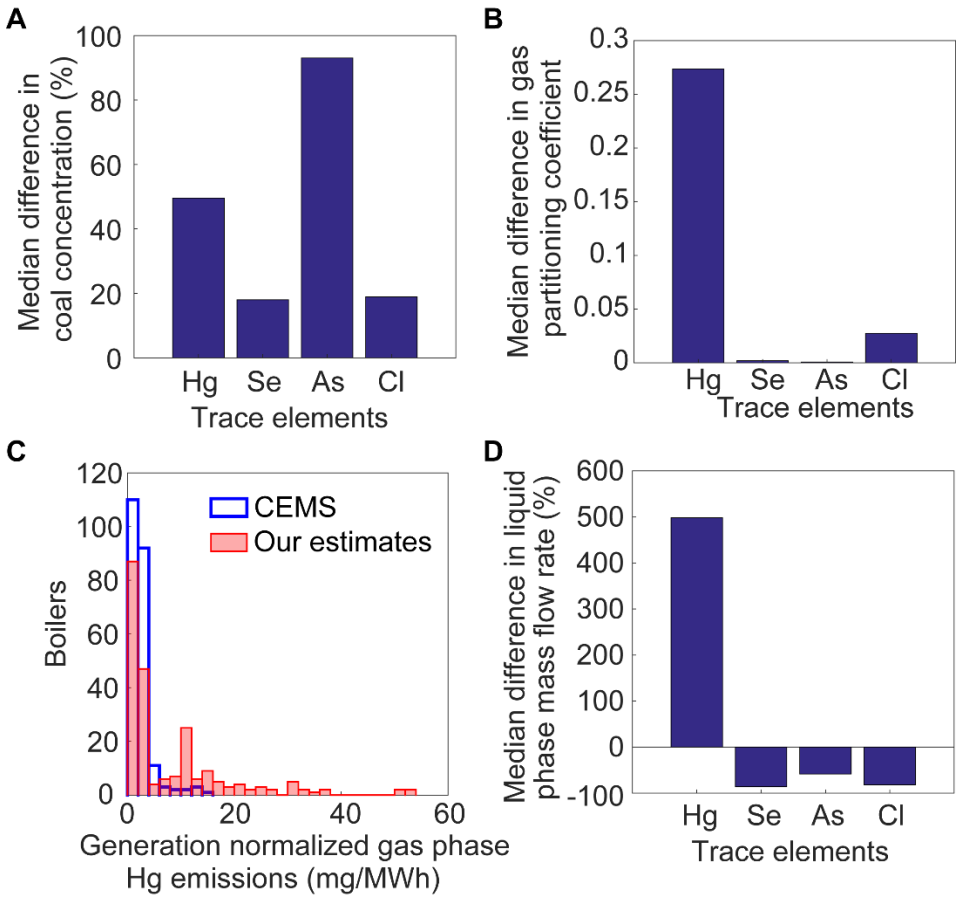

Figure 1.4: Summary of the comparison analyses. A) Median percent difference in plant-level trace element composition of coal between model estimates and data reported in the MATS ICR; B) Median difference in boiler-level trace element partitioning to the gas phase between model estimates and data reported in MATS ICR; C) Histogram of generation normalized boiler level gas phase Hg emissions estimated from model and reported in the CEMS in 2015; D) Median percent difference in liquid phase mass flow rates estimated at the fleet level compared to average mass flow rates for the 88 plants sampled and reported in the Environmental Assessment of the Effluent Limitation Guidelines.

1.4.2 Data Needs to Improve Future Emissions Modeling Efforts

There are several areas that warrant attention in future studies and data gathering efforts, including data on coal quality and trace element behavior. The first gap for improving modeling of coal quality involves updating the National Coal Resources Data System that underlies the COALQUAL database to focus on coal from active mines using analytical techniques with lower detection limits would reduce uncertainty from coal trace element concentrations and allow us to model correlations between concentrations. Second, more systematic efforts to sample coal at power plants would be useful in validating the coal blend models used in this work. Third, the effect of coal cleaning and preparation on trace element removal is another source of uncertainty that should be studied in the future.

Better characterizing trace element partitioning behavior will require well-designed trace element mass balance studies at CFPPs. These studies should sample the coal burned while accounting for the residence time in the flue gas treatment train in order to link measured concentrations in the combustion gasses with actual coal concentrations. Furthermore, sampling should be conducted during periods of plant ramping, shutdown. and partial loading. The difference in operation in these periods may explain some of the discrepancy between modeled and sampled emissions data. Advanced air pollution treatment technologies (i.e., dry sorbent injection, activated carbon injection, and selective catalytic reduction) will impact the removal or arsenic, selenium, and chloride in FGD and particulate matter control systems, but a lack of data forces us to assume these processes have no impact. Knowing the validity of this assumption is important in enabling accurate modeling these processes, something that will be critical as installations have increased and will continue to increase in recent years in response to the Cross State Air Pollution Rule and MATS. Finally, as noted above, a crucial source of error in the FGD system partitioning coefficients is the partitioning between gypsum and the FGD slurry. Filling this gap will assist plants in achieving compliance with the ELGs.

Correlations between the trace element partitioning coefficients in APCDs may exist. Establishing these correlations would require either mechanistic models of trace element behavior in each unit process or a sufficient number of studies that systematically measure multiple trace element partitioning coefficients in identical APCDs, neither of which exist. Future sampling activities are needed to study correlations in trace element partitioning that would inform future analysis using this open-source modeling framework.

1.5 Discussion

This model estimates CFPP trace element mass flow rates in the solid, liquid, and gas phase waste streams using publicly available data for trace element content in coal and partitioning fractions by air pollution control devices from the literature. Our method provides first order estimates of trace element concentrations in coal, mass flow rates, generation normalized mass flow rates, and air emissions to the environment. Despite important limitations to our model, the framework we use has the potential to address policy questions surrounding the impact of regulatory interventions on criteria air pollutants (e.g. PM, SO_2, NO_x) on changes on trace element emissions from CFPPs. For instance, the model could be used to quantify how the shift away from high-sulfur Appalachian coal and towards low-sulfur Powder River Basin coal following the passage of 1990 Clean Air Act Amendments may have also affected trace element mass flows into CFPPs. To answer such questions, general trends derived from first-order estimates are useful.

There are three main limitations. First, the model uses decades-old coal sample data (the most recent publicly available data source for trace element concentrations for in-ground coal in the U.S.). We also assume that the coal blend combusted in the boilers is reflective of recent coal purchases, ignoring any stockpiling of coal on site. Second, the model estimates trace element partitioning within air pollution control devices by generalizing partitioning behavior from data collected at a subset of CFPPs. The model also assumes the partitioning behavior of trace elements is 1) independent of installed pollution control devices upstream and downstream of the modeled device and 2) independent of the order of installed air pollution control devices. Finally, our model does not account for the introduction of trace metals from chemicals used in other plant processes, such as lime used in FGD. These sources of uncertainty may contribute to poor model alignment with existing validation data available from the MATS ICR, ELG rule development process, and the Hg emissions monitoring data reported in CEMS.

Given these limitations, this model is unlikely to be applicable for estimating specific emissions loadings from individual plants. However, it does highlight several important trends that are of relevance to the selection of pollution control technologies at the plant and the design of regulations across the fleet. First, there is a connection between the removal of trace elements from the gas phase and the resulting concentrations in either the liquid or solid phases. For example, we find that particulate matter controls and sulfur dioxide controls divert nearly all Hg, As, and Se from the flue gas into the solid waste stream. Trace element management strategies will maximize human health benefits by considering the ultimate fate of the trace element and the relative ease of long-term sequestration in that phase.

Second, this modeling framework is useful to regulators and policy analysts who are interested in monitoring trace element emissions and their cumulative impacts at the fleet level.[96] This is especially true for trace elements without continuous emissions monitoring and those in the liquid or solid phases. This model can also be useful in understanding broad trends in trace element flow rates in coal and to the gas, solid, liquid phases over the past few decades as coal plants responded to new regulations such as the 1990 Clean Air Act Amendments, the Mercury and Air Toxics Standards, and the Cross-State Air Pollution Rule. Without continuous monitoring data, trace element mass flow rate models are critical for understanding major point source emissions to the environment. Therefore, more effort is required to improve data quality and perform model validation in order to better inform risk assessment and policy design.

2 A bounding analysis of emissions consequences from weaker environmental regulations or from increased use of coal in the U.S.

Abstract: Under the Trump administration various policies have been proposed to increase coal-fueled electricity by either weakening environmental regulations or changing market rules to favor coal. While it is unlikely that a coal resurgence will materialize given other market forces, we explore the potential consequences of such policies on emissions of CO_2 and of pollutants that affect health and the environment (SO_2 and NO_x). We use two bounding scenarios: 1) we assume that environmental regulations are weakened so that coal plants turn off their wet flue gas desulfurization (wFGD) and selective catalytic reduction (SCR) devices and 2) we assume coal electricity becomes cheaper to operate than natural gas and displaces natural gas electricity. We assume no new coal construction and use data from the Environmental Protection Agency to characterize plant emissions. Turning off wFGD and SCR devices leads to SO_2 and NO_x emissions twice to three times the emissions observed in 2017. These emission levels were last observed about 7-10 years ago. A resurgence of coal that would displace natural gas would increase SO_2, NOx, and CO_2 emissions by 41%, 45%, and 21% compared to 2017 levels.

A version of this chapter is in preparation for submission to *Energy Policy* as: **Sun, X., Yang, J., Tong, D., Mauzerall, D., Azevedo, I. L. "Estimating the emissions consequences from increasing the use of coal in the U.S."**

2.1 Introduction

Current federal policy has supported coal electricity by rolling back environmental and climate protections, such as repealing the Stream Protection Rule and the Clean Power Plan. Under the Clean Air Act, the Cross-State Air Pollution Rule (CSAPR) and the Mercury Air Toxics Standards (MATS) are two of the more recent rules promulgated by the Environmental Protection Agency (EPA) which require electric generating units to reduce their sulfur dioxide (SO_2) and nitrogen oxides (NO_x) emissions. These pollutants are precursors of secondary $PM_{2.5}$ (particulate matter smaller than 2.5 microns in diameter). NO_x also reacts with carbon monoxide (CO) and volatile organic compounds (VOCs) to form ground-level ozone (O_3) in the presence of sunlight. CSAPR, implemented in 2015 and the successor to the 2009 Clean Air Interstate Rule (CAIR), allows states to allocate SO_2 and NO_x budgets to electrical generating units to meet the National Ambient Air Quality Standards.[3] CSAPR is currently still in effect.

The 2011 MATS requires coal and oil-fired power plants to reduce emissions of toxic pollutants, such as Hg, and $PM_{2.5}$, including $PM_{2.5}$ precursors such as SO_2 and NO_x, to meet the National Emissions

Standards for Hazardous Air Pollutants.[4] As a result, coal-fired power plants (CFPPs) are required to treat flue gas with wet flue gas desulfurization (wFGD) and selective catalytic reaction (SCR) to protect public health and welfare. SCR and wFGD also improve mercury capture. The SCR system oxidizes mercury, which becomes more water soluble and can then be removed by the wFGD system.[94] These policies decrease the number of premature mortalities in the U.S. by reducing SO_2 and NO_x emissions from CFPPs.[3,4,97,98] While MATS is still in effect, the EPA, at the time of writing, is seeking comments to determine if the MATS should be vacated.[12] If the EPA successfully vacates the rule, it is unclear how SO_2 and NO_x emissions might increase.

The Environmental Protection Agency estimates that the MATS and CSAPR are responsible for net benefits to society on the order of tens to hundreds of billions of dollars annually based on reductions in premature mortalities.[5,99] Furthermore, rollbacks of environmental regulations might impact human health, as Thomson et al. (2018) estimate that if the 2016 coal fleet had the same emissions as in 2007, before CAIR, CSAPR, and MATS, there would be 17,000 to 39,000 more premature mortalities annually.[98]

In September 2017, the Department of Energy proposed the "Grid Resiliency Pricing Rule," which would allow "for the recovery of costs of fuel-secure generation units" by directing the Federal Energy Regulatory Commission (FERC) to "develop and implement market rules that accurately price generation resources necessary to maintain reliability and resiliency."[13] Based on a Department of Energy report on electricity markets and reliability from August 2017, the fuel-secure generation units refer to coal and nuclear units.[100] While allowing cost recovery for nuclear may help reduce greenhouse gas emissions, pushing for coal could displace the use of cleaner energy sources and increase damages to public health, the environment and climate. Shawhan and Picciano argue that if this rule is enacted, then approximately 25 GW of coal capacity may delay retirement causing about 27,000 premature deaths in the U.S. over 25 years due to the increase of criteria air pollutant emissions such as SO_2, NO_x, and $PM_{2.5}$.[14] FERC has rejected the Grid Resiliency Rule,[15] but the push to increase the competitiveness of coal remains a goal of the current administration. If an increase in coal generation materializes, it would most likely displace natural gas generation given that nuclear power operates as base load and is not easily ramped up and down, and renewable electricity will generate regardless of market conditions.

To date, there has been no assessment of which we are aware of the potential damages of coal displacing natural gas, but there is extensive work in the literature that quantifies the benefits of natural gas replacing coal. Using a life-cycle perspective, these studies find that electricity produced using natural gas can lead

to more or less warming than coal depending on whether a 20 year or 100 year global warming potential is used. [25,101,102] Jenner and Lamadrid compare different life cycle analyses and conclude that a transition in the U.S. from coal to shale gas, including accounting for methane leakages, would yield public health benefits and create a smaller greenhouse gas footprint.[103] Lu et al. use an econometric model, which regressed the fraction of electricity generated by coal versus natural gas against the costs of generating coal relative to costs of generating natural gas and natural gas capacity. The authors find that fuel switching prompted by low natural gas prices, without accounting for methane leakages, reduced the greenhouse gas emissions of the U.S. electricity sector by 4% in 2008.[104] Potential coal plant retirements in unstructured electricity markets can reduce life-cycle greenhouse gas emissions by at most 4% while SO_2 and NO_x emissions can decrease by up to 30%.[105] Lastly, Lueken et al. find that if all coal in the U.S. had been replaced by natural gas in 2016 the human health benefits would have been valued at $20-$50 billion annually.[106]

In this chapter, we estimate the potential emissions of reactive pollutants and carbon dioxide (CO_2) under two bounding scenarios: 1) our first scenario assumes that environmental regulations are repealed or enforcement of those regulations are weakened so that coal plants can turn off their wFGD and SCR devices (and thus reducing their operational costs) and 2) our second scenario assumes that coal electricity becomes cheaper to operate than natural gas and displaces natural gas electricity (we are agnostic on whether this would be due to a policy intervention or market forces as our focus is to understand the emissions consequences).

The first scenario assumes that if there is a roll back of environmental regulations or if enforcement weakens, CFPPs may consider ceasing operations of their air emission controls to reduce their operating costs. It is worth noting that turning off SCR would mean not injecting the equipment with ammonia reagent but over time, the acidic flue gas will damage the catalysts. Turning off wFGD equipment would function by redirecting emissions to an air vent, which is accomplished by changing the operation of the fans. We choose wFGD and SCR as the focus of our analysis because they treat the largest share of coal generation in the U.S.[87] If in fact this scenario was to materialize, CFPPs operating costs would likely be lower, which in turn would shift coal further to the left in the merit order dispatch (an ordering of the generators used to meet demand from cheapest to most expensive operating costs). This would increase coal generation even further. However, for simplicity, we ignore that effect.

The second scenario focuses on a situation where coal would become competitive to operate when compared to natural gas. This situation could arise if market prices are altered to favor coal with policies similar to the Grid Resiliency Rule.[13] While we are fully aware that the extreme scenarios we are showing

are unlikely to materialize, this research can inform policy makers on the value of keeping current policies in place.

The rest of the chapter is organized as follows: in section 2.2, we provide the data and methods and in section 3 we provide our results. In section 2.3, we start by presenting the estimates of current CO_2, NO_x, and SO_2 emissions from the U.S. electricity sector, which provide the emissions baseline to which we will compare our two bounding scenarios. We then provide the emissions estimates for CO_2, NO_x, and SO_2 for our two scenarios. In section 2.4, we conclude and discuss policy implications.

2.2 Data and Methods

The baseline and scenario assumptions are shown in Table 2.1. For all cases, we assume the 2017 electricity generation fleet and that changes occur overnight. In all cases, we include the SO_2, NO_x, and CO_2 emissions.

Table 2.1: Overview of the baseline and scenarios considered in this work.

Baseline	U.S. electricity sector SO_2, NO_x, and CO_2 emissions observed in 2017.
Air pollution rollbacks	U.S. electricity sector SO_2, NO_x, and CO_2 emissions in 2017 if coal plants were to turn off their wFGD and SCR equipment.
Increase in coal generation	U.S. electricity sector SO_2, NO_x, and CO_2 emissions in 2017 if coal electricity were to displace natural gas electricity in each Emissions & Generation Resource Integrated Database (eGRID) sub-region.

Estimating base case emissions: We use hourly SO_2, NO_x, and CO_2 emissions, generation, and heat input in 2017 from each boiler from all coal and natural gas power plants with capacities greater than 25 MW from the Environmental Protection Agency Continuous Emissions Monitoring System (CEMS).[85] This data source is used to establish baseline emissions and annual generation. We also compute the hourly emissions intensity for each pollutant using the emissions and generation data from CEMS. The CEMS data includes some misreported entries, which we remove from our dataset. Specifically, we remove any boilers from our dataset that: (i) have a positive gross generation and a positive heat input, but report zero emissions for any pollutant; (ii) report zero or missing gross generation, zero or missing heat input, and nonzero emissions for any pollutant; and (iii) report positive gross generation, positive heat input, but have an emission factor less than 300 kg CO_2/MWh (because most efficient, state-of-the-art natural gas combined cycle generators have an emission factor of 300 kg CO_2/MWh).[106] We then present the annual emissions of each pollutant by region, using eGRID sub-regions as our geographical boundaries. The eGRID sub-regions are 26 regions of the U.S. defined by the EPA to mimic the regional transmission

organizations and the independent system operators across the U.S (in the SI, section 1, we provide a map of the 26 eGRID sub-regions).[107]

We combine CEMS, Energy Information Administration (EIA), and eGRID datasets at the plant level. EIA data provides the capacity at the plant level and eGRID data identifies the eGRID sub-region of each plant. We include only plants that are present in all three datasets. Our final dataset includes 855 natural gas and 280 coal plants with a total capacity of 435 GW and 296 GW, respectively, and total gross generation of 1050 TWh and 1250 TWh, respectively. These numbers correspond to 83% and 106% of the total gas and coal capacity,[31] and 90% and 98% of the U.S. electricity gross generation from natural gas and coal, respectively. We overrepresent coal capacity in this work because we identify capacity at the plant level, so plants with multiple boilers that use different fuel sources, such as coal and natural gas, are incorporated as a single fuel source based on the fuel source with the highest head input, which is the method also used in eGRID.[108] Furthermore, it corresponds to 62% of U.S. total generation capacity and 57% of total electricity generation.

Estimating the emissions consequences of air pollution control rollbacks: We simulate the emissions that would occur if wFGD and/or a SCR device ceased to operate as follows: for each boiler *b* with a wFGD and/or a SCR device installed downstream, we assume the hourly emissions at hour *h* would be:

$$emissions_{b,p,h}^{air\ pollution\ rollbacks} = \frac{emissions_{b,p,h}^{baseline}}{1-removal_{a,p}} \quad (4)$$

Where *a* is the air pollution control device and *p* is the pollutant. The combination of *a* and *p* represent either a SCR device for NO_x removal or a wFGD device for SO_2 removal. From the literature, we find that air pollution control removal efficiencies by SCR is 70-90% for NOx emissions, and by wFGD is 80-98% for SO_2 emissions.[109,110] We assume a baseline removal of 80% for SCR and 90% for wFGD, and test the effect of these assumptions in our sensitivity analysis in Appendix B.1. The wFGD does not remove any NO_x and the SCR does not remove any SO_2, so we can treat those two removal rates independently.

Estimating the effect of an increase in coal generation: For each eGRID subregion, we calculate the total hourly unused coal generation, in MWh, against hourly observed natural gas generation, and we assume that the generation would be provided by coal instead of natural gas. In instances where the hourly available unused coal capacity is larger than natural gas generation, we assumed that the electricity generated by natural gas plants would be fully displaced. If there is not enough coal capacity to fully substitute natural gas generation, we assume that the difference is still met by natural gas. We displace

natural gas generation equally across natural gas power plants and we replace them with the coal plants from lowest to highest SO_2 emissions intensity. This strategy provides us with a lower bound regarding the emissions that would be induced by coal. We assume that the capacity factor of each coal plant used to displace natural gas would increase from the actual observed value to a maximum of 90% (we do not use 100% to be more conservative and account for the fact that plants may need maintenance or other operations that require the plant to be offline temporarily). Lastly, we split the generation increase at each plant proportionally across all boilers, which assumes that power plants will operate more active boilers before operating less active, and potentially less efficient boilers. This strategy is used for each eGRID sub-region separately to account for the fact that coal plants would replace natural gas plants within the same region of operation. We assume that trade would not occur between regions.

Since this calculation requires capacity data from EIA, which are linked to CEMS at the plant level and not the boiler level, we also identify the fuel type of each plant (i.e., the primary fuel with the largest heat input into the plant in 2017 – this is the method used in eGRID).[108]

We estimate the hourly emissions induced or avoided by each coal or natural gas boiler by multiplying generation by the respective boiler's emissions factor. If a coal boiler does not report an hourly emission factor (because it is offline at that hour), we use one of the following emission factors:

- If the boiler was operating sometime in that month, we use the that month's average emission factor from CEMS.
- If the boiler was not operating in that month, we use the boiler's annual average emission factor from CEMS.
- Otherwise we use the plant's average annual emission factor.

We note that we find significant variations in the hourly emission factors for coal and natural gas plants, as shown in Appendix B.2.

Natural gas combined cycle (NGCC) boilers do not necessarily report gross generation from both steam and combustion turbines. This missing data raises an issue on emissions allocation for these units. We mark all NGCC boilers that report generation from the combustion turbine but not the steam turbine by analyzing the ratio of EIA net generation to CEMS gross generation. If the ratio of EIA net generation to CEMS gross generation for an NGCC boiler is much greater than 1, we assume that boiler does not report total gross generation and we scale their generation up by the combustion plus steam generation to combustion generation ratio, which we calculate using EIA generator data.[88] There are 63 NGCC plants (out of 514 total NGCC plants in the dataset) that misreport generation.

There are also non-NGCC plants that report generation from only a subset of their boilers. We treat these plants using a method similar to our treatment of NGCC plants. There are 40 non-NGCC plants that misreport generation out of 855 natural gas plants in our dataset.

2.3 Results

In Figure 2.1, we show the observed SO_2, NO_x and CO_2 emissions in each eGRID sub-region in 2017 (See Appendix B.3 for a map of the eGRID sub-regions). Nationwide emissions from the U.S. power sector were 1.2 million metric tons SO_2, 0.9 million metric tons NOx, and 1.6 billion metric tons CO_2. For context, total CO_2 emissions from energy consumption in the U.S. is 5.1 billion metric tons.[111] The sub-regions with the largest SO_2, NO_x, and CO_2 emissions are sub-regions with relatively high proportions of coal plants (ERCT, MROW, RFCW, SPSO, and the SRMW). These sub-regions are predominantly in the Midwest and in the south. Our 2017 estimates match those reported annually by CEMS.

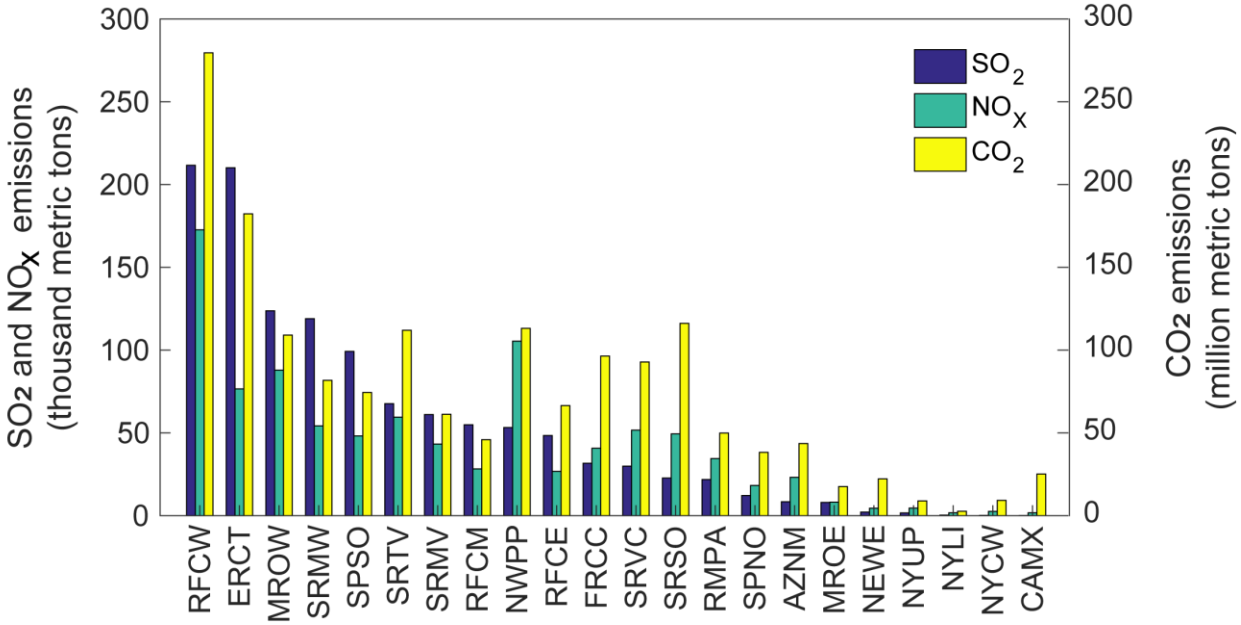

Figure 2.1: Observed 2017 emissions for each eGRID sub-region for SO_2 (blue), NO_x (green), and CO_2 (yellow). See Figure 2.3 or Appendix B.3 for a map of the eGRID sub-regions.

In Figure 2.2, we show the annual SO_2, NO_x, and CO_2 emissions emitted by the U.S. electricity sector for each scenario. We find that environmental air pollution control rollbacks for the power sector that would lead to turning off wFGD and SCR equipment would lead to annual emissions of SO_2 and NO_x of about 4 million metric tons and 2 million metric tons, respectively. These emissions levels would correspond to triple the observed levels of SO_2 emissions and double the observed levels of NOx emissions. These emissions levels were last observed in 2008-2011,[31] when coal constituted 42-48% of the U.S. electricity

fuel mix[112], and, according to 2010 CEMS data, when only 137 and 133 coal plants reported a unit with wFGD and SCR installed, respectively, out of a total of 484 coal plants.[85] CO_2 emissions do not change from the historically observed emissions as we neglect the energy benefit of turning off air emission controls.

Finally, we also estimate the emissions associated with increasing coal use in electricity generation (while assuming that the wFGDs and SCRs, if installed, would continue to operate). We find that in this case, the emissions would be 1.7 million metric tons for SO_2, 1.4 million metric tons for NOx, and 2 billion metric tons for CO_2. This translates to an increase of more than 40% from observed values for SO_2 and NO_x and a 20% increase in CO_2 emissions. The emission increases in this scenario are smaller than the wFGD and SCR scenario, in part, because there is not enough coal to displace all the natural gas at the eGRID sub-region level, and because several of the plants have wFGDs and SCRs that lower the emissions of SO_2 and NOx. We find that coal plants would be able to displace between 16% (in NEWE) and 100% (in SRMW) of natural gas generation in eGRID sub-regions (See Appendix B.4 for analysis). The total natural gas generation displaced is 551 TWh, which is 45% of total natural gas generation in 2017. In 2017, coal boilers combusted 540 teratons of coal to generate 1250 TWh of electricity.[88] Assuming a 551 TWh increase in coal generation, then an additional 238 teratons of coal would be needed to meet the electricity increase.

We also highlight that in this scenario air pollution control technologies continue to operate as usual: if plants did not use emission controls, the emissions would be higher. Emissions may also increase if we changed the dispatch order instead of increasing the capacity of coal plants with the lowest SO_2 emission factors first. In Appendix B.5, we perform a back of envelop estimate of emission increases using the average eGRID sub-region SO_2, NO_x, and CO_2 emission factor for coal and natural gas plants. We find an additional 1% increase in SO_2 emissions and a 12% and 3% decrease in NO_x and CO_2 emissions respectively, suggesting that plants with low SO_2 emission factors do not necessarily have low NO_x and CO_2 emission factors. The emission levels in this scenario were last observed in 2014-2015.[31] The fuel mix in 2014-2015 was 33-39% coal and 28-33% natural gas.

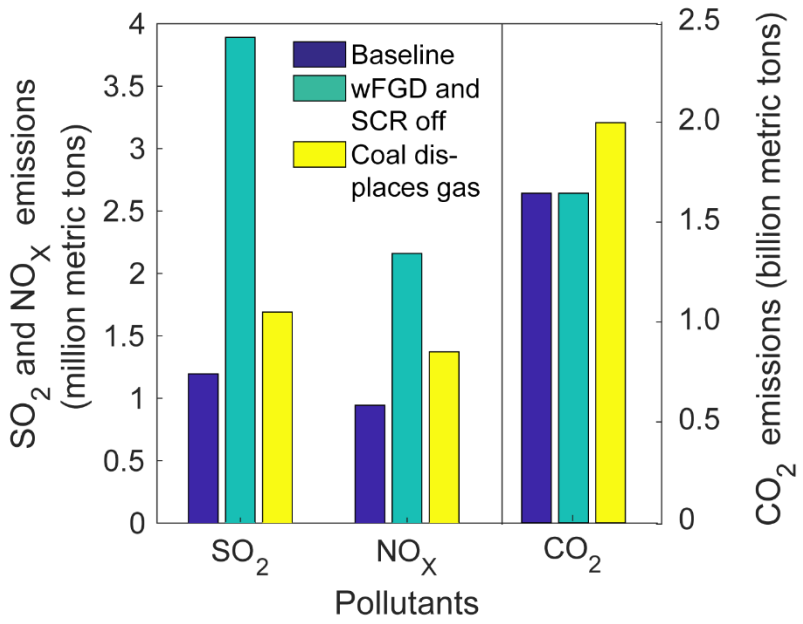

Figure 2.2: SO_2, NO_x and CO_2 emissions in the U.S. electricity sector. The blue bar corresponds to the observed emissions in 2017, the teal bar represents the scenario where wFGD and SCR devices are turned off at coal plants, and the yellow bar represents the scenario where coal generation displaces natural gas generation.

Figure 2.3 shows the change in emissions in each eGRID sub-region for our two scenarios, when compared with the baseline emissions. The largest SO_2 emission increases occur in SRMP, where emissions increase by 550% in the scenario where environmental regulations are relaxed, and by 900% in NYUP in the scenario where coal use displaces gas. Four coal plants in NYUP have among the highest emission factors across all sub-regions, averaging 2.2 kg SO_2/MWh and 1.0 kg NO_x/MWh (See Appendix B.6 for plant-level emission factors of the coal and natural gas fleet across the entire U.S. and the eGRID sub-regions). Furthermore, 40% of NYUP's natural gas generation is displaced in the scenario where coal generation is increased, leading to an 8-fold increase in coal generation.

In the scenario where coal displaces natural gas, all sub-regions but NEWE and RFCE see an increase in their coal generation by up to 110% from what was observed in 2017 (See Appendix B.4 for CFPP capacity and generation level in each eGRID subregion in 2017).

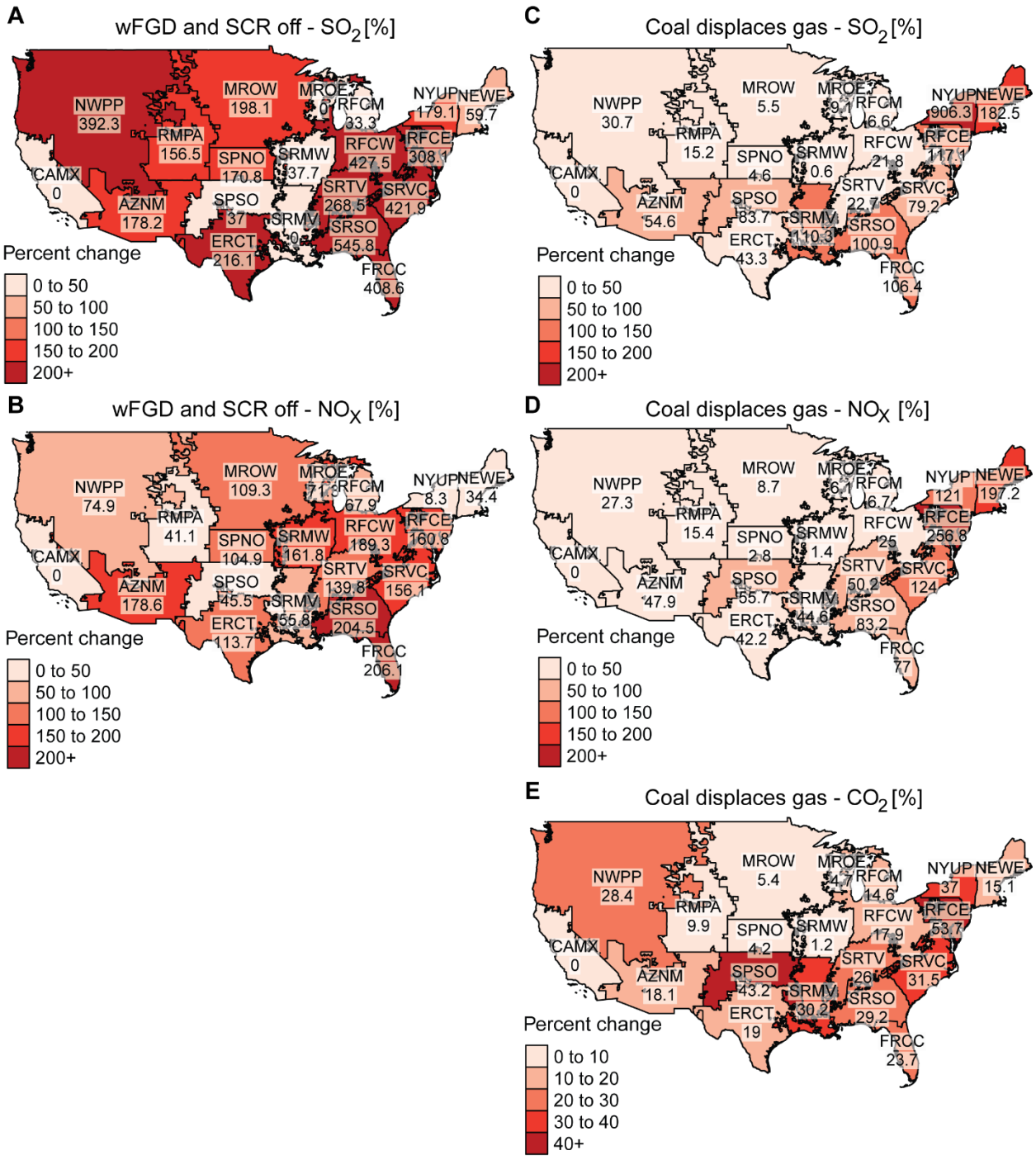

Figure 2.3: Increase in pollutant emissions from the baseline resulting from turning off wFGD and SCR devices at coal boilers (A-B) and by coal generation displacing natural gas generation (C-E). Results are expressed as a percentage of the baseline for SO_2 (A&C), NO_x (B&D) and CO_2 (E). NYCW and NYLI eGRID sub-regions are excluded because those sub-regions have zero coal plants in our dataset. wFGD and SCR – CO_2 plot is excluded because wFGD and SCR do not affect CO_2 emissions.

The emission increases are important to consider at the state level, given that state level policies are still in effect even if policies favoring coal are implemented at the federal level. In Table 2.2, we show the SO_2 and NO_x emissions budget mandated by the Cross State Air Pollution Rule that the federal government requires states to have state implementation plans to meet.[99] Of the 23 states with emission budgets, 13 states will have emissions greater than the budget for at least one pollutant when wFGD and SCR devices are turned off and 6 states will have emissions greater than the budget for at least one pollutant when coal displaces natural gas. Because the state implementation plans are executed at the state level, it is unlikely that states will allow emissions to exceed their states' budget. Therefore, the emission budgets listed in Table 2.2 could set a limit of how much emissions could potentially increase. In Appendix B.7, we show the emission increases for the two scenarios at the state level relative to the baseline.

Table 2.2: SO_2 and NO_x emissions compared to the 2017 state-level budget allocated by the Cross-State Air Pollution Rule when wFGD and SCR devices are turned off at coal plants and coal displaces natural gas.[99] In red are emissions that exceed the 2017 budget.

	SO2 (thousand metric tons)			NOx (thousand metric tons)		
State	2017 Budget	wFGD and SCR off	Coal displaces natural gas	2017 Budget	wFGD and SCR off	Coal displaces natural gas
Alabama	194	60	16	65	54	34
Georgia	123	85	28	49	84	55
Illinois	113	72	40	44	46	20
Indiana	151	250	66	99	166	74
Iowa	68	36	30	34	49	23
Kansas	38	24	5	29	26	12
Kentucky	97	212	63	70	107	55
Maryland	26	24	45	15	8	58
Michigan	131	78	63	57	50	33
Minnesota	38	40	13	27	17	17
Missouri	151	146	99	44	114	46
Nebraska	62	46	47	27	39	19
New Jersey	5	2	3	7	6	6
New York	25	5	18	20	9	15
North Carolina	52	109	31	38	91	57
Ohio	129	505	96	82	158	58
Pennsylvania	102	291	79	108	84	45
South Carolina	88	38	17	30	29	42
Tennessee	53	62	44	18	48	33
Texas	268	705	374	125	204	132
Virginia	32	13	7	30	16	20

West Virginia	69	204	55	50	103	48
Wisconsin	44	17	16	30	39	23

In Figure 2.4, we show the historical emissions for CO_2, SO_2, and NO_x and compare them with our scenarios. Historical emissions have been steadily decreasing over time due to technological advances, market and regulatory conditions. The levels of emissions of SO_2 and NO_x expected if wFGD and SCR devices are turned off were last observed in 2011 and 2008, respectively, suggesting that weakening of enforcement of existing environmental policies could potentially undo 7-10 years of air pollutant emission reductions and technological improvements.

On the other hand, the increased use of coal would lead to SO_2, NO_x, and CO_2 emissions that were last observed in 2015, 2014, and 2014 respectively, and thus have relatively modest impacts, suggesting that coal-favored policies which promote fuel switching would move us backwards in terms of air quality less than the weakening of emission standards or enforcement. If a push towards the increased use of coal were successful, it would have adverse impacts on health, but the magnitude of damages would be constrained by the operation of wFGD and SCR equipment at coal plants and the decrease in available coal capacity caused by coal plant retirements. For example, in 2008, net summer capacity for coal was 313 GW and dropped to 267 GW by 2016, while during the same time period, net summer capacity for natural gas plants increased from 397 GW to 447 GW.[31] The generation mix showed similar changes with coal decreasing from 48% to 30% and natural gas increasing from 24% to 34% from 2008-2016.[31] Even if there was enough coal to displace all 1050 TWh of natural gas generation in 2017, assuming 0.9 kg SO_2/MWh, which is the SO_2 emission factor of the coal fleet in our dataset, SO_2 emissions would increase by 964 thousand metric tons. These emission increases would result in approximately an 80% increase from the baseline, or an additional 40% increase from the coal displacing natural gas scenario.

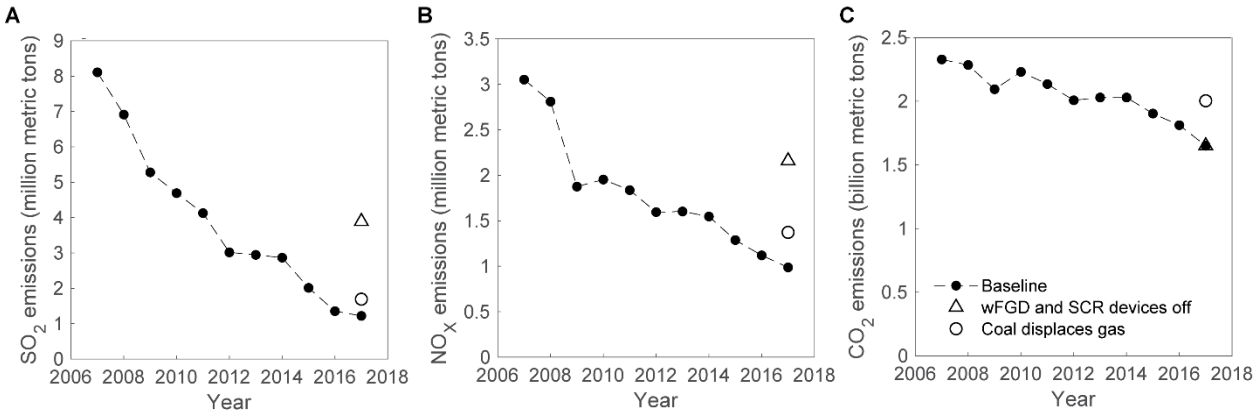

Figure 2.4: Annual A) SO_2, B) NO_x, and C) CO_2 emissions from 2007-2016 for scenarios: baseline, air pollution rollbacks, and coal displace natural gas generation.

2.4 Conclusions and Policy Implications

In this paper, we estimate the potential emissions' consequences of coal-favored energy policies in the U.S. We utilize two bounding scenarios to encapsulate two different types of energy policies, one which weakens environmental regulations and one which makes coal more economically viable so that the electricity sector switches from natural gas to coal. Weakening environmental air pollution regulations or enforcement of coal electricity can increase SO_2 and NO_x emissions up to 2-3 times more than the national baseline emissions without affecting CO_2 emissions. Coal displacing natural gas can increase SO_2 and NO_x emissions by 40-50% and CO_2 emissions by 21%.

Generally, we find that policies that weaken environmental regulations or enforcement result in larger emission increases than policies that motivate more coal generation. However, some eGRID sub-regions, especially those in the northeast, face larger emission increases from increased coal generation than weakened environmental regulations. Additionally, there is significant spatial variability in emission increases resulting from each type of coal-favoring policy. This variation introduces spatial inequities as some eGRID sub-regions may suffer greater adverse human health impacts than other sub-regions.

To avoid these emission increases and their health and climate consequences, federal decision makers, such as EPA and FERC, need to continue to enforce environmental regulations and prevent changes to the electricity market price structures in ways which benefit coal-fired power plants for electricity generation. Either policy directive has the potential to undo years of emission reductions and weaken the electricity sector's ability to decarbonize. Though different coal-favored policies have been proposed over the last two years, few of them have been approved. Thus, we acknowledge that it is highly unlikely for the scenarios proposed in this work to fully come to pass. Turning off wFGD and SCR devices would require the federal government to stop enforcing the Clean Air Act and for states to ignore their own rules. Coal

will not displace natural gas unless natural gas becomes more expensive than coal. States, under the Cross-State Air Pollution Rule, are also required to not exceed the SO_2 and NO_x emissions budget that EPA allocated. There are several states where emissions resulting from either turning off wFGD and SCR devices or from coal displacing natural gas would exceed these budgets. However, if federal requirements change so that states no longer must enforce these budgets, then states may choose to weaken their enforcement. At the time of writing, we find that states do not have ambient air pollution standards or air pollution rules that would stay in effect if the Clean Air Act is not enforced, except for California, which has its own Ambient Air Quality Standards with emission stringencies comparable to the National Ambient Air Quality Standards.[113] We believe that it is important to investigate the potential emission outcomes of energy policies that favor coal over other fuels, especially natural gas.

Additionally, power plants may see minor economic benefits if they turn off the wFGD and SCR devices. By turning off these control devices, power plants can save operational costs on purchasing reagents and increase overall efficiency by turning off auxiliary processes and leaving only the fans necessary to draw the flue gas out of the equipment. Based off of an example 500 MW plant, turning off auxiliary wFGD processes, such as dewatering, reagent prep, and pumps, overall plant efficiency can be increased by 1%,[114] but it is not clear how significant the efficiency gains would be from turning off a SCR device. Turning off the SCR also poisons the catalyst layers, which could be a significant cost.[114] Catalysts need to be replaced once every three years,[114] so a power plant may wait until the end of the catalyst's lifetime to turn off the control.

One limitation of our methods is the lack of unit-level capacity data in CEMS, which meant fuel types had to be determined at the plant level instead of the unit level. Therefore, power plants with boilers of mixed fuel types had to be reduced to a single fuel type. In our dataset, 143 natural gas boilers or 5% of boilers are incorporated into coal plants. In the coal displacing natural gas scenario, because coal plants with lower SO_2 emission factors are selected to increase generation first, actual emissions may be higher than simulated due to this modeling preference.

Further inquiries into coal-favoring energy policies can also a more incremental approach that estimates emission increases as individual air pollution regulations, such as the MATS rule, are undone or the marginal price of coal electricity decreases. Further study should also estimate and monetize the human health and climate impacts of potential emission increases from possible changes to existing environmental regulations, enforcement, and possible increases in coal power generation to fully understand the potential ramifications of these policies. Such studies can also analyze how damages vary across space and whether the spatial variation observed in this work leads to inequities. These

characterizations can help articulate the need to transition from more harmful forms of energy to a cleaner energy future.

3 Land use and ecological impacts of deep decarbonization of Pennsylvania's electricity sector

Abstract: The Pennsylvania Department of Environmental Protection aims to reduce greenhouse gas emissions from Pennsylvania to 20% of 2005 levels by 2050. A deep decarbonization is crucial for mitigating the effects of climate change, but the infrastructure required to implement deep decarbonization can also create significant land and forest impacts, which in turn may disrupt habitats and negatively impact the ecology. In this work, we model a variety of pathways to deep decarbonize Pennsylvania's electricity sector, quantify the land and forest land use from these pathways, and estimate potential ecological impacts using fragmentation indices. If carbon capture and sequestration is not used, Pennsylvania would need to replace all coal and retiring nuclear generation with renewables, which constitutes 64% of the fuel mix. Even if all the coal plants retire, the emissions from current natural gas plants exceed the decarbonization goals, suggesting that natural gas cannot be a bridge fuel. If only wind is built, the total land use is 13,300 km^2 (Pennsylvania is 119,000 km^2), with direct land use and forest land use impacts of 520 km^2 and 370 km^2, respectively. Solar farms are constructed across Pennsylvania, as there is insufficient land in the southeast where resources are highest, impacting 2400 km^2 of forested land. As such, solar contributes to a greater loss of landscape than wind, but wind requires significantly more land allocated to deep decarbonize the PA electricity sector. Carbon capture and sequestration can play an important role in deep decarbonization by reducing renewables penetration and reducing land impacts by up to half.

A version of this chapter is in preparation for submission to *Environmental Science and Technology* as: **Sun, X., Griffin, M.; Azevedo, I. L. "Land use and ecological impacts of deep decarbonization of Pennsylvania's electricity sector."**

3.1 Introduction

Pennsylvania (PA) accounts for 4.6% of CO_2 emissions from electricity across all U.S. states, fourth amongst all states.[115] In 2018, PA's Department of Environmental Protection announced plans to reduce all greenhouse gas emissions emitted in PA to 20% of 2005 levels by 2050,[22] which aligns with previous 2016 U.S. mid-century deep decarbonization strategy.[21] Timely deep decarbonization can reduce the severity of climate change impacts, such as more frequent and intense heat waves, droughts, extreme weather events, and disrupted ecosystems.[21]

Deep decarbonization of the electricity sector requires significant changes to the fuel mix. Although PA has yet to focus on deep decarbonization research, previous deep decarbonization assessments for the U.S. find that the electricity sector needs an assortment of conservation, wind, solar, nuclear, and carbon capture and sequestration (CCS), while constraining fossil fuels to about 20% of the fuel mix.[25–30] State-level deep decarbonization analyses focus primarily on California, where demand-supply models and capacity expansion models find that fossil fuel needs to be less than 10% of the fuel mix to reduce CO_2 emissions to less than 80% of 1990 levels.[116–118] As such, PA may need to make drastic changes to their fuel mix considering the 2016 fuel mix is 25% coal and 32% natural gas.[88] Also, 39% of PA's fuel mix is nuclear, all of which may retire by 2050 given that the plants are approaching the end of their useful life and up for relicensing by 2049.[119]

Deep decarbonization in PA could result in significant land use change due to infrastructure required for renewable capacity increases, transmission for new electricity production, and pipelines for CCS.[32–37] Various studies examining U.S. deep decarbonization with high renewables use find that 6,000 km^2 to 90,000 km^2 land can be impacted, where the range depends on CO_2 emissions or renewable penetration goals, technologies utilized, and the assumed land use factors.[24,120–123] Renewables use and associated land use change are known to have adverse effects on wildlife via forest fragmentation and habitat disruption.[32,34,38–40] Therefore, these impacts should be quantified to understand potential impacts and inform policy makers of the strategies that could meet decarbonization goals and minimize ecosystem impacts.

In this chapter, we define potential pathways to reduce CO_2 emissions by 80% of 2005 levels by 2050 for the PA electricity sector, quantify the land-use and forested land-use requirements, and measure forest fragmentation metrics of several potential pathways. We discuss the impact and tradeoffs of PA deep decarbonization.

3.2 Data and Methods

Deep decarbonization pathways: We assume electricity generation in 2050 is the same as in 2016 because electricity generation in PA has not changed significantly over the last ten years (See Appendix C.1, where we show the PA electricity generation since 2001).[124] We assume PA will not electrify the transportation sector by 2050. We estimate the CO_2 emissions from each fuel source by multiplying the CO_2 emissions factor by the electricity generated by that fuel type. Table 3.1 shows the CO_2 emission factors we assume for this analysis and the source of those emission factors. Generation produced by fuel type in PA is from EIA.[115]

Table 3.1: CO_2 emission factors by fossil fuel type with the source of each emission factor.

Fuel category	CO_2 emission factor (kg/MWh)	Source
Coal	1000	Schivley et al.[125]
Natural Gas	414	Schivley et al.[125]
State-of-the-art Natural Gas Combined Cycle (NGCC)	300	Lueken et al.[106]

We assume CCS reduces CO_2 emissions from coal and natural gas plants by 90%, which is the assumed CCS efficiency used in other theoretical studies.[126] We also assume that all of PA's nuclear power plants retire by 2050 and replaced by renewables since they will be up for relicensing by 2049.[119]

We identify five scenarios that deep decarbonize the PA electricity sector. Those scenarios are given in Table 3.2.

Table 3.2: Description of the baseline and the five deep decarbonization scenarios examined for the land and forested land impacts analysis along with the number of farms and the amount of installed capacity needed to deep decarbonize. In Scenarios 1-5, we install CCS and replace natural gas with state of the art NGCC until power plants reduce 80% of 2005 CO_2 emissions.

Scenario	Description	Farms needed to deep decarbonize	Capacity needed to deep decarbonize (GW)
0. Baseline	Current 2016 fuel mix and demand in Pennsylvania	-	-
1. Wind and CCS	Wind replaces all electricity generated by nuclear in 2016 and CCS is installed on coal and natural gas plants.	451	31.6
2. Wind only	Wind replaces all electricity generated by coal and nuclear in 2016. Existing natural plants are retrofitted with state of the art NGCC.	832	52.2
3. Solar and CCS	Solar replaces all electricity generated by nuclear in 2016 (83 TWh) and CCS is installed on coal and natural gas plants.	3053	61.1
4. Solar only	Solar replaces all electricity generated by coal and nuclear in 2016 (137 TWh). Existing natural gas plants are retrofitted with state of the art NGCC	5145	102.9
5. Solar, wind, and CCS	CCS, solar, and wind each reduce PA carbon dioxide emissions by a third of 80% of 2005 levels. Solar and wind replaces electricity generated by nuclear plants first and then coal plants in 2016.	342 (wind) 1974 (solar)	20.3 (wind) 39.5 (solar)

Land and forested land use of different pathways to deep decarbonize: We estimate land use change and forest fragmentation for the five different deep decarbonization pathways given in Table 3.2.

Impacts from CCS: If a plant installs CCS, the plant needs to transport and inject the CO_2 underground into an appropriate reservoir for storage. We assume plants with CCS construct pipelines with a 40 m right-of-way, which is the same right of way for transmission lines, to the boundary of the nearest saline formation. Pipeline construction could clear forests and cause forest fragmentation, but plants that sit directly above a reservoir can inject CO_2 underground into the reservoir, which minimizes impact. We assume each plant site has sufficient storage, since actual storage capacity of the reservoir is dependent on-site characteristics that can only be assessed in person. The National Energy Technology Laboratory provide saline reservoir maps which were developed to determine CCS storage capacity.[127]

Impacts from solar and wind farms: In Appendix C.2 we provide all the data sources used to estimate land and forested land impacts. We identify forested and non-forested land using the 2011 National Land Cover Database, which contains land use type at 30m x 30m resolution. We then exclude land where solar and wind cannot be built, such as urban areas, roads, bodies of water etc. (In Appendix C.2, we list the exclusion criteria used in the analysis).

We assume all wind and solar farms are built on land with the highest renewable resource first. For solar, we estimate the generation of solar panels using National Renewable Energy Laboratory's PVWatts, which estimates generation of a solar panel given its capacity and coordinates.[128] Each solar farm is a utility-scale solar farm with 20 MW built with fixed, open rack arrays. We do not build rooftop solar farms. In Appendix C.3, we show a distribution of solar farm capacity across the U.S. and find that there are 293 out of a total of 2306 solar farms with capacity equal or greater than 18 MW. Each solar farm is built on an 800 m x 800 m grid cell, so that each solar farm has a land impact factor of 28 MW/km^2. For comparison, NREL estimates the fixed, open rack solar farms built before 2013 had an median impact factor of 33 MW/km^2.[129]

We estimate the generation from wind farms by converting wind speeds to generation (see Appendix C.4). The National Renewable Energy Laboratory's mid-Atlantic wind resource maps provide the wind class at 1/4 degree latitude and 1/3 degree longitude resolution.[130] We build wind farms on a 4 km x 4 km grid and build the highest possible capacity with the wind available at each grid cell. We make this assumption because wind developers would attempt to maximize the capacity they can build and so that we can present a more conservative estimate of land use and forested land use. According to an NREL analysis of wind projects built prior to 2009, capacity density wind farms range from 1.0 to 11.2 MW/km^2 with an median land impact factor of 3.4 MW/km^2.[131] At the highest wind class, a 128 MW wind farm

can be built, which has a capacity density factor of 8.0 MW/km^2. In Appendix C.3, we show the distribution of wind farm capacity in the U.S. and find that at least 100 existing projects have a capacity of at least 128 MW. To convert capacity to generation, we assume each wind farm has a capacity factor of 0.3.

New renewable capacity creates two types of impacts: indirect and direct. Indirect impacts are land impacts created by spacing turbines for optimal operation or to enclose solar farms within their boundaries.[129,131] Although indirect impacts do not convert land from one purpose to another, they need to be tracked for permitting reasons. Direct impacts are impacts created by conversion of land, such as roads and infrastructure for power generation. The direct impacts of wind farms can be either permanent or temporary. Permanent impacts are caused by the turbine pad and access roads and temporary impacts are caused by temporary roads and storage space used during construction. Land impacted temporarily is expected to recover after a few years.[131] According to NREL, the median permanent direct land use factor of wind is 0.2 hectares/MW and temporary direct land use factor of wind is 0.5 hectares/MW (1 km^2 = 100 hectares).[131] The direct impact of solar farms are always permanent. The median direct land use factor of solar is 2.4 hectares/MW.[129]

For each wind and solar farm constructed, we assume a transmission line is built from the center of the farm to either the nearest transmission substation or the nearest newly constructed solar or wind farm. We assume each transmission line requires a right of way of 40 m.[132]

We perform a sensitivity analysis of the total area and the direct area for wind only and solar only scenarios. We fix the capacity and recalculate the total and direct area using the area-per-capacity impact factor of every farm reported in the appendices of the NREL land impact analyses for wind and solar.[129,131] For solar, out of 192 solar farms, we find the total land factor use varied from 1.2-7.0 hectares/MW and the direct impact factor varied from 0.9-4.9 hectares/MW. The median total and direct land use factors are 3.2 hectares/MW and 2.4 hectares/MW, respectively. For wind, out of 192 wind farms, the total impact factor ranged from 4.3-228 hectares/MW with a median of 29 ha/MW. The direct impact factor of wind ranged from 0.1-5.7 hectares/MW with a median of 0.7 ha/MW.

Fragmentation Analysis: We use three fragmentation indices to analyze the potential ecological impact of the deep decarbonization scenarios. The fragmentation indices are Number of Core Patches (NCP), the Percent of Habitat Available in the Landscape (PLAND) relative to the total baseline land, defined as $PLAND_{total}$, and the PLAND relative to the forested baseline land, defined as $PLAND_{forest}$. The NCP is the number of patches greater than 4 ha that are greater than a 100 m from a non-forest opening.[35] For the

NCP, we buffered each solar and wind project by the radius of the grid cell plus an additional 100 m to account for edge effects. Therefore, we buffered solar farms by 450 m, wind farms by 2100 m, and transmission lines by 140 m. All land within the buffer are removed.

We define the PLAND in equations 1 and 2:

$$PLAND_{land} = \frac{land_{scenario}}{land_{baseline}} \quad (1)$$

$$PLAND_{forest} = \frac{forest_{scenario}}{forest_{baseline}} \quad (2)$$

Where the $land_{baseline}$ and $forest_{baseline}$ are the land and forested land area in PA without manmade infrastructure, respectively. We remove manmade infrastructure because new infrastructure could not be built over existing infrastructure and habitats of interest exist outside of land occupied by manmade infrastructure. Land excluded is specified in Appendix C.2. The $land_{scenario}$ and $forest_{scenario}$ are the land and forested land area of a given scenario after removing direct impacts, respectively. These definitions of $PLAND_{land}$ and $PLAND_{forest}$ differentiate generic land use impacts from forested land use impacts.

These metrics serve as a proxy to understand the ecological damages caused by the land-use change from the various deep decarbonization scenarios. The specific impacts on species, habitat, and mobility will require on-site impact assessments.

3.3 Results

Deep decarbonization pathway analysis to create the scenario suite: If the PA electricity sector emits 24 million metric tons CO_2 by 2050, then it will reduce CO_2 emission by 80% of 2005 levels, which was 122 million metric tons of CO_2. In 2016, the PA electricity sector emitted 83 million metric tons of CO_2 (68% of 2005 levels), of which 55 and 28 million metric tons of CO_2 were emitted by coal and natural gas plants, respectively.

In Figure 3.1, we show carbon dioxide emissions as a function of coal and natural gas generation treated by CCS keeping the fuel mix and demand fixed. Installing CCS on all coal reduces CO_2 emissions to 34 million metric tons, which is insufficient to meet the deep decarbonization goal. To reach an 80% reduction, CCS needs to treat all emissions from coal generation and 37% of emissions from natural gas generation. Conversely, one can install CCS on all natural gas generation and 68% of coal generation. Thus, without changes to the fuel mix, CCS must play a significant role to deep decarbonize the PA electricity sector.

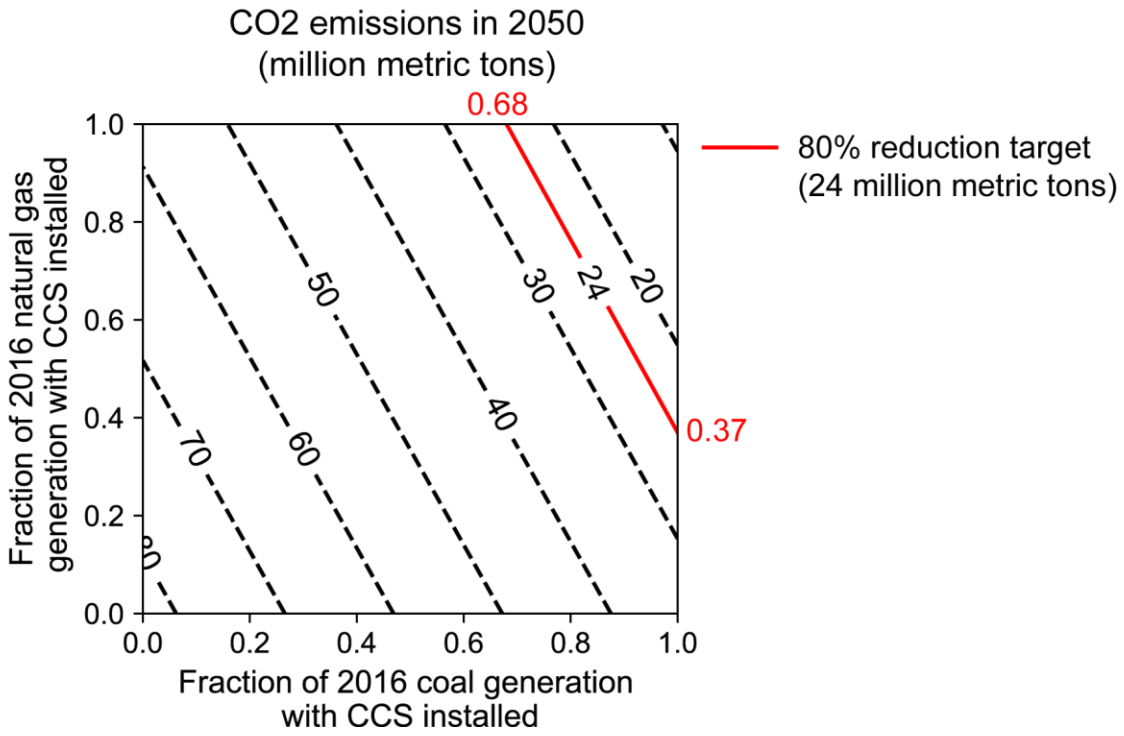

Figure 3.1: CO_2 emissions of the PA electricity sector in 2050 as a function of the fraction of natural gas generation with CCS installed and the fraction of coal generation with CCS installed. The fuel mix is the same as the fuel mix in 2016. The dashed lines show annual million metric ton of CO_2 emitted in 2050. The red line highlights the 80% reduction target and the red numbers illustrate the fraction of fossil fuel needed to deep decarbonize assuming the other fossil fuel 100% treated with CCS.

Changes to the fuel mix create more options for deep decarbonization. In Figure 3.2, we show CO_2 emissions emitted by the PA electricity sector in 2050 assuming the fuel mix is comprised of natural gas with CCS and renewables or state-of-the-art natural gas with CCS and renewables. If the share of natural gas in the fuel mix in 2050 is the same as 2016 and the rest of the fuel mix is renewables, the electricity sector would emit 28 million metric tons of CO_2, exceeding the target goal. Therefore, even if all coal retired, the PA electricity sector cannot decarbonize without either retiring natural gas until it is 27% of the fuel mix or installing CCS so that it treats 18% of natural gas generation. The PA electricity sector cannot, however, continue to build more natural gas as a bridge fuel without driving further away from 80% reduction goals.

CO_2 emissions can decrease significantly when fossil fuel plants are replaced by state-of-the-art NGCC plants and renewables. If state-of-the-art NGCC made up 57% of the fuel mix, which is the share of fossil fuels in the fuel mix, the PA electricity sector emits 37 million metric tons. About 38% of the fossil fuel generation will require CCS to reach the decarbonization goal.

We also sought to understand if deep decarbonization goals could be attained without CCS, given that CCS has yet to demonstrate commercial viability at a large scale.[133] If the entire coal fleet is replaced by renewables, and the entire natural gas fleet is retrofitted for state-of-the-art NGCC, then the electricity sector emits 20 million metric tons of CO_2, reaching the deep decarbonization goal. Assuming no changes to demand, this fuel mix is the only pathway to deep decarbonization without the use of CCS.

Based on the results of Figure 3.2, we created the five deep decarbonization scenarios in Table 3.2. In the wind and CCS and solar and CCS scenarios, we assume 100% of coal generation and 37% of natural gas generation is treated with CCS. For the wind only and solar only scenarios, we assume coal retires and state-of-the-art NGCC replaces the existing natural gas fleet until fossil fuel plants emit 24 million metric tons. For the solar, wind, and CCS scenario, we reach 24 million metric tons by changing the fuel mix and installing CCS. Solar and wind displace coal until CO_2 emissions decrease by two-thirds of 80% (55 million metric tons to 16 million metric tons). CCS on the remaining coal generation and 20% of natural gas generation reduces CO_2 emissions by one-third of 80%. We believe these five scenarios create illustrative examples and bounds to evaluate land use and forested land use impacts caused by deep decarbonization.

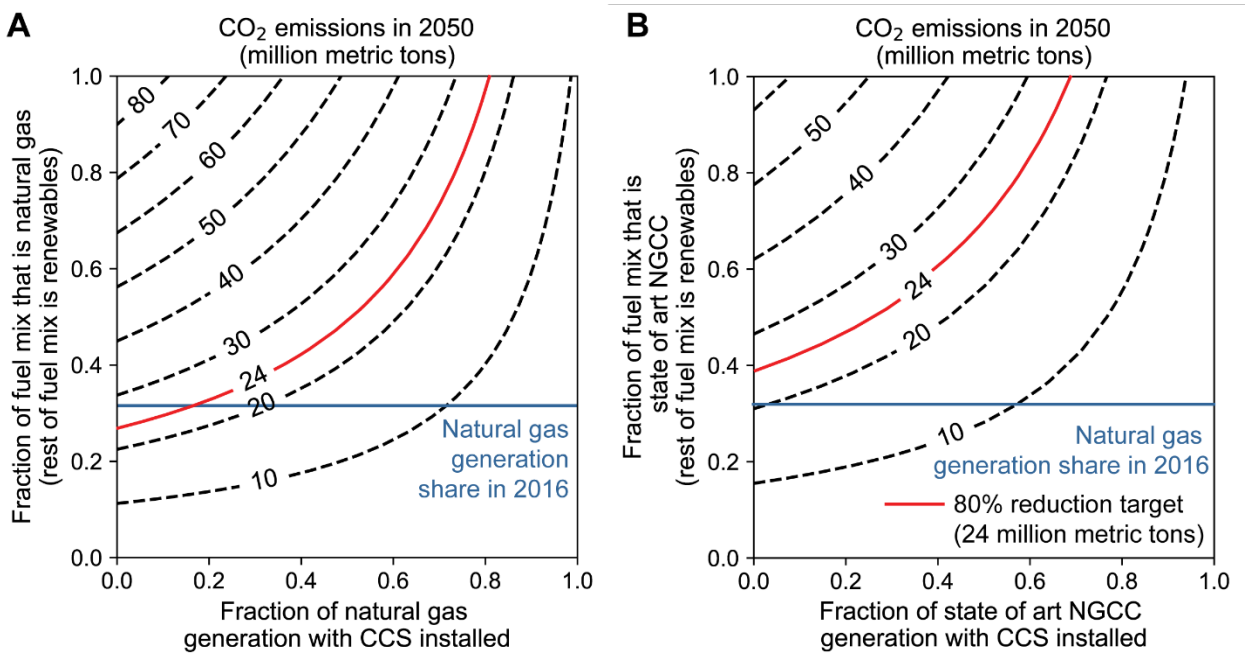

Figure 3.2: CO_2 emissions of the PA electricity sector in 2050 as a function of A) natural gas and renewables in the fuel mix and the fraction of natural gas generation with CCS installed and B) state-of-the-art NGCC and renewables in the fuel mix and the fraction of state-of-the-art NGCC generation with CCS installed. The dashed lines show annual million metric ton of CO2 emitted in 2050. The red line highlights the 80% reduction target.

Land and forested land use of different pathways to deep decarbonize

Impacts from CCS: CCS can deep decarbonize the entire PA electricity sector by treating all coal generation and at least 37% of natural gas generation with CCS. In Figure 3.3, we show the location of every coal and natural gas plant in PA along with the location of saline reservoirs in PA. In Appendix C.5, we provide a table of each plant with their generation, fuel type, and coordinates. Each plant located above a reservoir can build injections wells on site. Every coal plant except for plant 3140 sits directly above a saline reservoir. Plant 3140 is 70 km away from the saline reservoir. Installing CCS on all these coal plants reduces CO_2 emissions 68% of 2005 levels to 28% of 2005 levels.

Natural gas plants above saline formations generated 18.9 TWh or 28% of natural gas generation. To reach deep decarbonization goals, CCS needs to treat an additional 6.1 TWh of natural gas generation. In the blue circle in Figure 3.3, plants 3148 and 55667 generated 4.4 TWh and 3.9 TWh respectively. Both plants are about 33 km away from the nearest reservoir.

CCS requires about 136 km of pipeline from plants 3140, 3148, and 55667 to the saline reservoir boundary. Assuming a 40 m pipeline right-of-way, CCS pipelines would clear 5.4 km^2 of land. The bulk of the land and forest impacts will be caused by renewables infrastructure.

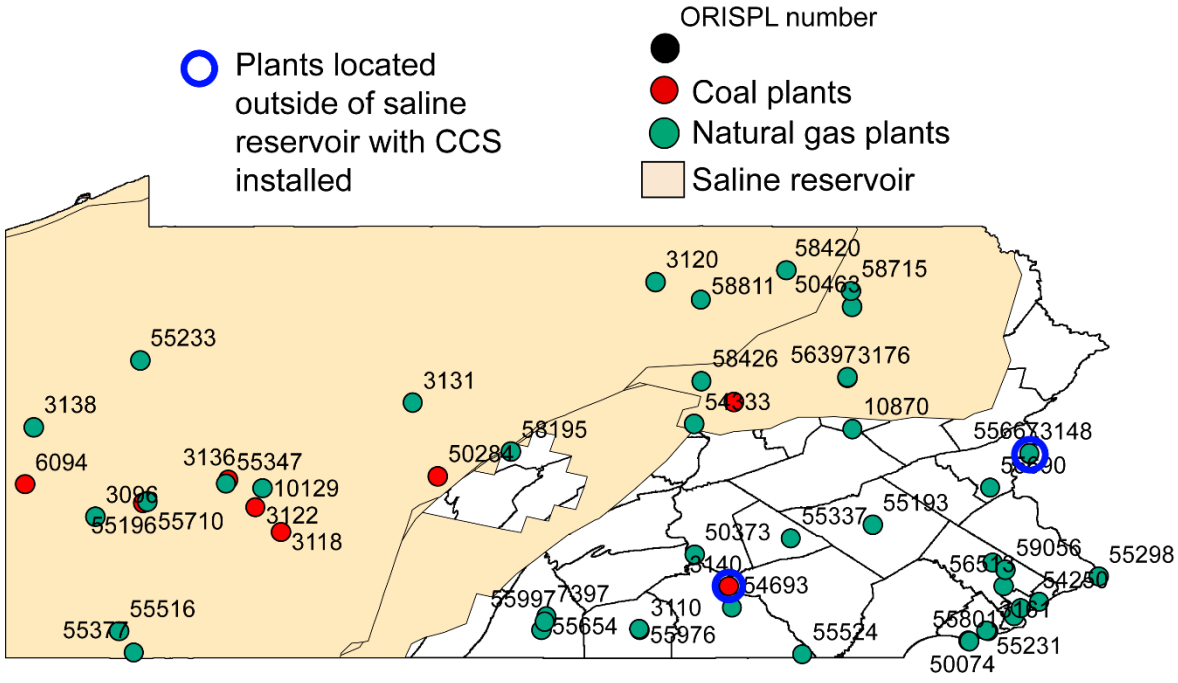

Figure 3.3: Coal (red) and natural gas (green) plants with their ORISPL numbers (black numbers) in PA in 2016.[87,88] Plants that are above saline reservoirs (yellow) can build pipelines for carbon capture and

sequestration directly underground and create negligible forest impacts. In the blue circle is the natural gas plant 3148 and 55667 and the coal plant 3140. These three plants generated which generated 3.9 TWh, 4.4 TWh, and 3.3 TWh, respectively in 2016. The natural gas plants 3148 and 55667 are about 33 km away from reservoir boundary and the coal plant 3140 is about 70 km away from the reservoir boundary.

Impacts from solar and wind farms: Table 3.2 shows the number of farms and capacity needed in each deep decarbonization scenario. Figure 3.4 illustrates the solar and wind farms that would be sited in PA for the scenarios. The average wind farm capacity is 59-70 MW across the different scenarios. The average capacity factor of a solar farm is 0.151-0.155 across the different scenarios.

In the wind and CCS and wind only scenarios, wind farms are sited throughout central PA, except for Allegheny National Forest, which is excluded from our analysis because it is a protected area. Wind farms appear on PA ridgelines, which are important areas for species conservation.[134] Solar farms are sited in the southeast first, where solar resources are highest in PA. In the solar only scenario, solar farms are built across central PA and into western PA to augment the production in southeast PA. As CCS use allows for fossil energy production it can be used to mitigate land impacts in central PA and western PA.

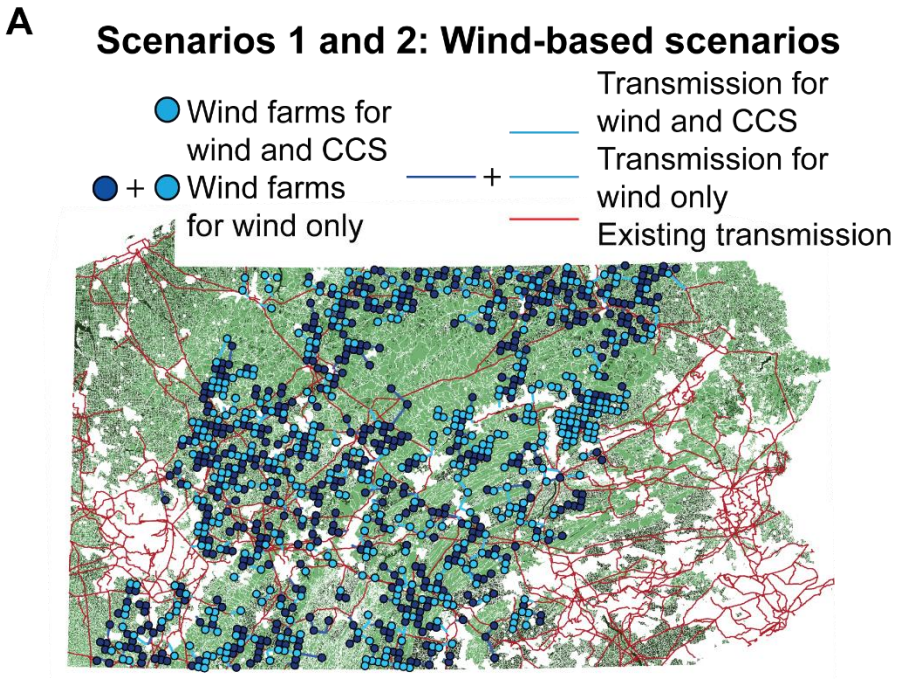

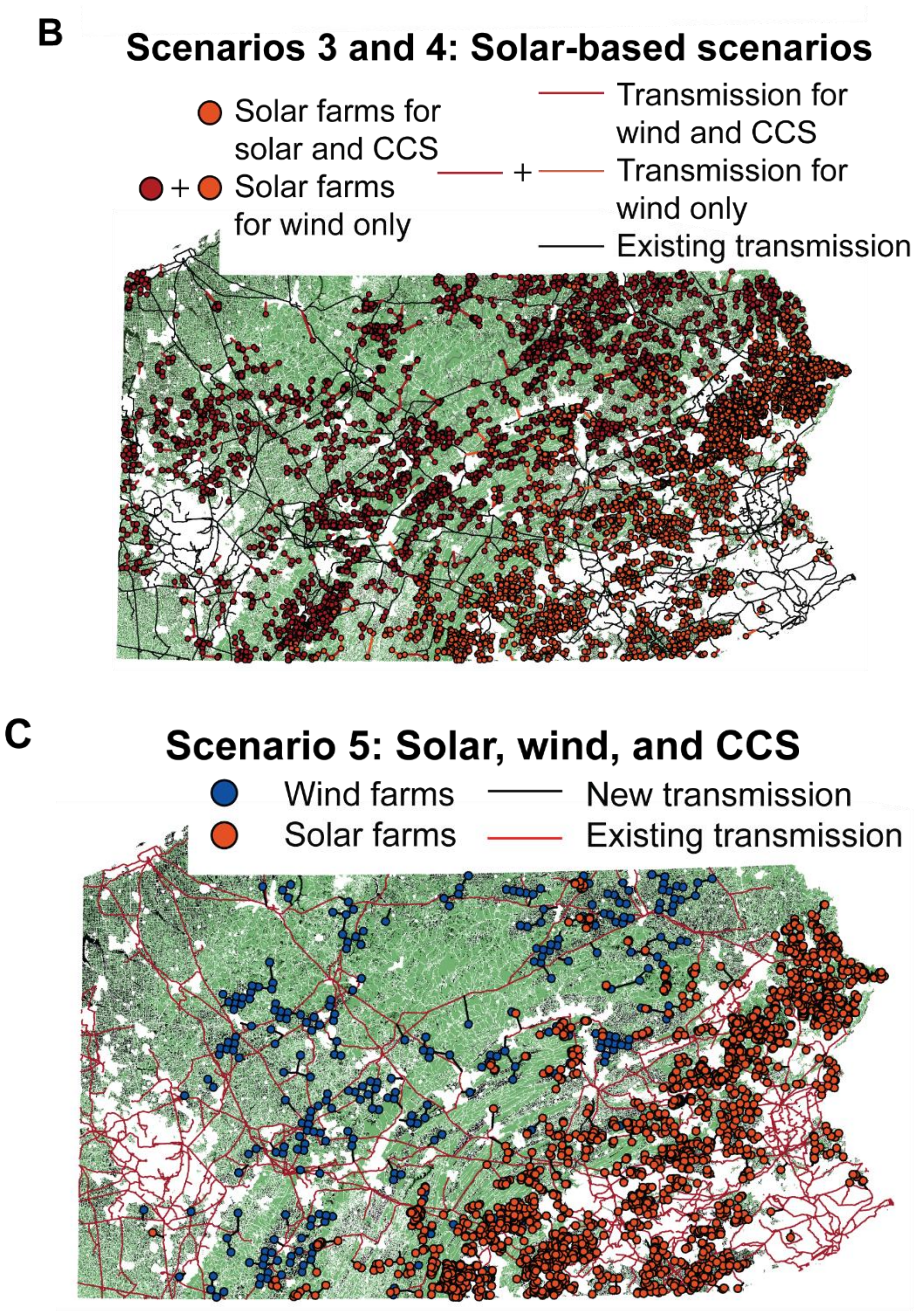

Figure 3.4: A map of PA showing new renewables capacity and transmission lines built for A) wind-based scenarios: wind and CCS and wind only, B) solar-based scenarios: solar and CCS and solar only, and C) solar, wind, and CCS scenario. In addition to new infrastructure, we also show the existing transmission network and a base map, where green are forested regions, black are non-forested regions, and white are areas with existing manmade infrastructure, where renewables infrastructure cannot be built.

Figure 3.5 shows the land and forested land area directly and indirectly impacted by new solar farms, wind farms, and transmission. The results provide upper and lower bounds for the land use needed to

deep decarbonize PA, assuming no changes to demand. The wind-based scenarios have the largest land and forested land impacts. In wind only, the amount of land and forested land allocated to site wind turbines is 13,300 km^2 and 9400 km^2 or 11% and 14% of total land and total forested land in PA, respectively. However, the bulk of wind impacts are indirect due to the amount of space required between wind turbines. The direct land and direct forested land impacts of wind only are 380 km^2 and 270 km^2, which are nearly two order of magnitudes less than the total impacts. In fact, direct impacts from wind farms are 73-78% less than direct impacts in solar and CCS and solar only scenarios.

Our results are similar to those described by others. Siting 102.9 GW of solar in the solar only scenario directly impacts 3300 km^2. Shum finds that adding 300-400 GW of solar in the U.S. can impact 5700-18,000 km^2 of land.[123] For wind, the Nature Conservancy estimates that 30,000 turbines could lead to 200 km^2 of direct impact to forests.[34] Assuming farms are composed of 1.5-2 MW turbines, then the wind only scenario requires about 30,000 turbines to build 52.2 GW and impacts 270 km^2 of forest directly, 35% greater than the Nature Conservancy's estimate.

Scenarios with CCS impact 54-61% of the direct and indirect land compared to scenarios without CCS. Therefore, CCS can be used to decrease land impacts in PA. In the solar and CCS scenario, 2.3% and 2.4% of land and forested PA land are needed, respectively. This scenario is the best-case scenario for minimizing total land impacts. Meanwhile, wind and CCS minimizes direct impacts. Only 0.5% and 0.4% of land and forested PA land are needed, respectively.

Lastly, the transmission impacts in the solar scenarios are 260-280% higher than the wind scenarios. The greater transmission impacts are caused by the fact that 6-7 times more solar farms need to be sited to deep decarbonize compared to wind. More solar farms are needed because our model assumes solar farms with capacity (20 MW) smaller than wind farm capacity (59-70 MW on average).

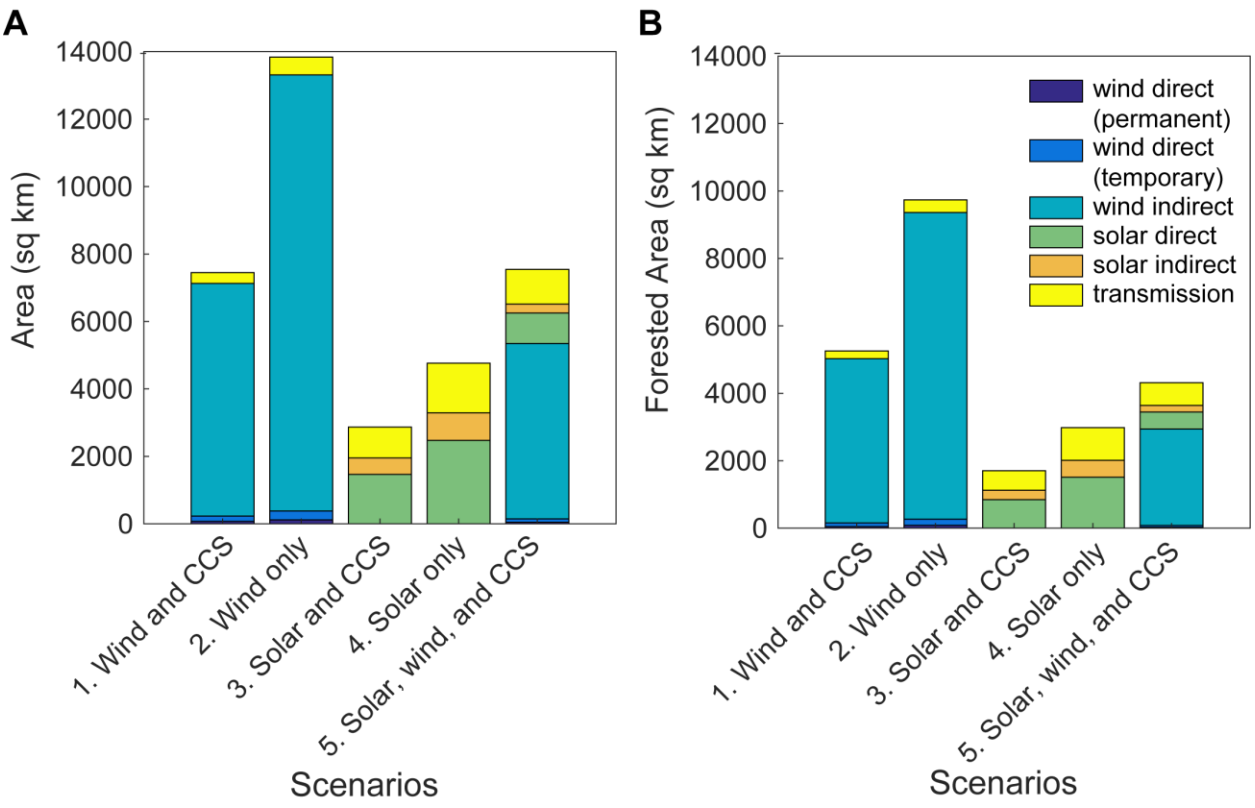

Figure 3.5: Land area (A) and forested area (B) required to deep decarbonize PA. Direct impacts cause changes to the land while indirect impacts include area needed to contain the project, such as turbine spacing or boundary enclosures. Temporary impacts are land cleared temporary roads and storage space cleared that can recover in a few years while permanent impacts are land cleared by roads and farms that are not expected to recover during the lifetime of the project.

In Figure 3.6, we perform a sensitivity analysis of the total and direct area for the wind only and solar only scenarios. We assume the same capacity of renewables needed to deep decarbonize in the two scenarios, which is 55.2 GW for wind only and 102.9 GW for solar only.

Based on Figure 3.6, solar tends to have less total area impacts than wind. Assuming the highest solar area-per-capacity impact factor, solar only has the highest total land impact if the wind impact factor is less than 12 ha/MW, which is true for 5% of all land impact factors. However, the lowest wind land impact factor at 4.3 ha/MW creates a total land impact smaller than 84% of solar total impacts, which is an encouraging signal for wind if wind farms can be consistently built at such high densities.

We also find that wind tends to have less direct area impacts than solar. About 12% of wind farms have direct area impacts that are higher than the possible direct area impacts of a solar farm. Therefore, even if

solar farms are constructed with the lowest possible area-per-capacity impact factor, solar farms are likely to produce greater direct area than a wind farm.

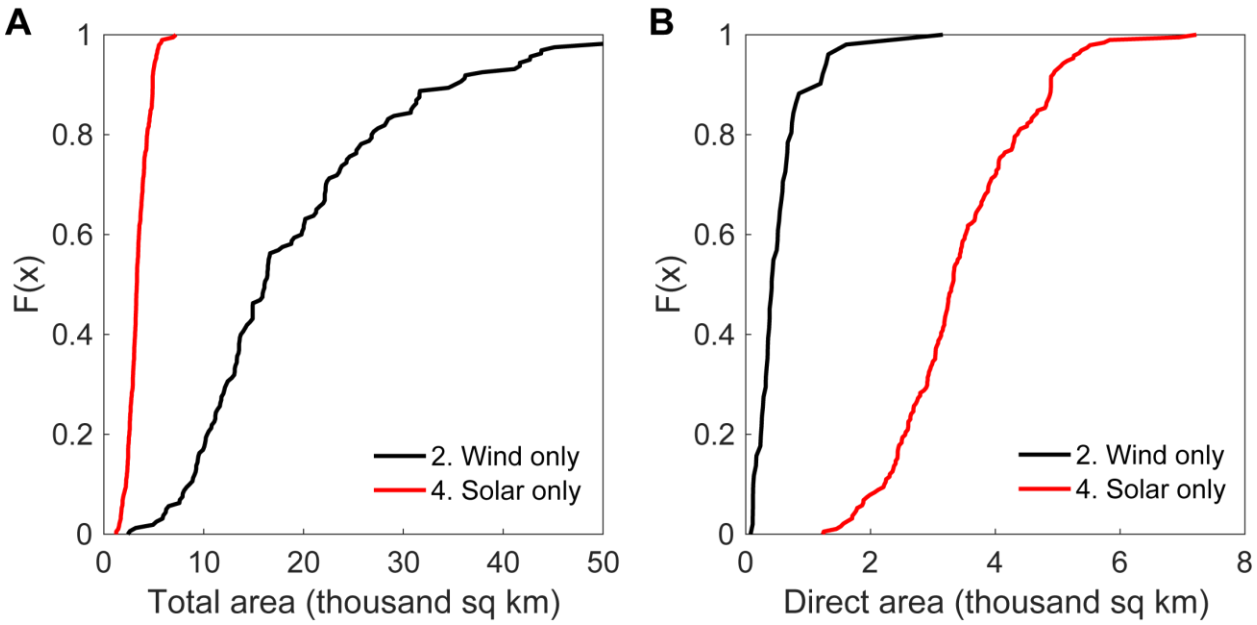

Figure 3.6: Cumulative distribution functions illustrating the A) total area and B) direct area of the wind only and solar only scenarios where we calculate the area using the same capacity needed to deep decarbonize and the area-per-capacity impact factor of every solar and wind farm provided by NREL's land impact analysis.[129,131] The x-axis of A) the total area figure is cut-off at 50 thousand km^2 to make the figure more readable. The largest total area of the wind only scenario is 125 thousand km^2.

Fragmentation analysis

For the fragmentation analyses, we compare the deep decarbonization scenarios against a baseline map, which excludes all manmade infrastructure (See Appendix C.3 for a list of exclusion criteria). The baseline has 43,800 NCP, 47,080 km^2 of forested land, and 63,900 km^2 of land.

In Table 3.3 we summarize the fragmentation results for each of the five scenarios. When solar is the renewable energy source, we find that the NCP increases from the baseline, implying that building new solar and transmission will fragment forests in PA, which can be harmful to existing habitats. However, when wind is the renewable energy source, we find that NCP decreases from the baseline. When a wind farm is sited, all land within the boundary of that farm is impacted and removed from core patch counts. Since each farm is 16 km^2 and each core patch is at least 4 ha or 0.04 km^2, a new wind farm can eliminate existing core patches. Therefore, instead of fragmenting the forest, the presence of large wind farms removes core patches, also creating potential damage to habitats and sensitive species. In the solar, wind, and CCS scenario, we observe a tension between the increase in fragmentation caused by solar farms and removal of core patches by wind farms, where ultimately more core patches are removed than created.

The $PLAND_{total}$ and $PLAND_{forest}$ show that the solar and CCS and solar only scenarios affect a larger percentage of the landscape than the wind and CCS scenario, suggesting that solar may have greater overall impact on habitat. Consistent with our findings from Figures 3 and 4, we find solar will have greater impacts on both total landscape and forested landscape, where solar could remove up to 5% of forested landscape from the baseline. Relying more on CCS could reduce some of the forest impacts presented in Table 3.3.

Table 3.3: Fragmentation indices by scenario. NCP is the number of core patches, are patches with greater than 4 ha of area. The $PLAND_{total}$ and $PLAND_{forest}$ are the percent of total habitat in the landscape defined in Equations 1 and 2 based on the total area map and the forest area map, respectively.

Scenario	NCP (thousands)	$PLAND_{total}$ (%)	$PLAND_{forest}$ (%)
0. Baseline	43.8	-	-
1. Wind and CCS	42.4	99	99
2. Wind only	40.6	98	98
3. Solar and CCS	44.3	96	97
4. Solar only	46.3	94	95
5. Solar, wind, and CCS	43.1	96	97

3.4 Discussion

We find pathways to deep decarbonize the PA electricity sector (20% of 2005 carbon dioxide emissions by 2050) assuming there are no changes to demand and the nuclear fleet retires by 2050. We estimate the land and forested land required to deep decarbonize, selecting pathways that represent bounding scenarios, and quantify potential ecosystem damages via fragmentation indices.

Carbon dioxide emissions from current natural gas plants exceed deep decarbonization goals. Thus, the PA electricity sector cannot increase the use natural gas fired electricity production from current use. While replacing coal with natural gas will reduce emissions, ultimately, these plants must be replaced by renewables to achieve deep decarbonization.

CCS plays an important role in deep decarbonization if the PA electricity sector wants to minimize changes to its fuel mix. If PA wants to deep decarbonize without CCS, it needs to replace all its coal and nuclear with renewables and retrofit all its natural gas with state-of-the-art NGCC, assuming demand in 2050 is the same as in 2016. More CCS may be necessary if demand were to increase due to electrification of vehicles or other end-uses. However, CCS may not be ready to deploy at such a massive scale given that only three plants operate post-combustion CCS in the U.S. and Canada.[133] If deep decarbonization is a priority, decision-makers must accelerate the development and deployment of CCS, as it may be an important solution while minimizing ecological impacts.

Solar and wind will also require fast deployment if PA wants to reach deep decarbonization goals in time. In our mixed strategy, we estimate that PA needs to install 20.3 GW of wind and 39.5 GW of solar. Assuming a 30-year window, they need to install 680 MW of wind and 1300 MW of solar annually. Presently, PA has installed in total 1400 MW of wind and 400 MW of solar.[87,135]

Using only wind to deep decarbonize causes the least direct land impacts (1050 sq km or 0.9% of total PA area). Using only solar requires 4580 km^2 or 3.9% of total PA area. Overall, solar poses more potential damage to forested land, as there is insufficient land in southeast PA site enough renewables penetration for deep decarbonization. One way to minimize the effect solar and wind on land use is to prioritize renewables development on already used land, but the scale requirement may overwhelm this approach. The obvious approach to reducing land perturbation is to preserve nuclear based electricity production, but this comes with a cost tradeoff considering the public support required.[136,137]

There are some important limitations to this work. Infrastructure costs are excluded and renewables might locate in prohibitively expensive areas. Second, land use factors are uncertain and based on prior literature assessing past solar and wind projects, where future projects may introduce more efficient wind

turbines and photovoltaics with smaller land impact factors. Third, transmission from new renewable capacity is directed to the nearest substation or renewable farm without considering the difficulty of siting transmission in communities or the needs of the transmission system.[138] Reaching >60% renewables penetration introduces curtailment and grid reliability issues.[26,139] Lastly, assuming CCS can perform onsite injections with minimized land use impacts, pore space availability, injectivity, and costs of displaced brine treatment might limit utility.[140]

The important issue raised in this work is that deep decarbonization has environmental and ecological costs that we seek to protect by addressing climate change. We should understand if addressing climate change does not inadvertently cause impacts that might leave society worse off. Instead of assuming every state must address "their fair share," an understanding of potential tradeoffs may suggest a different, yet more sustainable approach by going beyond artificial political boundaries. A major first step beyond this work is to quantify the benefits and costs of deep decarbonization so that these tradeoffs can be measured against each other.

Conclusions

In Chapter 1, I model trace element mass flow rates from coal-fired power plants. Trace metal mass flow rates are predominantly in the solid phase, and chlorine mass flow rates are predominantly in the liquid and gaseous phase. These emissions partition into their respective phases because of the air pollution controls downstream of the boiler, where wet flue gas desulfurization devices create liquid waste streams and all other air pollution control devices generate solid waste streams. Therefore, trace element management that maximize human health and environmental benefits should consider the final fate of the trace element exiting the power plant. The model can also be useful to regulator and policy analysts who are interested in monitoring trace element mass flow rates at the plant or fleet level. However, the validation assessments demonstrate that modeling efforts of trace elements need to improve in accuracy before they can be used to assess policy options on the coal-fired fleet, predict mass flows to environmental systems, or replace liquid-phase or gas-phase monitors. Accuracy improvements can come from more available robust data of trace element concentrations at the plant-level. One major step that can be taken is to require coal plants to sample the concentration of trace elements in the coal blend prior to combustion. This measurement, when combined with fuel combustion data, can quantify the total trace elements entering the coal-fired power plant system and can predict the total trace element mass flows discharged to the environment. While such a requirement is helpful for modeling efforts, the time and resources required for coal plants to maintain high fidelity data may not be worth the information gained.

In Chapter 2, I model potential SO_2, NO_x, and CO_2 emissions of the U.S. electricity under two bounding scenarios, one which assumes environmental regulations are weakened and one which assumes coal becomes more profitable than natural gas. These scenarios are extreme scenarios of current federal energy policies which advance coal in the U.S. I find that these scenarios can increase emissions by 30%-300% of current emissions while increasing emissions to levels last observed ten years ago. Emission increases differ across the U.S. depending on the controls installed at coal plants and the mix of coal and natural gas plants at the eGRID sub-region level. While FERC recently voted down the Grid Resiliency Pricing Rule. the Environmental Protection Agency has yet to give assertive signals to regulate and enforce existing regulations on coal or create new regulation that target coal plants and push them toward retirement. These federal signals also create a tension with the behavior of state agencies. State agencies could enforce regulations to protect public health in their state, but if they are compelled to enforce due to a federal regulation and EPA weakens enforcement, then the states may follow suit, even if, for example, coal plants violate the CSAPR state budget emissions.

In Chapter 3, I estimate the fuel mix and infrastructure necessary to deep decarbonize the Pennsylvania electricity sector by 80% of 2005 levels and the potential land-use and forested land-use of a few deep decarbonization pathways. From a deep decarbonization perspective, Pennsylvania cannot build more natural gas if it plans to reach the deep decarbonization goal and will need a combination of retiring coal from the fuel mix and installing CCS on coal power plants. Deep decarbonization will also require a significant fraction of the fuel mix to be renewables that may be an order of magnitude greater than the existing wind and solar renewables capacity. Pennsylvania decision-makers will need to prioritize the development and deployment of renewables and CCS if they want to meet the deep decarbonization goals set out by the Department of Environmental Protections. Excluded from the analysis is consideration of grid reliability, where the large renewables capacity will likely provide loads at different hours of the day and could cause curtailment. Future decarbonization planning will also need to include methods for stabilizing the grid, which would require more infrastructure on top of the existing infrastructure needed to decarbonize. From the ecological perspective, deep decarbonization may require significant amount of land and cause fragmentation of forests. Therefore, deep decarbonization planning will need to account for various ecological species and include methods of protecting habitats. However, it is also conceivable that the amount of infrastructure needed may overwhelm the amount of non-habitat land available and make ecological impacts unavoidable. Extending the nuclear fleet beyond 2050 becomes an increasingly attractive option for reducing ecological impacts as more nuclear would reduce some of the need for solar and wind.

References

(1) Caiazzo, F.; Ashok, A.; Waitz, I. A.; Yim, S. H. L.; Barrett, S. R. H. Air pollution and early deaths in the United States . Part I : Quantifying the impact of major sectors in 2005. *Atmos. Environ.* **2013**, *79*, 198–208.

(2) Committee on Health Environmental and Other External Costs and Benefits of Energy Production and Consumption; National Research Council. *Hidden costs of energy*; 2010.

(3) U.S. Environmental Protection Agency. *Regulatory Impact Analysis of the Cross State Air Pollution Rule*; Washington D.C., 2011.

(4) U.S. Environmental Protection Agency. *Regulatory Impact Analysis for the Final Mercury and Air Toxics Standards*; U.S. Environmental Protection Agency: Research Triangle Park, NC, 2011.

(5) U.S. Environmental Protection Agency. *Mercury and Air Toxics Standards*; U.S. Environmental Protection Agency: Washington D.C., 2012.

(6) U.S. Environmental Protection Agency. *Steam Electric Power Generating Effluent Guidelines - 2015 Final Rule*; U.S. Environmental Protection Agency: Washington D.C., 2015.

(7) U.S. Environmental Protection Agency. *Disposal of Coal Combustion Residuals from Electric Utilities*; U.S. Environmental Protection Agency: Washington D.C., 2015.

(8) U.S. Environmental Protection Agency. *National Emission Standards for Hazardous Air Pollutants From Coal and Oil-Fired Electric Utility Steam Generating Units and Standards of Performance for Fossil-Fuel-Fired Electric Utility, Industrial-Commercial Institutional, and Small Industrial Commerc*; U.S. Environmental Protection Agency: Washington D.C., 2012.

(9) U.S. Environmental Protection Agency. *Environmental Assessment for the Effluent Limitation Guidelines and Standards for the Steam Electric Power Generating Point Source Category*; U.S. Environmental Protection Agency: Washington D.C., 2015.

(10) Harkness, J. S.; Sulkin, B.; Vengosh, A. Evidence for Coal Ash Ponds Leaking in the Southeastern United States. *Environ. Sci. Technol.* **2016**, *50* (12), acs.est.6b01727.

(11) Bruggers, J. Coal ash is contaminating groundwater in at least 22 states, utility reports show. *Inside Climate News*. January 2019.

(12) US Environmental Protection Agency. *National Emission Standards for Hazardous Air Pollutants: Coal- and Oil-Fired Electric Utility Steam Generating Units—Reconsideration of*

Supplemental Finding and Residual Risk and Technology Review; 2019.

(13) U.S. Department of Energy. *Grid resiliency pricing rule*; Washington D.C., 2017.

(14) Shawhan, D.; Picciano, P. *Costs and Benefits of Saving Unprofitable Generators: A Simulation Case Study for U.S. Coal and Nuclear Power Plants*; Washington D.C., 2017.

(15) Federal Energy Regulatory Commission. *Order terminating rulemaking proceeding, initiating new proceedings, & establishing additional procedures re Grid Reliability & Resilience Pricing under RM18-1 et al.*; 2018.

(16) Osborne, J. Perry says he's "thrown a lot of jello at the wall," on coal, nuclear closures. *Houston Chronicle*. March 13, 2019.

(17) Field, C. B.; Barros, V. R.; Dokken, D. J.; Mach, K. J.; Mastrandrea, M. D.; Bilir, T. E.; Chatterjee, M.; Ebi, K. L.; Estrada, Y. O.; Genova, R. C.; et al. *Climate Change 2014: Impacts, Adaptation, and Vulnerability. Contribution of Working Group II to the Fifth Assessment Report of the Intergovernmental Panel on Climate Change*; 2014.

(18) Stocker, T. F.; Qin, D.; Plattner, G.-K.; Tignor, M.; Allen, S. K.; Boschung, J.; Nauels, A.; Xia, Y.; Bex, V.; Midgley, P. M. *Climate Change 2013: The Physical Science Basis. Contribution of Working Group I to the Fifth Assessment Report of the Intergovernmental Panel on Climate Change*; 2014.

(19) Edenhofer, O.; Pichs-Madruga, R.; Sokona, Y.; Farahani, E.; Kadner, S.; K.; Seyboth; Adler, A.; I. Baum, S.; Brunner, .; et al. *Climate Change 2014: Mitigation of Climate Change. Contribution of Working Group III to the Fifth Assessment Report of the Intergovernmental Panel on Climate Change*; 2014.

(20) Williams, J. H.; Jones, R.; Kwok, G.; Haley, B. *Deep Decarbonization in the Northeastern United States and Expanded Coordination with Hydro-Québec*; 2018.

(21) The White House. *United States Mid-Century Strategy for Deep Decarbonization*; Washington D.C., 2016.

(22) Pennsylvania Department of Environmental Protection. *Pennsylvania Climate Action Plan (Draft)*; 2018.

(23) Haley, B.; Kahrl, F.; Moore, J.; Jones, A. D.; Torn, M. S.; Mcjeon, H. Deep Decarbonization. **2015**.

(24) Pacala, S.; Socolow, R. Stabilization Wedges : Solving the Climate Problem for the Next 50 Years

with Current Technologies. *Science (80-.).* **2004**, *305* (968).

(25) Myhrvold, N. P.; Caldeira, K. Greenhouse gases, climate change and the transition from coal to low-carbon electricity. *Environ. Res. Lett.* **2012**, *7*.

(26) MacDonald, A. E.; Clack, C. T. M.; Alexander, A.; Dunbar, A.; Wilczak, J.; Xie, Y. Future cost-competitive electricity systems and their impact on U.S. carbon dioxide emissions. *Nat. Clim. Chang.* **2016**, *6* (5), 526–531.

(27) Cochran, J.; Mai, T.; Bazilian, M. Meta-analysis of high penetration renewable energy scenarios. *Renew. Sustain. Energy Rev.* **2014**, *29*, 246–253.

(28) Tu, J.; Xia, Z.-G. Examining spatially varying relationships between land use and water quality using geographically weighted regression I: Model design and evaluation. *Sci. Total Environ.* **2008**, *407* (1), 358–378.

(29) Mai, T.; Mulcahy, D.; Hand, M. M.; Baldwin, S. F. Envisioning a renewable electricity future for the United States. *Energy* **2014**, *65*, 374–386.

(30) Cole, W.; Beppler, R.; Zinaman, O.; Logan, J.; Cole, W.; Beppler, R.; Zinaman, O.; Logan, J. *Considering the Role of Natural Gas in the Deep Decarbonization of the U.S. Electricity Sector*; 2016.

(31) U.S. Energy Information Administration. Electric Power Annual https://www.eia.gov/electricity/annual/.

(32) Hernandez, R. R.; Easter, S. B.; Murphy-Mariscal, M. L.; Maestre, F. T.; Tavassoli, M.; Allen, E. B.; Barrows, C. W.; Belnap, J.; Ochoa-Hueso, R.; Ravi, S.; et al. Environmental impacts of utility-scale solar energy. *Renew. Sustain. Energy Rev.* **2014**, *29*, 766–779.

(33) Hernandez, R. R.; Hoffacker, M. K.; Murphy-mariscal, M. L.; Wu, G. C.; Allen, M. F. Solar energy development impacts on land cover change and protected areas. *Proc. Natl. Acad. Sci.* **2015**, *113* (44).

(34) Johnson, N.; Gagnolet, T.; Ralls, R.; Zimmerman, E.; Eichelberger, B.; Tracey, C.; Kreitler, G.; Orndorff, S.; Tomslinson, J.; Bearer, S.; et al. *Pennsylvania Energy Impacts Assessment*; 2010.

(35) Abrahams, L. S.; Griffin, W. M.; Matthews, H. S. Assessment of policies to reduce core forest fragmentation from Marcellus shale development in Pennsylvania. *Ecol. Indic.* **2015**, *52* (1), 153–160.

(36) Sekar, A.; Williams, E.; Chester, M. Siting is a constraint to realize environmental benefits from

carbon capture and storage. *Environ. Sci. Technol.* **2014**, *48* (19), 11705–11712.

(37) Wu, G. C.; Torn, M. S.; Williams, J. H. Incorporating land-use requirements and environmental constraints in low-carbon electricity planning for California. *Environ. Sci. Technol.* **2015**, *49* (4), 2013–2021.

(38) Goodale, M. W.; Milman, A. Cumulative adverse effects of offshore wind energy development on wildlife. *J. Environ. Plan. Manag.* **2016**, *59* (1), 1–21.

(39) Eichhorn, M.; Drechsler, M. Spatial trade-offs between wind power production and bird collision avoidance in agricultural landscapes. *Ecol. Soc.* **2010**, *15* (2), 10.

(40) Fahrig, L. How much habitat is enough? *Biol. Conserv.* **2001**, *10*, 65–74.

(41) Union of Concerned Scientists. Climate Change in Pennsylvania. **2008**, 54.

(42) Ruhl, L.; Vengosh, A.; Dwyer, G. S.; Hsu-kim, H.; Deonarine, A.; Bergin, M.; Kravchenko, J. Survey of the potential environmental and health impacts in the immediate aftermath of the coal ash spill in Kingston, Tennessee. **2009**, *43* (16), 6326–6333.

(43) Winkel, L. H. E.; Johnson, C. A.; Lenz, M.; Grundl, T.; Leupin, O. X.; Amini, M.; Charlet, L. Environmental selenium research: From microscopic processes to global understanding. *Environ. Sci. Technol.* **2012**, *46* (2), 571–579.

(44) Utsunomiya, S.; Jensen, K. A.; Keeler, G. J.; Ewing, R. C. Direct identification of trace metals in fine and ultrafine particles in the Detroit urban atmosphere. *Environ. Sci. Technol.* **2004**, *38* (8), 2289–2297.

(45) Vengosh, A.; Coyte, R.; Karr, J.; Harkness, J. S.; Kondash, A. J.; Ruhl, L. S.; Merola, R. B.; Dywer, G. S. Origin of hexavalent chromium in drinking water wells from the Piedmont aquifers of North Carolina. *Environ. Sci. Technol. Lett.* **2016**, *3* (12), 409–414.

(46) Agusa, T.; Kunito, T.; Fujihara, J.; Kubota, R.; Minh, T. B.; Kim Trang, P. T.; Iwata, H.; Subramanian, A.; Viet, P. H.; Tanabe, S. Contamination by arsenic and other trace elements in tube-well water and its risk assessment to humans in Hanoi, Vietnam. *Environ. Pollut.* **2006**, *139* (1), 95–106.

(47) Zahir, F.; Rizwi, S. J.; Haq, S. K.; Khan, R. H. Low dose mercury toxicity and human health. *Environ. Toxicol. Pharmacol.* **2005**, *20* (2), 351–360.

(48) Brandt, J. E.; Bernhardt, E. S.; Dwyer, G. S.; Giulio, R. T. Di. Selenium ecotoxicology in freshwater lakes receiving coal combustion residual effluents: A North Carolina example. *Environ.*

Sci. Technol. **2017**, *51* (4), 2418–2426.

(49) Mathews, T. J.; Fortner, A. M.; Jett, R. T.; Morris, J.; Gable, J.; Peterson, M. J.; Carriker, N. Selenium bioaccumulation in fish exposed to coal ash at the Tennessee Valley Authority Kingston spill site. *Environ. Toxicol. Chem.* **2014**, *33* (10), 2273–2279.

(50) Ruhl, L.; Vengosh, A.; Dwyer, G. S.; Hsu-Kim, H.; Schwartz, G.; Romanski, A.; Smith, S. D. The impact of coal combustion residue effluent on water resources: A North Carolina example. *Environ. Sci. Technol.* **2012**, *46* (21), 12226–12233.

(51) Jiao, W.; Chen, W.; Chang, A. C.; Page, A. L. Environmental risks of trace elements associated with long-term phosphate fertilizers applications: A review. *Environ. Pollut.* **2012**, *168*, 44–53.

(52) Samsøe-Petersen, L.; Larsen, E. H.; Larsen, P. B.; Bruun, P. Uptake of trace elements and PAHs by fruit and vegetables from contaminated soils. *Environ. Sci. Technol.* **2002**, *36* (14), 3057–3063.

(53) Ikem, A.; Egiebor, N. O.; Nyavor, K. Trace elements in water, fish and sediment from Tuskegee Lake, southeastern U.S.A. *Water. Air. Soil Pollut.* **2003**, *149* (1), 51–75.

(54) US Environmental Protection Agency. 2014 National Emissions Inventory (NEI) Data https://www.epa.gov/air-emissions-inventories/2014-national-emissions-inventory-nei-data.

(55) Carey, T. R.; Hargrove, O. W. J.; Richardson, C. F.; Chang, R.; Meserole, F. B. Factors affecting mercury control in utility flue gas using activated carbon. *J. Air Waste Manage. Assoc.* **1998**, *48* (12), 1166–1174.

(56) Berkenpas, M. B.; Rubin, E. S.; Smith, D. N.; Gibbon, G. A. Preliminary cost and performance models for mercury control at coal-fired power plants. In *The EPA/DOE/EPRI Mega Symposium*; 2001; pp 1–19.

(57) Meij, R.; te Winkel, H. The emissions of heavy metals and persistent organic pollutants from modern coal-fired power stations. *Atmos. Environ.* **2007**, *41* (40), 9262–9272.

(58) Flora, J. R. V.; Hargis, R. A.; Dowd, W. J. O.; Pennline, H. W.; Vidic, R. D. Modeling sorbent injection for mercury control in baghouse filters: II - pilot-scale studies and model evaluation. *J. Air Waste Manag. Assoc.* **2003**, *53*, 489–496.

(59) Linak, W. P.; Wendt, J. O. . Toxic metal emissions from incineration: Mechanisms and control. *Prog. Energy Combust. Sci.* **1993**, *19* (2), 145–185.

(60) Scala, F. Modeling mercury capture in coal-fired power plant flue gas. *Ind. Eng. Chem. Res.* **2004**, *43* (10), 2575–2589.

(61) Senior, C. L. Oxidation of mercury across selective catalytic reduction catalysts in coal–fired power plants. *J. Air Waste Manage. Assoc.* **2006**, *56* (1), 23–31.

(62) Senior, C. L.; Lignell, D. O.; Sarofim, A. F.; Mehta, A. Modeling arsenic partitioning in coal-fired power plants. *Combust. Flame* **2006**, *147* (3), 209–221.

(63) Senior, C.; Otten, B. Van; Wendt, J. O. L.; Sarofim, A. Modeling the behavior of selenium in pulverized-coal combustion systems. *Combust. Flame* **2010**, *157* (11), 2095–2105.

(64) Zeng, T.; Sarofim, A. F.; Senior, C. L. Vaporization of arsenic, selenium and antimony during coal combustion. *Combust. Flame* **2001**, *126* (3), 1714–1724.

(65) Helble, J. J. Model for the air emissions of trace metallic elements from coal combustors equipped with electrostatic precipitators. *Fuel Process. Technol.* **2000**, *63* (2), 125–147.

(66) Kittner, N.; Fadadu, R. P.; Buckley, H. L.; Schwarzman, M. R.; Kammen, D. M. Trace Metal Content of Coal Exacerbates Air-Pollution-Related Health Risks: The Case of Lignite Coal in Kosovo. *Environ. Sci. Technol.* **2018**, acs.est.7b04254.

(67) Wang, S.; Zhang, L.; Zhao, B.; Meng, Y.; Hao, J. Mitigation potential of mercury emissions from coal-fired power plants in China. *Energy & Fuels* **2012**, *26* (8), 4635–4642.

(68) Zhu, C.; Tian, H.; Cheng, K.; Liu, K.; Wang, K.; Hua, S.; Gao, J.; Zhou, J. Potentials of whole process control of heavy metals emissions from coal-fired power plants in China. *J. Clean. Prod.* **2016**, *114*, 343–351.

(69) Zhang, L.; Wang, S.; Wang, L.; Wu, Y.; Duan, L.; Wu, Q.; Wang, F.; Yang, M.; Yang, H.; Hao, J.; et al. Updated emission inventories for speciated atmospheric mercury from anthropogenic sources in China. *Environ. Sci. Technol.* **2015**, *49* (5), 3185–3194.

(70) Liu, K.; Wang, S.; Wu, Q.; Wang, L.; Ma, Q.; Zhang, L.; Li, G.; Tian, H.; Duan, L.; Hao, J. A Highly-resolved Mercury Emission Inventory of Chinese Coal-fired Power Plants. *Environ. Sci. Technol.* **2018**, acs.est.7b06209.

(71) Good, K. D.; Vanbriesen, J. M. Power Plant Bromide Discharges and Downstream Drinking Water Systems in Pennsylvania. *Environ. Sci. Technol.* **2017**, *51* (20), 11829–11838.

(72) Good, K. D.; VanBriesen, J. M. Wet flue gas desulfurization bromide discharges to U.S. watersheds and their contributions to drinking water sources. *Environ. Sci. Technol.* **2018**, *(in press)*, 213–223.

(73) Granite, E. J.; Pennline, H. W.; Hargis, R. A. Novel Sorbents For Mercury Removal From Flue

Gas. *Ind. Eng. Chem. Res.* **2000**, *39*, 1020–1029.

(74) Granite, E. J.; Pennline, H. W.; Senior, C. *Mercury Control: for Coal-Derived Gas Streams*; John Wiley & Sons, 2015.

(75) Pekney, N. J.; Martello, D. V; Schroeder, K.; Granite, E. Measurement of mercury flux from coal utilization by-products with a laboratory flux chamber. *Fuel* **2009**, *88* (5), 890–897.

(76) Granite, E. J.; King, W. P.; Stanko, D. C.; Pennline, H. W. Implications of mercury interactions with band-gap semiconductor oxides. *Main Gr. Chem.* **2008**, *7* (3), 227–237.

(77) Electric Power Research Institute. TRI for Power Plants RY2015 https://www.epri.com/#/pages/product/3002007002/ (accessed Apr 1, 2018).

(78) Rubin, E. S.; Berkenpas, M. B.; Frey, H. C.; Toole-O'Neil, B. Modeling the uncertainty in hazardous air pollutant emissions. In *EPRI Second International Conference on "Managing Hazardous Air Pollutants";* 1993; pp 1–20.

(79) Rubin, E. S.; Toole-O'Neil, B. The PISCES Model: A new tool for chemical effluents assessment and control. In *EPRI International Clean Water Conference*; La Jolla, California, 1995.

(80) Rubin, E. S.; Neil, B. T. A computer simulation model for power plant air toxics emissions. In *Fossil Simulation Program*; Phoenix, AZ, 1995.

(81) Rubin, E. S. Toxic releases from power plants. *Environ. Sci. Technol.* **1999**, *33* (18), 3062–3067.

(82) Wu, Y.; Wang, S.; Streets, D. G.; Hao, J.; Chan, M.; Jiang, J. Trends in anthropogenic mercury emissions in China from 1995 to 2003. *Environ. Sci. Technol.* **2006**, *40* (17), 5312–5318.

(83) Meij, R. Trace element behavior in coal-fired power plants. *Fuel Process. Technol.* **1994**, *39* (1–3), 199–217.

(84) U.S. Environmental Protection Agency. Mercury Air Toxic Standards Information Collection Request https://www3.epa.gov/airtoxics/utility/utilitypg.html (accessed Sep 1, 2017).

(85) U.S. Environmental Protection Agency. Air Markets Program Data Tool https://ampd.epa.gov/ampd/.

(86) Palmer, C. A.; Oman, C. L.; Park, A. J.; Luppens, J. A. *The U.S. geological survey coal quality (COALQUAL) database version 3.0*; 2015.

(87) U.S. Energy Information Administration. Annual Electric Generator Data https://www.eia.gov/electricity/data/eia860/ (accessed Sep 1, 2017).

(88) U.S. Energy Information Administration. Annual Electric Utility Data http://www.eia.gov/electricity/data/eia923/ (accessed Sep 1, 2017).

(89) Capes, C. E.; Mcllhinney, A. E.; Russell, D. S.; Sirianni, A. F. Rejection of trace metals from coal during beneficiation by agglomeration. *Environ. Sci. Technol.* **1974**, *8* (1), 35–38.

(90) Dutta, A.; Basu, P.; Ghosh, A.; Chakraborty, P. Innovative solution to the problem of mill rejects in thermal power plants. In *18th International Conference on Fluidized Bed Combustion*; 2005; pp 1–6.

(91) Clarke, L. B.; Sloss, L. L. *Trace Elements - Emissions From Coal Combustion and Gasification*; 1992.

(92) Swanson, S. M.; Engle, M. A.; Ruppert, L. F.; Affolter, R. H.; Jones, K. B. Partitioning of selected trace elements in coal combustion products from two coal-burning power plants in the united states. *Int. J. Coal Geol.* **2013**, *113*, 116–126.

(93) Otero-Rey, J. R.; López-Vilariño, J. M.; Moreda-Piñeiro, J.; Alonso-Rodríguez, E.; Muniategui-Lorenzo, S.; López-Mahía, P.; Prada-Rodríguez, D. Arsenic, mercury, and selenium flue gas sampling in a coal-fired power plant and their fate during coal combustion. *Environ. Sci. Technol.* **2003**, *37* (22), 5262–5267.

(94) National Risk Management Research Laboratory Office. *Control of Mercury Emissions from Coal Fired Electric Utility Boilers: An Update*; Research Triangle Park, NC, 2005.

(95) Electric Power Research Institute. *Hazardous Air Pollutants (HAPs) Emission Estimates and Inhalation Human Health Risk Assessment for U.S. Coal-Fired Electric Generating Units*; 2018.

(96) Chen, C. Y.; Driscoll, C. T.; Eagles-smith, C. A.; Eckley, C. S.; Gay, D. A.; Hsu-kim, H.; Keane, S. E.; Kirk, J. L.; Robert, P.; Obrist, D.; et al. A Critical Time for Mercury Science to Inform Global Policy. *Environ. Sci. Technol.* **2018**.

(97) Chan, H. R.; Chupp, B. A.; Cropper, M. L.; Muller, N. Z. The impact of trading on the costs and benefits of the Acid Rain Program. *J. Environ. Econ. Manage.* **2018**, *88*, 180–209.

(98) Thomson, V. E.; Huelsman, K.; Ong, D. Coal-fired power plant regulatory rollback in the United States: Implications for local and regional public health. *Energy Policy* **2018**, *123*, 558–568.

(99) U.S. Environmental Protection Agency. *Cross-State Air Pollution Rule*; U.S. Environmental Protection Agency: Washington D.C., 2015.

(100) U.S. Department of Energy. *Staff Report to the Secretary on Electricity Markets and Reliability*;

2017.

(101) Hayhoe, K.; Kheshgi, H. S.; Jain, A. K.; Wuebbles, D. J. Substitution of natural gas for coal: Climatic effects of utility sector emissions. *Clim. Change* **2002**, *54* (1–2), 107–139.

(102) Zhang, X.; Myhrvold, N. P.; Caldeira, K. Key factors for assessing climate benefits of natural gas versus coal electricity generation. *Environ. Res. Lett.* **2014**, *9* (11).

(103) Jenner, S.; Lamadrid, A. J. Shale gas vs. coal: Policy implications from environmental impact comparisons of shale gas, conventional gas, and coal on air, water, and land in the United States. *Energy Policy* **2013**, *53*, 442–453.

(104) Lu, X.; Salovaara, J.; McElroy, M. B. Implications of the recent reductions in natural gas prices for emissions of CO2 from the US power sector. *Environ. Sci. Technol.* **2012**, *46* (5), 3014–3021.

(105) Venkatesh, A.; Jaramillo, P.; Griffin, W. M.; Matthews, H. S. Implications of near-term coal power plant retirement for SO2 and NOX and life cycle GHG emissions. *Environ. Sci. Technol.* **2012**, *46* (18), 9838–9845.

(106) Lueken, R.; Klima, K.; Griffin, W. M.; Apt, J. The climate and health effects of a USA switch from coal to gas electricity generation. *Energy* **2016**, *109*, 1160–1166.

(107) U.S. Environmental Protection Agency. Emissions & Generationg Resource Integrated Database, eGRID2014 Version 2.0 (year 2014 data) https://www.epa.gov/energy/emissions-generation-resource-integrated-database-egrid (accessed Aug 1, 2017).

(108) U.S. Environmental Protection Agency. The Emissions & Generation Resource Integrated Database - Technical Support Document for the 9th Edition of eGRID with Year 2010 Data. **2014**.

(109) U.S. Environmental Protection Agency. *Air Pollution Control Technology Fact Sheet – SCR*; Washington D.C., 2003.

(110) U.S. Environmental Protection Agency. *Bituminous and Subbituminous Coal Combustion*; Washington D.C., 1998.

(111) U.S. Energy Information Administration. Monthly Energy Review https://www.eia.gov/totalenergy/data/browser/?tbl=T12.01#/?f=A&start=1973&end=2017&charted=0-1-13.

(112) U.S. Energy Information Administration. Electric Power Monthly https://www.eia.gov/electricity/monthly/epm_table_grapher.php?t=epmt_1_1.

(113) California Air Resources Board. California Ambient Air Quality Standards https://ww2.arb.ca.gov/resources/california-ambient-air-quality-standards.

(114) Kitto, J. B.; Stultz, S. C. *Steam: Its generation and use*, 41st ed.; The Babcock and Wilcox Company, 2005.

(115) U.S. Energy Information Administration. Pennsylvania Electricity Profile, Table 1. 2015 Summary statistics https://www.eia.gov/electricity/state/pennsylvania/ (accessed Jan 8, 2018).

(116) Yang, C.; Yeh, S.; Zakerinia, S.; Ramea, K.; McCollum, D. Achieving California's 80% greenhouse gas reduction target in 2050: Technology, policy and scenario analysis using CA-TIMES energy economic systems model. *Energy Policy* **2015**, *77*, 118–130.

(117) Mileva, A.; Johnston, J.; Nelson, J. H.; Kammen, D. M. Power system balancing for deep decarbonization of the electricity sector. *Appl. Energy* **2016**, *162*, 1001–1009.

(118) Williams, J. H.; Debenedictis, A.; Ghanadan, R.; Mahone, A.; Moore, J.; Iii, W. R. M.; Price, S.; Torn, M. S. The technology path to deep greenhouse gas emissions cuts by 2050: The pivotal role of electricity. *Science (80-.).* **2012**, *335*, 53–60.

(119) U.S. Energy Information Administration. Pennsylvania Nuclear Profile 2010 https://www.eia.gov/nuclear/state/pennsylvania/index.php (accessed Nov 1, 2017).

(120) Calvert, K. E. Measuring and modelling the land-use intensity and land requirements of utility-scale photovoltaic systems in the Canadian province of Ontario. *Can. Geogr.* **2018**, *62* (2), 1–12.

(121) Hernandez, R. R.; Hoffacker, M. K.; Field, C. B. Efficient use of land to meet sustainable energy needs. *Nat. Clim. Chang.* **2015**, *5* (4), 353–358.

(122) Arent, D.; Pless, J.; Mai, T.; Wiser, R.; Hand, M.; Baldwin, S.; Heath, G.; Macknick, J.; Bazilian, M.; Schlosser, A.; et al. Implications of high renewable electricity penetration in the U.S. for water use, greenhouse gas emissions, land-use, and materials supply. *Appl. Energy* **2014**, *123*, 368–377.

(123) Shum, R. Y. A comparison of land-use requirements in solar-based decarbonization scenarios. *Energy Policy* **2017**, *109*, 460–462.

(124) U.S. Energy Information Administration. State Energy Data System (SEDS): 1960-2015 (complete) https://www.eia.gov/state/seds/seds-data-complete.php?sid=PA#Consumption (accessed Jan 8, 2018).

(125) Schivley, G.; Azevedo, I. L.; Samaras, C. Assessing the evolution of power sector carbon intensity in the United States. *Environ. Res. Lett.* **2018**, *13*.

(126) Rubin, E. S.; Zhai, H. The cost of carbon capture and storage for natural gas combined cycle power plants. *Environ. Sci. Technol.* **2012**, *46* (6), 3076–3084.

(127) NETL. Carbon Storage Atlas - Fifth Edition (Atlas V). **2015**, *5*, 114.

(128) National Renewable Energy Laboratory. PV Watts v6 https://developer.nrel.gov/docs/solar/pvwatts/v6/.

(129) Ong, S.; Campbell, C.; Denholm, P.; Margolis, R.; Heath, G. *Land-Use Requirements for Solar Power Plants in the United States*; 2013.

(130) National Renewable Energy Laboratory. Wind Data https://www.nrel.gov/gis/data-wind.html.

(131) Denholm, P.; Hand, M.; Jackson, M.; Ong, S. *Land Use Requirements of Modern Wind Power Plants in the United States*; 2009.

(132) Pletka, R.; Khangura, J.; Rawlines, A.; Waldren, E.; Wilson, D. *Capital Costs for Transmission and Substations*; 2014.

(133) Folger, P. *Carbon Capture and Sequestration (CCS) in the United States*; 2017.

(134) Luzenski, A. J.; Rocca, C. E.; Harness, R. E.; Cummings, J. L.; Austin, D.; Luzenski, J.; Rocca, C. E.; Harness, R. E.; Cummings, J. L.; Austin, D. D.; et al. Collision avoidance by migrating raptors encountering a new electric power transmission line. *Condor Ornithol. Appl. 118* (2), 402–410.

(135) Solar Energy Industries Association. Pennsylvania Solar https://www.seia.org/state-solar-policy/pennsylvania-solar.

(136) Levy, M. Rescuing nuclear power plants could come with conditions. *York Dispatch*. March 3, 2019.

(137) Maykuth, A. Customers would pay millions to rescue PA nuclear reactors, including some that are already profitable. *The Inquirer*. March 9, 2019.

(138) Vajjhala, S. P.; Fischbeck, P. S. Quantifying siting difficulty: A case study of US transmission line siting. *Energy Policy* **2007**, *35* (1), 650–671.

(139) National Renewable Energy Laboratory. *Renewable Electricity Futures Study*; 2012.

(140) Popova, O. H.; Small, M. J.; McCoy, S. T.; Thomas, A. C.; Rose, S.; Karimi, B.; Carter, K.; Goodman, A. Spatial stochastic modeling of sedimentary formations to assess carbon dioxide storage potential. *Environ. Sci. Technol.* **2014**, *48* (11), 6247–6255.

(141) Yudovich, Y. E.; Ketris, M. P. Mercury in coal: A review. *Int. J. Coal Geol.* **2005**, *62* (3), 107–

134.

(142) Yudovich, Y. E.; Ketris, M. P. Selenium in coal: A review. *Int. J. Coal Geol.* **2006**, *67* (1–2), 112–126.

(143) Yudovich, Y. E.; Ketris, M. P. Arsenic in coal: A review. *Int. J. Coal Geol.* **2005**, *61* (3–4), 141–196.

(144) Yudovich, Y. E.; Ketris, M. P. Chlorine in coal: A review. *Int. J. Coal Geol.* **2006**, *67* (1–2), 112–126.

(145) Akers, D. J. The Redistribution of Trace Elements during the Beneficiation of Coal. In *Environmental Aspects of Trace Elements in Coal*; Swaine, D. J., Goodarzi, F., Eds.; Springer Netherlands: Dordrecht, 1995; pp 93–110.

(146) Chen, H. L.; Pagano, M. The Removal of Chlorine from Illinois Coal by High Temperature Leaching. *Fuel Process. Technol.* **1986**, *13*, 261–269.

(147) Cheng, C.-M.; Hack, P.; Chu, P.; Chang, Y.-N.; Lin, T.-Y.; Ko, C.-S.; Chiang, P.-H.; He, C.-C.; Lai, Y.-M.; Pan, W.-P. Partitioning of mercury, arsenic, selenium, boron, and chloride in a full-scale coal combustion process equipped with selective catalytic reduction, electrostatic precipitation, and flue gas desulfurization systems. *Energy & Fuels* **2009**, *23* (10), 4805–4816.

(148) Córdoba, P. Status of Flue Gas Desulphurisation (FGD) systems from coal-fired power plants: Overview of the physic-chemical control processes of wet limestone FGDs. *Fuel* **2015**, *144*, 274–286.

(149) Aunela-Tapola, L.; Hatanpää, E.; Hoffren, H.; Laitinen, T.; Larjava, K.; Rasila, P.; Tolvanen, M. A study of trace element behaviour in two modern coal-fired power plants. *Fuel Process. Technol.* **1998**, *55* (1), 13–34.

(150) Laird, C. P.; Smith, K. J.; Looney, B. Results of Dry Sorbent Injection Testing to Reduce HCl. *Paper No.*, 1–12.

(151) Felsvang, K.; Gleiser, R.; Juip, G.; Nielsen, K. K. Activated carbon injection in spray dryer/ESP/FF for mercury and toxics control. *Fuel Process. Technol.* **1994**, *39* (1–3), 417–430.

(152) Karlsson, H. T. Spray dry scrubbing of secondary pollutants from coal burning. In *Proceedings of the third annual Pittsburgh Coal Conference, MEMS*; 1986; pp 237–252.

(153) U. S. Energy Information Administration. State Profile and Energy Estimates https://www.eia.gov/state/data.php?sid=PA#ConsumptionExpenditures.

(154) Multi-Resolution Land Characteristics Consortium. National Land Cover Database 2011 Land Cover (CONUS) https://www.mrlc.gov/data.

(155) Multi-Resolution Land Characteristics Consortium. National Land Cover Database 2011 (NLCD2011) Legend https://www.mrlc.gov/data/legends/national-land-cover-database-2011-nlcd2011-legend.

(156) Miller, L. M.; Keith, D. W. Observation-based solar and wind power capacity factors and power densities. *Environ. Res. Lett.* **2018**, *13*.

Appendix A: Supplemental Information for Chapter 1

Appendix A.1: Data and model repository

We uploaded all MATLAB code and data spreadsheets used in this analysis in the following GitHub repository: https://github.com/xdansun/trace_elem_cfpp_model

Appendix A.2: Coal-fired generation included and excluded from analysis

In the analysis presented in the main manuscript, we estimate Hg, Se, As, and Cl mass flow rates for 276 plants that generated 1190 TWh of electricity, which is 63% of all coal plants and 89% of all coal electricity generation. For context there are 436 coal plants in the U.S. which generated 1330 TWh in 2015.[88]

We exclude some coal boilers in our analysis due to data limitations on coal boilers collected using EIA-923, Schedule 3, EIA-860, Schedule 6, and COALQUAL. These data limitations include:

Power plants with less than 1 MW capacity: Power plants with a total nameplate capacity less than 1 MW are not required to report generation or environmental control data using EIA-923, Schedule 3 and EIA-860, Schedule 6. Therefore, we do not know what percentage of plants are affected nor how much electricity these plants generated.

Boilers connected to multiple generators and vice-versa: Where boilers are connected to multiple generators and vice-versa, we are unable to attribute generation to a boiler or normalize mass flow rates based on electricity generation. About 24% of plants and 4.6% of coal generation are removed from our analysis due to this limitation.

Boilers without coal purchases: Without the location of coal purchases and quantity of coal purchased, we cannot estimate the concentrations of trace elements in the coal blend. This data limitation removes an additional 6.7% of plants and 3.1% of coal generation.

Boilers that burn foreign and/or waste coal: Our dataset for run-of-mill coal samples, COALQUAL, only includes domestic and non-waste coal samples, so we cannot estimate trace element concentrations in foreign or waste coal.[86] This data limitation removes an additional 5.3% of plants and 2.8% of coal generation.

Boilers that do not report fuel consumption: Without knowing how much fuel is combusted in the boiler, we cannot estimate the mass flow rates of trace elements from the coal blend. This data limitation removes an additional 0.3% of plants and 0.3% of coal generation.

The amount of generation excluded from our analysis due to the above limitations are listed in Table A1. Overall, at least 10.8% of coal generation is lost in the analysis, with 4.6% of total generation lost from boiler to generator linking issues and 6.2% of total generation lost from coal consumption and purchasing issues.

Table A1: Percent of total coal generation that is not included in our analysis due to data limitations in input data of coal plants. For context there are 436 coal plants in the U.S. which generated 1330 TWh in 2015.[88]

Data limitation	Plants excluded in analysis		Generation excluded in analysis	
	(plants)	(%)	(TWh)	(%)
Power plants with less than 1 MW capacity	Unknown	Unknown	Unknown	Unknown
Boilers connected to multiple generators and vice-versa	105	24.1	61	4.6
Power plants which did not report coal purchases	29	6.7	41	3.1
Boilers that burn foreign and/or waste coal	23	5.3	37	2.8
Boilers that do not report fuel consumption	1	0.2	4	0.3
Total	**158**	**36.3**	**144**	**10.8**

Table produced by the authors using data from COALQUAL, EIA-923, Schedule 3 and EIA-860, Schedule 6.[86–88]

Appendix A.3: Variability of coal within each county

COALQUAL reports trace element concentrations in coal samples across different counties in the U.S. For each county, the concentration of trace elements and the number of samples can vary. In Figure A1 we show the variability in the concentration of trace elements across five illustrative U.S. counties and for all samples reported in COALQUAL. We also report the number of samples reported in each county. We selected the five counties for each trace element by first, ordering the counties by range of trace element concentration in ascending order and second, choosing one county from each quintile of the ordered counties.

At the county level, we find significant variability in the concentration of trace elements even if there are a few samples from the county. For example, in Figure A2B, county 29011 has 8 selenium samples reported but the samples vary by a factor of 5 (lowest is 3.2 ppm and highest is 15.2 ppm). At the national level, there are many outliers in the COALQUAL database. About 2-8% of the reported data for each trace element are outliers, all of which are high values. We also find that range of measurements from the 75^{th} to 100^{th} percentiles is much greater than the range from 0^{th} to 25^{th} percentiles, which suggests that our data may have more outliers with high trace element concentrations that can lead to trace element concentrations in coal and subsequently, higher estimates of trace elements in the waste streams.

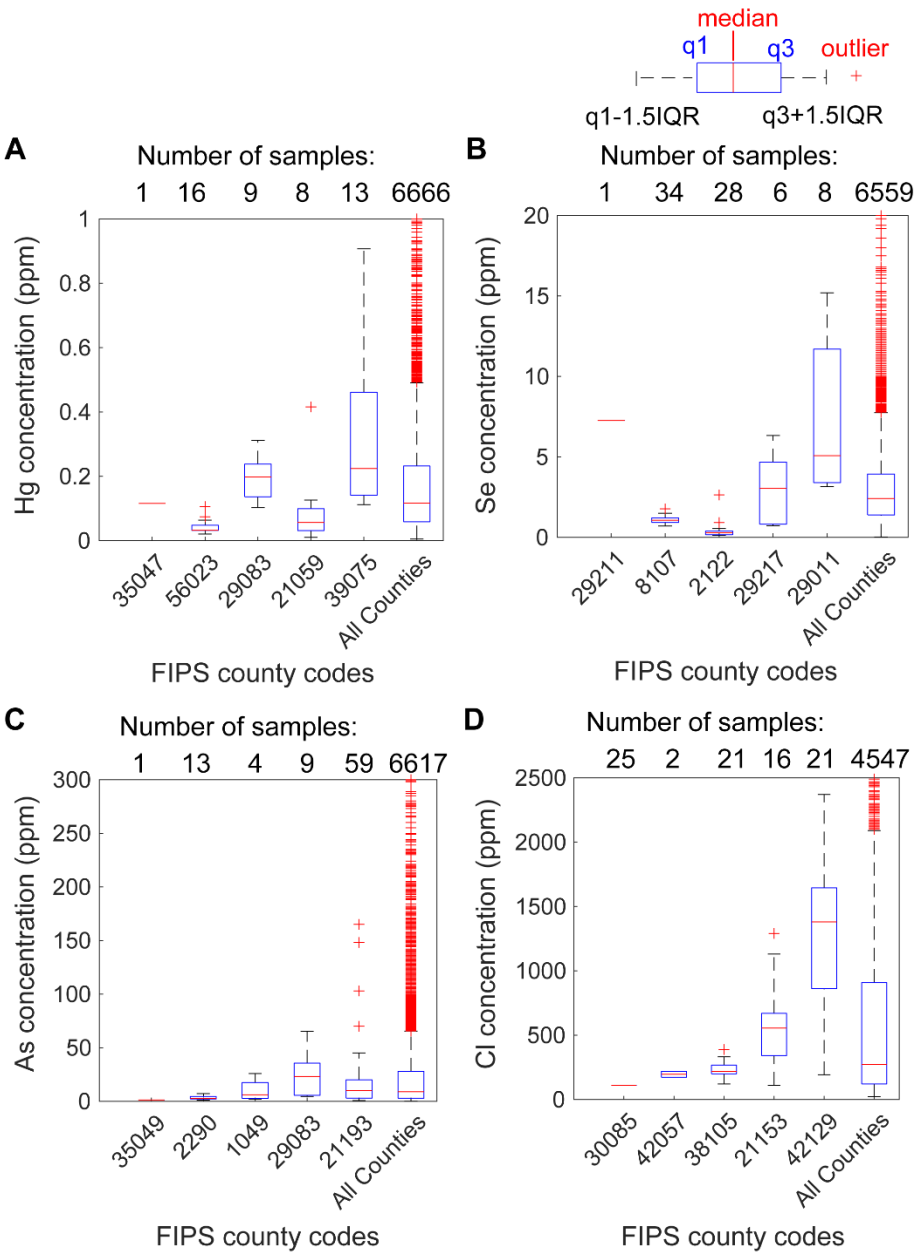

Figure A1: Boxplots of trace element concentrations in coal samples in COALQUAL at a few illustrative U.S. counties and all coal samples reported in COALQUAL for the trace elements A) Hg, B) Se, C) As, and D) Cl. The number of coal samples in each county are reported in A) and are the same across all four trace elements. The y-axis is cutoff for readability. The highest concentration reported is 3.3 ppm for Hg, 153 ppm for Se, 2200 ppm for As, and 8920 ppm for Cl. In the boxplot, the red line is the median, the blue lines are the first and third quartiles, the lower whisker is the first quartile minus 1.5 times the interquartile range, the upper whisker is the third quartile plus 1.5 times the interquartile range, and the red crosses are outliers. The figure is produced using COALQUAL data.[86]

Appendix A.4: Map of eGRID sub-regions

Figure A2 shows the 26 Emissions and Generation Resource Integrated Database (eGRID) sub-regions in the U.S. The EPA designed the eGRID sub-regions to mimic regional transmission organizations and independent system operators within North American Electric Reliability Corporation regions. In our study, we focus on the contiguous U.S.

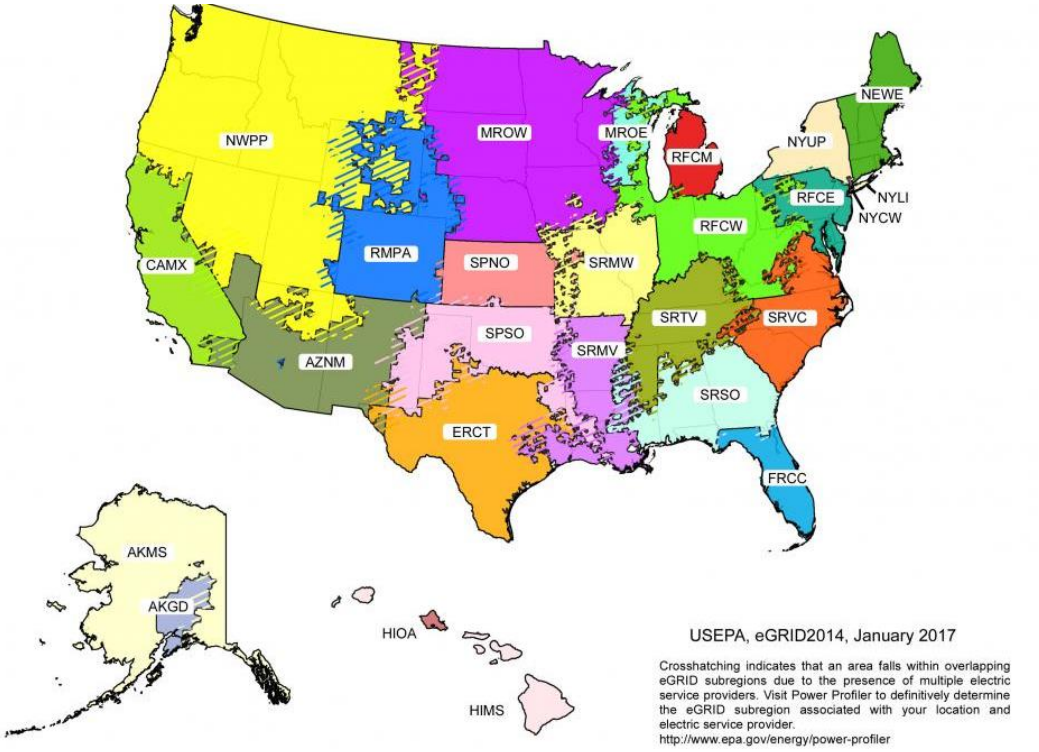

Figure A2: Map of eGRID sub-regions (source: https://www.epa.gov/energy/egrid-sub-region-representational-map)

Table A2 shows the number of plants with at least one boiler with coal as its primary fuel, coal generation, total coal capacity, and average capacity factor for all coal electrical generating units in each eGRID sub-region within the contiguous U.S. included in our modeling dataset (Appendix A.2 for more information on plant inclusion). The NYCW and NYLI sub-regions have no coal plants. The one coal plant in sub-region CAMX and the five coal plants in sub-region NEWE are removed from our analyses for the reasons listed in Appendix A.2. One plant, Roy S Nelson, does not have an eGRID sub-region reported and is therefore not included in any eGRID-level analysis in either Chapter 1 or Appendix A.

In Table A2 we also show the percentage of plants and percent of coal generation modeled for each eGRID sub-region. We find that we model 45-89% of coal plants and 68-96% of coal powered electricity generation in each eGRID sub-region. See Appendix A.2 for more details about coal plants included in the analysis.

Table A2: The number of coal plants, coal generation, coal capacity, and coal capacity factor in 2015 for all coal plants included in the model dataset in each eGRID sub-region.

eGRID sub-region[a]	Coal plants[b]	Generation (TWh)	Capacity (GW)	Average capacity factor	Coal plants modeled (%)	Coal generation modeled (%)
AZNM	7	24	4.6	0.59	71	96
ERCT	17	98	20.8	0.54	88	92
FRCC	11	41	10.2	0.46	45	56
MROE	12	15	3.5	0.49	50	94
MROW	63	111	21.6	0.59	54	96
NWPP	21	111	20.2	0.63	71	95
NYUP	7	2	1.9	0.14	57	85
RFCE	19	46	14.7	0.36	68	68
RFCM	24	52	11.5	0.52	50	78
RFCW	79	280	64.5	0.50	66	92
RMPA	17	46	7.9	0.67	76	99
SPNO	14	41	8.6	0.55	86	100
SPSO	18	67	14.6	0.53	89	92
SRMV	5	24	6.6	0.42	80	87
SRMW	29	107	22.2	0.55	62	88
SRSO	19	79	21.5	0.42	63	88
SRTV	28	103	26.3	0.45	71	91
SRVC	32	77	20.6	0.43	59	87
Roy S Nelson[c]	1	2.1	0.6	0.39	0	0

[a] We exclude sub-regions AKGD, AKMS, HIMS, and HIOA because they are not in the contiguous U.S. and sub-regions CAMX, NEWE, NYCW, and NYLI because there are no coal plants remaining in those sub-regions after applying the criteria mentioned in Appendix A.3.

[b] The number of plants with at least one boiler using bituminous, subbituminous, or lignite coals as its primary fuel.

[c] Roy S. Nelson power plant is excluded in all analysis in the manuscript and SI.

Note: Table produced using data from EIA-923, Schedule 3 and eGRID2014.[88,107]

Appendix A.5: Concentration of trace elements in coal blends

We estimate a distribution for the concentration Hg, Se, As, and Cl entering each U.S. coal plant in 2015 as described in the Methods section of the main manuscript. In Figure A3A-D, we show an illustration of the results for a few coal plants, and in Figure A3E-H we provide the distribution of median concentrations across our entire dataset. In Figure A4, we also show the distribution of median concentrations at each eGRID sub-region.

In Figure A3A-D, the five plants we chose are the Greene County plant in Alabama (ORISPL: 10), the Escalante plant in New Mexico (ORISPL: 87), the Limestone plant in Texas (ORISPL: 298), the Indian River Generating Station in Deleware (ORISPL: 594), and the E.D. Edwards plant in Illinois (ORISPL: 856). These 5 plants generated 2.2 TWh, 1.3 TWh, 9.2 TWh, 0.6 TWh, and 2.9 TWh respectively.

As explained in the methods section, for each plant, we bootstrap 10,000 draws, and in Figure A3H the median distribution shows the cumulative distribution function of the median for each plant (and the same strategy is pursued for the 25^{th} and 75^{th} percentiles). We find that the median of the median concentrations of trace elements across the plants in our dataset is 0.13 ppm for Hg, 1.4 ppm for Se, 3.4 ppm for As, and 122 for Cl. These concentrations are within the same order of magnitude as the median of the median concentration of trace elements from the MATS ICR, which are 0.08 ppm for Hg, 1.0 ppm for Se, 2.0 ppm for As, and 200 for Cl (See Appendix A.12 for more details).

There is significant variability in the concentrations of trace elements in combusted coal both within an individual plant and across the coal-fired fleet. For some power plants, variability associated with concentrations of trace element in coal is substantial (for illustration, plant 10 in Figure A3A has a Hg concentration in the coal blend ranging from 0.005 ppm to 1 ppm, representing a 200x difference between the lowest and highest estimated values), due to difference in the trace element in coal reported in the samples in COALQUAL and the variability in the monthly coal purchased from different counties. Across the fleet, the variability in trace element content is mostly determined by differences in the coal across U.S. regions, such as Wyoming Powder River Basin subbituminous coal versus eastern bituminous coal.[141–144] In the Appendix A.13, we also show these results for plants located in each eGRID sub-region, which highlights the regional diversity in the trace element content of coal combusted at CFPPs.

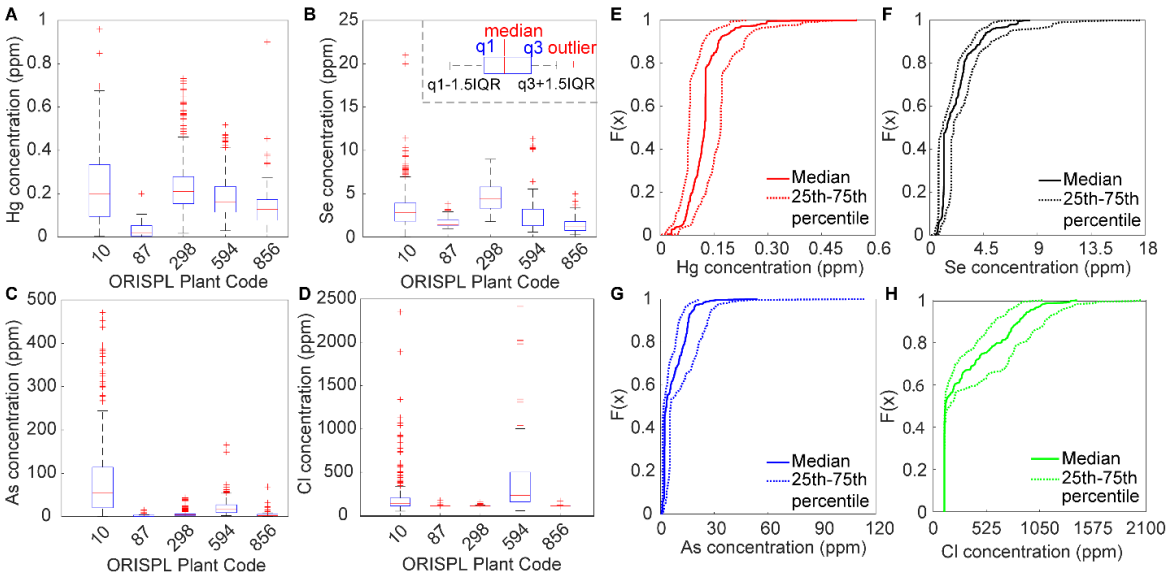

Figure A3: **(A-D)** Estimates of trace element concentration in coal entering a few illustrative U.S. coal-fired power plants. In the boxplot, the red line is the median, the blue lines are the first and third quartiles, the lower whisker is the first quartile minus 1.5 times the interquartile range, the upper whisker is the third quartile plus 1.5 times the interquartile range, and the red crosses are outliers. **(E-H)** Cumulative distribution functions of 25th percentile, median, and 75th percentile of the bootstrapped concentrations of trace elements in the coal blend across coal plants in the coal fleet. For the two panels, the following trace elements are represented: A/E) Hg, B/F) Se, C/G) As, and D/H) Cl

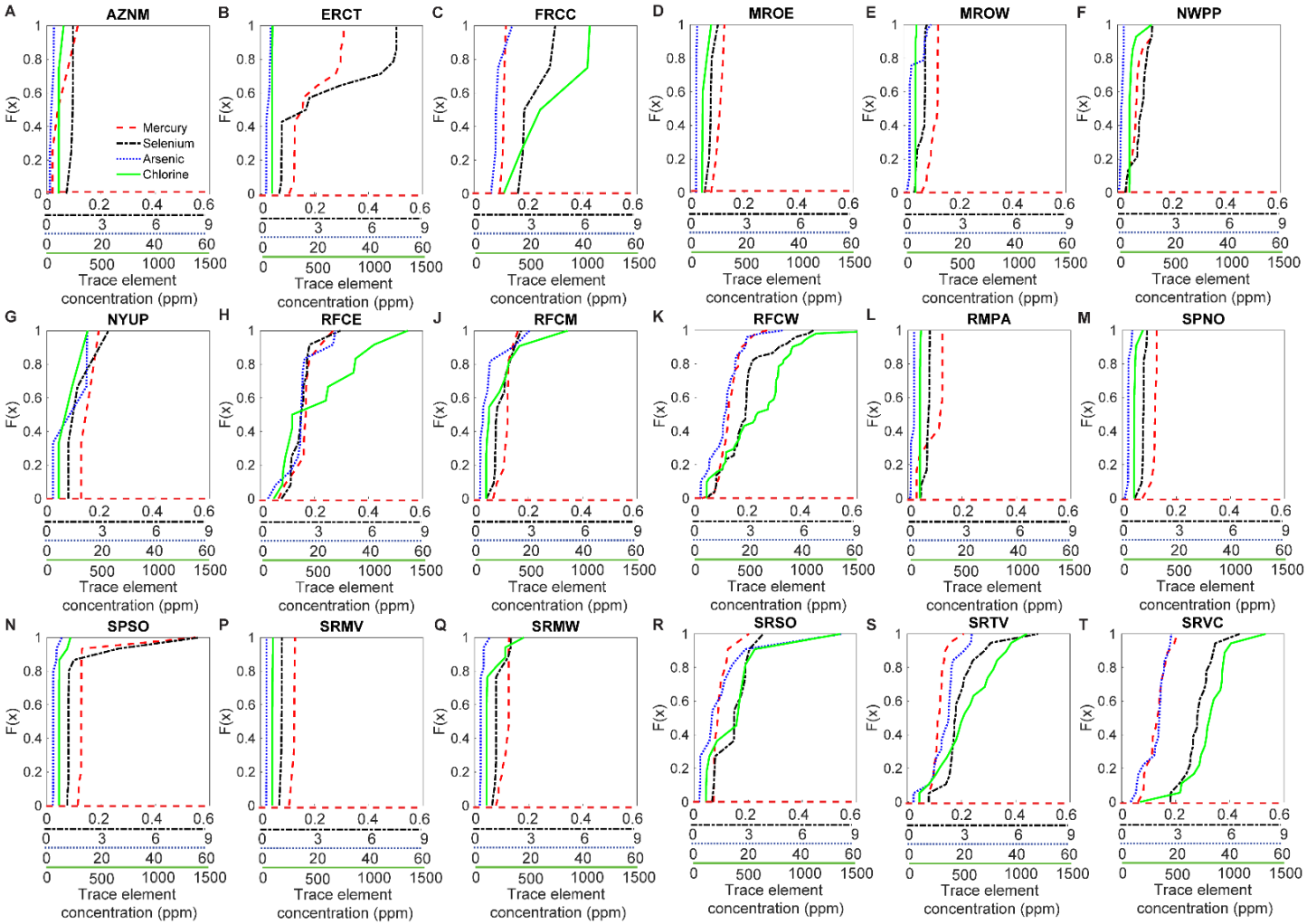

Figure A4: Cumulative distribution functions of the bootstrapped median Hg, Se, As, and Cl concentrations in the coal blend across coal plants in the eGRID sub-regions A) AZNM, B) ERCT, C) FRCC, D) MROE, E) MROW, F) NWPP, G) NYUP, H) RFCE, J) RFCM K) RFCW, L) RMPA, M) SPNO, N) SPSO, P) SRMV, Q) SRMW, R) SRSO, S) SRTV, V) SRVC. We excluded sub-regions AKGD, AKMS, HIMS, and HIOA because they are not in the contiguous US and sub-regions CAMX, NEWE, NYCW, and NYLI because there are no coal plants remaining in those sub-

regions after applying the criteria stated in Appendix A.3. Figure produced by the authors using data from COALQUAL and EIA-923 Schedule 5.[86,88]

Lastly, we compare estimates of trace element concentrations by bootstrapping coal samples by location and by taking the median of all coal samples at the location. We refer to the former as the "bootstrap approach" and the latter as the "median approach." The bootstrap approach is the approach utilized in the manuscript.

In Figure A5 we show the median concentration of trace elements using the bootstrap approach and the concentration of trace elements using the median approach. Although one may expect the median concentration of the bootstrap approach to nearly equal the median approach, they can produce different results at the plant level because the median is not a linear operator. A plant that purchases coal from multiple counties will have a higher chance of bootstrapping a sample away from the median, which skews toward values much greater than the median. Hence, each trace element has plants where the two approaches estimate different concentrations.

Although the two approaches have differences, the median approach performs reasonably well as a method to estimate trace element concentrations and is a simpler method to use. Ultimately, the median approach does not handle the variability of trace element concentrations at any level and can only generate point estimates. Thus, we use the bootstrap approach in our work.

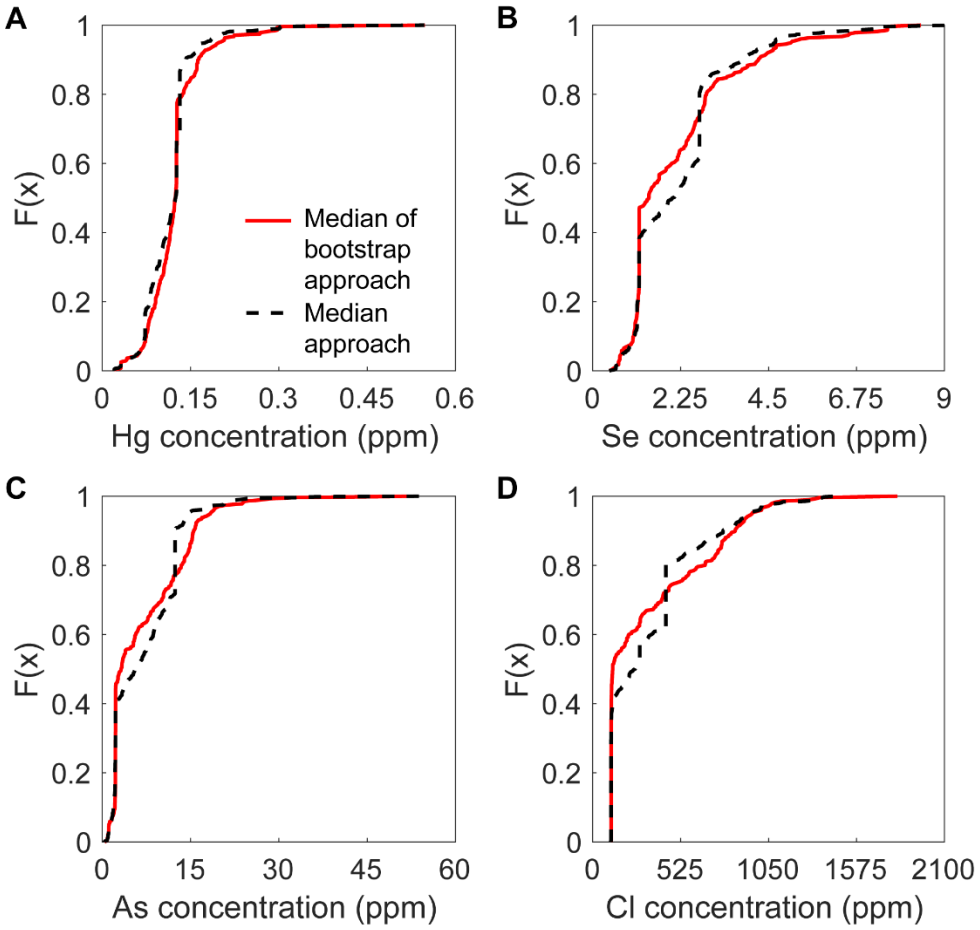

Figure A5: Cumulative distribution functions of concentrations of trace elements in the coal blend at the plant level using bootstrap approach and median approach for trace elements A) Hg, B) Se, C) As, and D) Cl. For the bootstrap approach, the median of the bootstrapped trace element concentration is shown.

Appendix A.6: Effect of COALQUAL lower detection limit assumptions on the concentration of trace elements in coal blends

In COALQUAL, there are 6666 Hg samples, 6560 Se samples, 6618 As samples, and 4548 Cl samples. Of these samples, about 4% of Hg samples, 3% of Se samples, 1% of As samples, and 21% of Cl samples are below the detection limit. COALQUAL assumes that samples below the detection limit have concentrations equal to 0.7 times the detection limit.

In Figure A6, we plot a cumulative distribution function showing the median concentration of trace elements in the coal blend at the plant level assuming samples below the detection limit have concentration equal to either 0 or equal to the lower detection limit. We find for Hg, Se, and As that the assumption in the lower detection limit has little effect on the concentration of trace elements at the plant level. Indeed, the median of the difference in median concentrations for Hg, Se, and As is 0.04 ppm, 0.004 ppm, and 0.04 ppm respectively. These results are not surprising given the small percentage of samples in COALQUAL that are below the detection limit.

However, we find that Cl concentrations in the coal blend of half of the coal fleet can change by up to 130 ppm depending on whether we assume samples below the detection limit equals zero or equals the detection limit. Even though only 21% of Cl samples are below the detection limit, these results are still surprising because they affect half of the coal fleet. This result suggests that nearly half of the fleet purchase coal from counties where COALQUAL only has samples that are below the detection limit. Therefore, the detection limit issue highlights one additional problem with the COALQUAL data, especially when estimating Cl concentrations in coal blends.

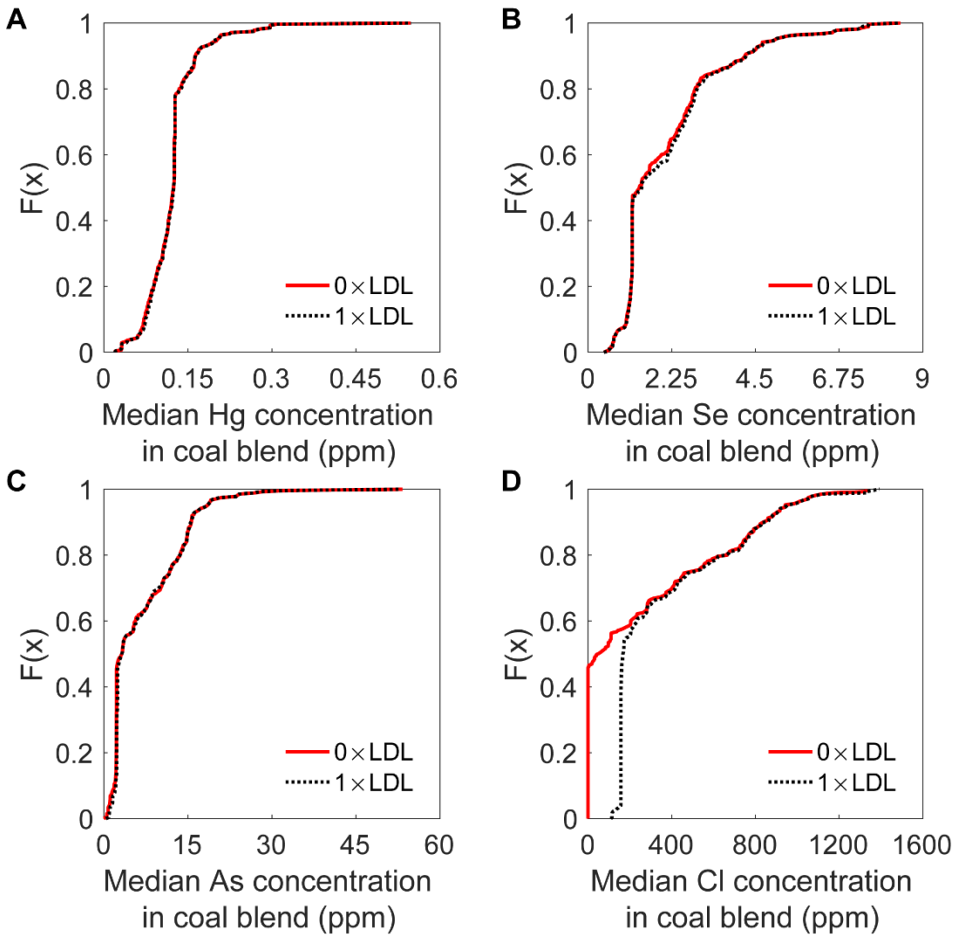

Figure A6: Cumulative distribution functions of trace elements in the coal blend at the plant level assuming all samples with concentrations lower than the detection limit have concentration equal to zero or equal to the detection limit for trace elements A) Hg, B) Se, C) As, and D) Cl. COALQUAL assumes all samples below the lower detection limit have concentration equal to 0.7 times the detection limit.

Appendix A.7: Coal purchases from preparation plants

Coal plants report coal purchases from mines and preparation plants in EIA-923, Schedule 5. In 2015, coal plants purchased nearly 780 million tons of coal, of which only 42 million tons were purchased from coal preparation plants. Thus, less than 6% of total coal purchases coming from coal preparation plants.[88] This has been consistent since 2009, with about 4-8% of coal purchases from coal preparation plants, as shown in Figure A7. Additionally, less than 1% of trace metals are removed by on-site coal pulverization prior to combustion.[89,90] Because cleaned coal purchases account for a small percentage of total coal purchases, and on-site processing does not remove a significant fraction of trace elements, we assume coal cleaning does not affect our trace element inputs.

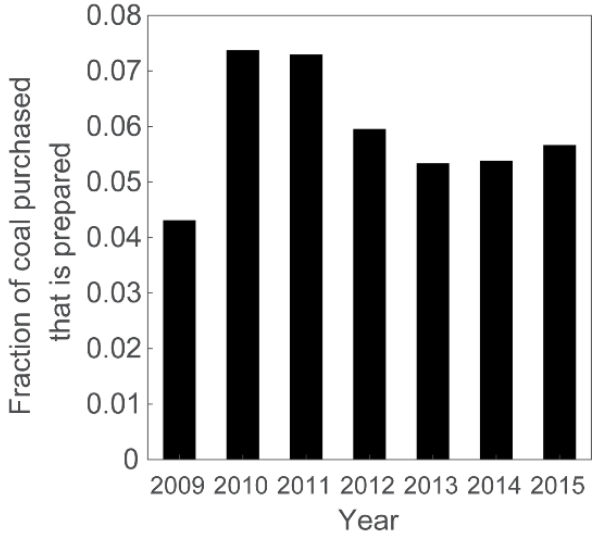

Figure A7: Fraction of prepared coal purchased to total coal purchased made by coal plants from 2009 to 2015. Figure produced using data from EIA-923, Schedule 5.[88]

Modeling coal cleaning is not simple, due to a lack of information about the processes that take place at different coal preparation plants. We perform a conservative analysis where we assume coal cleaning removes the highest concentration of trace elements observed in the literature for all coal samples in a county with a preparation plant. The highest removals we observed for Hg, Se, As, and Cl from coal cleaning are 78.3%, 80.3%, 84.6%, and 68%.[145,146] We rerun our model after adjusting for coal concentrations using the aforementioned coal cleaning removals and recreate Figure 4 from the manuscript.

As shown in Figure A8, model accuracy changes modestly. The notable changes are in the Hg CEMS result, where the median estimate is 1.8 mg Hg/MWh, which is an improvement from the previous result of 2.8 mg/MWh. However, we still observe 81 boilers, which is close to a third of boilers in the Hg CEMS validation analysis, that exceed 5.9 mg Hg/MWh, which is the regulated mercury emissions limit for high-rank coal units. Therefore, even with this conservative coal cleaning assumption, we still overestimate Hg emissions to the gas phase.

The other notable improvement is with the validation against the wet flue gas desulfurizer mass flow rate observed by the EPA during the ELG rulemaking. We find that the Hg validation improves from a 500%

difference between our estimate and EPA's to 360% under the coal cleaning assumption. This improvement gets the model closer to the EPA estimated values, but still represents an overestimate of Hg mass flow rate.

Ultimately, while we find some improvements with a conservative coal cleaning assumption, we find that our conclusions are the same. Data quality improvements and more data of lesser documented processes, such as bromine addition, are more important to bridging the gap between model estimates of trace element mass flow rates to the ground truth. Therefore, we believe coal cleaning is a second-order effect and that we can safely not account for it.

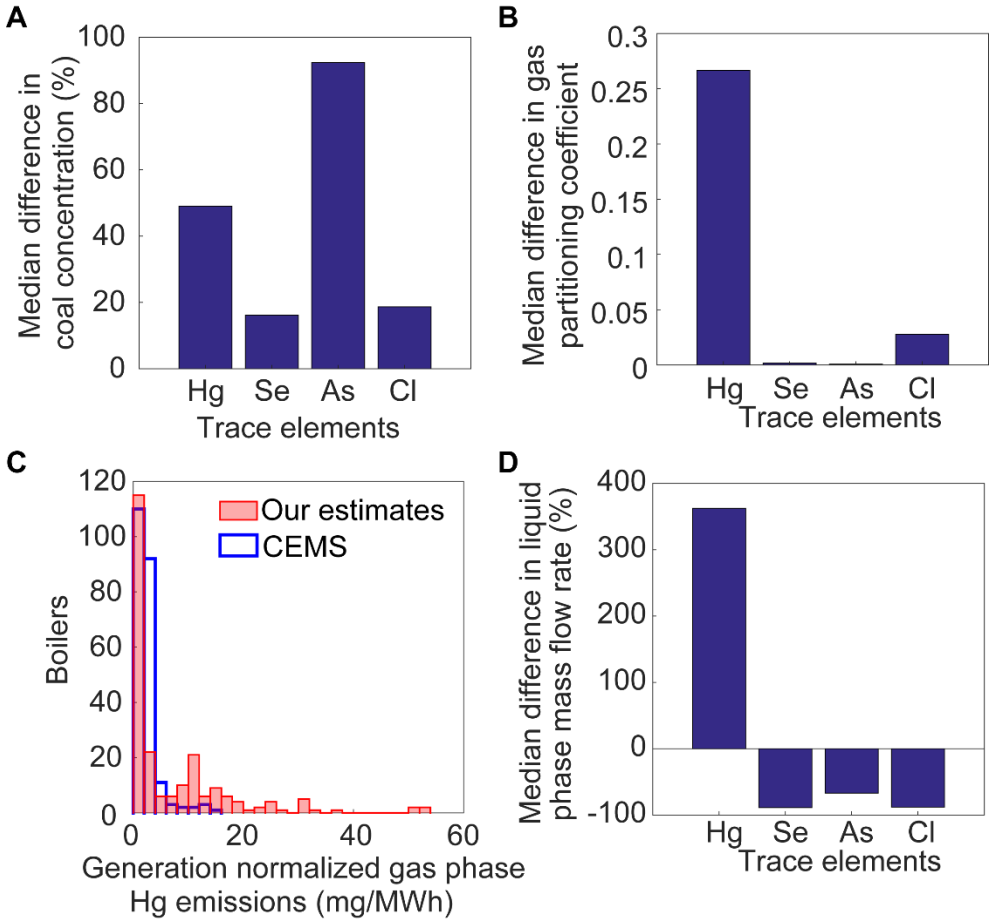

Figure A8: Summary of the comparison analyses under the assumption that all coal purchased from counties with coal preparation plants are cleaned to the maximum extent. A) Median percent difference in plant-level trace element composition of coal between model estimates and data reported in the MATS ICR; B) Median difference in boiler-level trace element partitioning to the gas phase between model estimates and data reported in MATS ICR; C) Histogram of generation normalized boiler level gas phase Hg emissions estimated from model and reported in the CEMS in 2015; D) Median percent difference in liquid phase mass flow rates estimated at the fleet level compared to average mass flow rates for the 88 plants sampled and reported in the Environmental Assessment of the Effluent Limitation Guidelines.

Appendix A.8: Studies on partitioning of trace elements by air pollution control

In Table A3 we list the removal fraction of trace elements by the boiler and different air pollution control devices for each study included in the model. For those studies that include several boilers or plants, we calculate the partitioning factors for each plant and use the average removal to represent that study. We only include trace element partitioning estimates from U.S. CFPPs. We assume all waste exiting particulate matter controls and the gypsum stream of wet flue gas desulfurizers is in the solid phase, all waste exiting the chloride purge stream of wet flue gas desulfurizers is in the liquid phase, and all remaining wastes exit the plant in the gaseous phase. We assume wet flue gas desulfurization is always the last air emission control downstream of the boiler.

A significant fraction of trace metals are removed by particulate matter controls because of the presence of particulate bound trace metals in the flue gas and high fly ash removal rates of particulate matter controls.[147] Particulate matter controls are more efficient at removing Se and As from the flue gas than Hg because Se and As are less volatile than Hg.[147] However, the addition of activated carbon injection combined with a particulate matter control can remove up to 80% of Hg in the flue gas, which is comparable to the removal of Se and As by particulate matter controls.

A fraction of trace metals is also removed by sulfur dioxide controls. There are two types of post-combustion sulfur dioxide controls: wet flue gas desulfurizers and dry/semi-dry flue gas desulfurizers. Wet flue gas desulfurizers capture a significant fraction of the fine particles that are not captured by upstream particulate matter controls, which leads to conversion of trace metals from gas phase to solid phase.[148] Specifically for Hg, the selective catalytic reactor helps promote the oxidation of Hg^0 into Hg^{+2} so that wet flue gas desulfurizers can direct more Hg into liquid waste streams, but it is not clear that selective catalytic reactors have the same effect on other trace metals.[94] Dry and semi-dry flue gas desulfurizers serve a similar function as the wet flue gas desulfurizer but produce zero liquid phase waste. Waste products from dry flue gas desulfurizers are entrained in the flue gas and removed by a downstream particulate matter control, typically a fabric filter though some dry flue gas desulfurizers will have an additional waste for a fraction of the byproducts.[149]

Chloride exists predominantly as hydrochloric acid in flue gas, which is not affected by particulate matter controls but easily removed by any of the sulfur dioxide controls, including dry sorbent injection. Dry sulfur dioxide controls will direct chloride into solids that are removed by downstream particulate matter controls.[150] Wet flue gas desulfurizers will direct chloride into the liquid phase.

Within each air pollution control device, the partitioning of trace elements varies across different studies due to differences in coal composition and operating conditions. For simplicity, we assume selective catalytic reactors and activated carbon injection only affect mercury partitioning, dry sorbent injection only affects chlorine partitioning, and all pollution controls not included in Table A3 do not affect trace element partitioning.

For studies with multiple samples, we calculate the partitioning factor for each sample and use the average partitioning to represent the study. However, we use the partitioning factor of each sample to represent the study if they sample air pollution control devices that are not well studied so that we can increase the sample size in our bootstrapping analysis. Therefore, we use sample level data for mercury partitioning by fabric filters and combinations of activated carbon injection and particulate matter

controls. We also use sample level data for chloride partitioning by dry sorbent injection. Those studies where we use sample level data are listed in Table A3.

Additionally, some combinations of air pollution control devices are best modeled as a single unit. For example, the particulates created in a dry flue gas desulfurizer are typically removed by a fabric filter. We treat the following air pollution control device combinations as a single device: dry sorbent injection and any particulate matter control device,[150] dry flue gas desulfurizers with any particulate matter control device,[151] and selective catalytic reactors with wet flue gas desulfurization for Hg.[94] Due to a lack of Cl partitioning data for hot-side electrostatic precipitators and fabric filters, we assume those particulate matter controls partition Cl in an identical manner as a cold-side electrostatic precipitator. This assumption is not expected to significantly impact the study results because Cl is generally unaffected by particulate matter controls.[147]

Several studies of plants with electrostatic precipitators installed do not report whether the technology is a cold-side electrostatic precipitator or a hot-side electrostatic precipitator. We assume that all unspecified electrostatic precipitators are cold-side electrostatic precipitators, because they are more prevalent than hot-side electrostatic precipitators (58% of coal generation vs. 8% of coal generation as shown in Table A4 in Appendix A.11). Swanson et al.[92] describe that fly ash from cold-side and hot-side electrostatic precipitators are mixed before trace elements were sampled, and so we assume the partitioning factors for cold-side and hot-side electrostatic precipitators are the same in that study.

Multiple studies report partitioning of trace elements by wet flue gas desulfurizers. However, only Cheng et al.[147] specify the partitioning of trace elements exiting the wet flue gas desulfurizer into the liquid chloride purge and solid gypsum stream, and so we assume these same partitioning between liquid and solid phases hold for other studies. The ratio of liquid to solid trace element exiting the wet flue gas desulfurizer based on Cheng et al. is 0.11 for Hg, 0.04 for Se, 9e-4 for As, and 0.98 for Cl.

Table A3: Removal fraction of trace elements listed by study, boiler or air pollution control, and pollutant for studies included in the model.

		Removal by boiler				Removal by PM control				Removal by SO_2 control				Source	Data type	Other
	APCDs	Hg	Se	As	Cl	Hg	Se	As	Cl	Hg	Se	As	Cl			
Brekke et al. (1995)[9]	csESP					0.3	0.2							Coal plants	Removal fractions	
	FF					0.6	0.65									
Brown et al. (1999)[10 a, b]	csESP, wFGD					0.3				0.411				Coal plants	Reported from another study	assume csESP
	FF					0.65										
						0.85										
						0.90										
						0.55										
						0.65										
						0.68										
						0.95										
						0.99										
						0.98										
						0.99										
						0.50										
						0.65										
						0.67										
Cheng et al. (2009)[8]	SCR, csESP, wFGD	0.003	0.069	0.064	0.004	0.174	0.604	0.946	0.024	0.946	0.86	0.997	0.988	Coal plants	Mass flows	assume csESP
Chu and Porcella (1995)[11]	csESP, wFGD					0.3				0.15				Coal plants		
	FF					0.3										
Devito et al. (2002)[12]	csESP, wFGD	0.029				0.161				0.444				Coal plants	Removal fractions	assume csESP
	dFGD, FF									0.333	0.998	0.999		Coal plants	Removal fractions	

Felsvang et al. (1994)[151]	ACI, dFGD, FF									0.990						
Flora et al. (2003)[13, b]	ACI, FF					0.122								Coal plants	Removal fractions	
						0.841										
						0.887										
						0.682										
						0.31										
						0.428										
						0.656										
						0.627										
						0.037										
						0.054										
						0.90										
						0.875										
						0.796										
						0.965										
						0.808										
						0.732										
						0.328										
						0.967										
						0.925										
						0.918										
						0.877										
						0.862										

						0.102										
Helble (2000)[14]	csESP					0.289	0.491	0.961						From EPRI and DoE		assume csESP
Karlsson (1984)[152]	dFGD, FF												0.97	Coal plants	Removal fractions	
Klein et al. (1975)[15]	csESP	0.019	0.163	0	0.006	0.038	0.038	0.805	0.818	0.011				Coal plants	Mass flows	
Laird et al. (2013)[150, b]	DSI												0.917	Coal plants	Mass flows	
													0.989			
													0.9996			
													0.969			
													0.969			
													0.71			
													0.78			
													0.64			
													0.84			
													0.77			
Laudal et al. (2000)[16]	csESP, wFGD					0.034				0.19				Coal plants	Mass flows	assume csESP
NRMRL (2005)[17, b]	ACI, csESP					0.65								Coal plants	Removal fractions	
						0.70										
						0.73										
						0.85										
						0.94										
						0.94										
	ACI, hsESP					0.40										
						0.80										
Ondov et al. (1979)[18]	csESP, wFGD						0.941	0.921	0		0.05	0.075	0.964	Coal plants	Removal fractions	
Pavlish et al. (2003)[30 a]	csESP, wFGD					0.233				0.403				From 1999 EPA ICR	Removal fractions	

	hsESP, wFGD					0.128				0.29					
	FF, wFGD					0.323				0.103					
Rubin (1999)[20] [c]	csESP	0.008	0.015	0.014	0.001	0.254	0.252	0.595	0.96	0				From model	Removal fractions	assume csESP
Swanson et al. (2013)[7]	csESP	0	0	0.04		0.02	0.2	0.5						Coal plants	Removal fractions	
	hsESP	0	0	0.04		0.02	0.2	0.5								

[a] We incorporate data from only one of the studies cited within the review paper, because the other studies overlapped with another study already included in our table. We cite the review paper, because we were unable to obtain copies of the original paper cited in the review.

[b] To increase sample size for the bootstrapping analysis, we use sample level data for this study.

[c] Rubin estimated partitioning of trace elements using data from a combination of empirical samples and literature data.[81] His results are summarized as point estimates, which we use for bootstrapping.

Notes: Studies either sampled data from CFPPs or perform secondary analysis using reported data from other studies. The partitioning of trace elements is reported in either fractions removed or in mass flows across different air pollution controls. Plants that did not specify if they were csESP or hsESP were assumed to be cold-side ESP. Studies used in the model are indicated in bold. Only studies that included U.S. CFPPs are included. The controls are: ACI – activated carbon injection; csESP – cold-side electrostatic precipitator; dFGD – dry flue gas desulfurizer, DSI – dry sorbent injection, FF – fabric filter; hsESP – hot-side electrostatic precipitator; SCR – selective catalytic reactor; wFGD – wet flue gas desulfurizer.

Appendix A.9: Partitioning of trace elements to the solid, liquid, and gas phase at each coal boiler

In Figure A9, we show the cumulative distribution functions of bootstrapped partitioning fractions of trace elements into solid, liquid, and gas phases for each U.S. coal boiler in our dataset. As expected, a small fraction of trace metals and a large fraction of chlorine will end up in liquid waste. For CFPPs with a wet flue gas desulfurizer, trace element partitioning into the liquid phase ranges from 0.003 to 0.105 for Hg, 0.005 to 0.035 for Se, $4x10^{-5}$ to $9x10^{-4}$ for As, and 0.13 to 0.97 for Cl. Trace element partitioning into the solid phase ranges from 0.02 to 0.99 for Hg, 0.20 to 0.98 for Se, 0.52 to 1.0 for As, and 0.001 to 0.86 for Cl. The partitioning factors to solid phase observed in Figure A9 are consistent with the chemistry of these trace elements, as less volatile trace elements, such as Se and As, are more likely to condense out of the gas phase, while less volatile elements, such as Hg and Cl are less likely to condense out.[92,93]

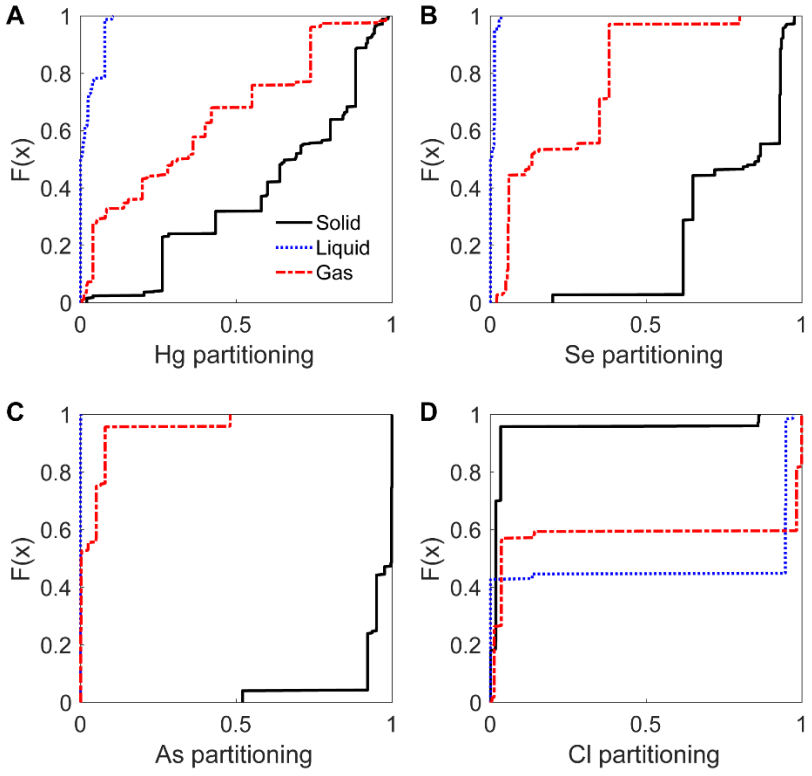

Figure A9: Bootstrapped cumulative distribution functions of trace element partitioning into solid, liquid, and gas phases at each boiler across the coal fleet for A) Hg, B) Se, C) As, and D) Cl. Figure produced by the author using data from Table A3.

Appendix A.10: Comparing partitioning fractions estimated matching individual air pollution control devices against matching combinations of air pollution control devices

In the manuscript, we estimate trace element partitioning fractions at the boiler level by estimating the partitioning fraction for each air pollution control downstream of the boiler and combining as shown in Equation A1.

$$x^{link}_{boiler,\phi,TE} = x_{PM,\phi,TE} + x_{PM,\phi=gas,TE} \times x_{SO_2,\phi,TE} \text{ (A1)}$$

Where $x^{link}_{boiler,\phi}$ is the overall partitioning fraction for the boiler for a phase ϕ and a trace element *TE*. Also $x_{PM,\phi,TE}$ is the partitioning fraction at the particulate matter control and activated carbon injection and $x_{SO_2,\phi,TE}$ is the partitioning fraction at the sulfur dioxide control and the selective catalytic reactor, both of which are derived from the literature. We call this method the "link" method.

The method presented in Equation A1 assumes that partitioning is independent of the plant processes before or after the air pollution control. To test this assumption of independence, we estimate the partitioning fraction of trace elements at the boiler-level by matching the combination of air pollution controls downstream of the boiler against the exact combination of controls in the literature data. This new formulation is shown in Equation A2.

$$x^{system}_{boiler,\phi,TE} = x_{PM,SO_2,\phi,TE} \text{ (A2)}$$

Where $x_{PM,SO_2,\phi,TE}$ is the partitioning fraction of trace element *TE* into phase ϕ for the combination of particulate matter and sulfur dioxide controls. We call this method the "system" method.

We assumed partitioning by air pollution controls is independent to model mass flow rates from a greater fraction of the fleet. We can estimate mass flow rates for 89% of coal generation using the link method but only 67-89% of coal generation using the system method.

In Figure A10, we show a histogram of the difference between the partitioning fraction calculated using the link method and the system method. For all four trace elements, we observe differences of at most two percent in the partitioning fraction to liquid phase across the two methods. For partitioning to solids, we observe differences greater than 10% between the link and system method for Hg, Se, and As. The differences in partitioning are driven by the method that determines which set of literature studies included. Because of the variability in trace element partitioning observed across literature studies for each air pollution control, the median partitioning fraction will shift depending on which study is included. Therefore, the assumption of independence across different air pollution controls will not affect partitioning estimates for most coal boilers, but will affect partitioning estimates of some specific trace elements and pollution controls.

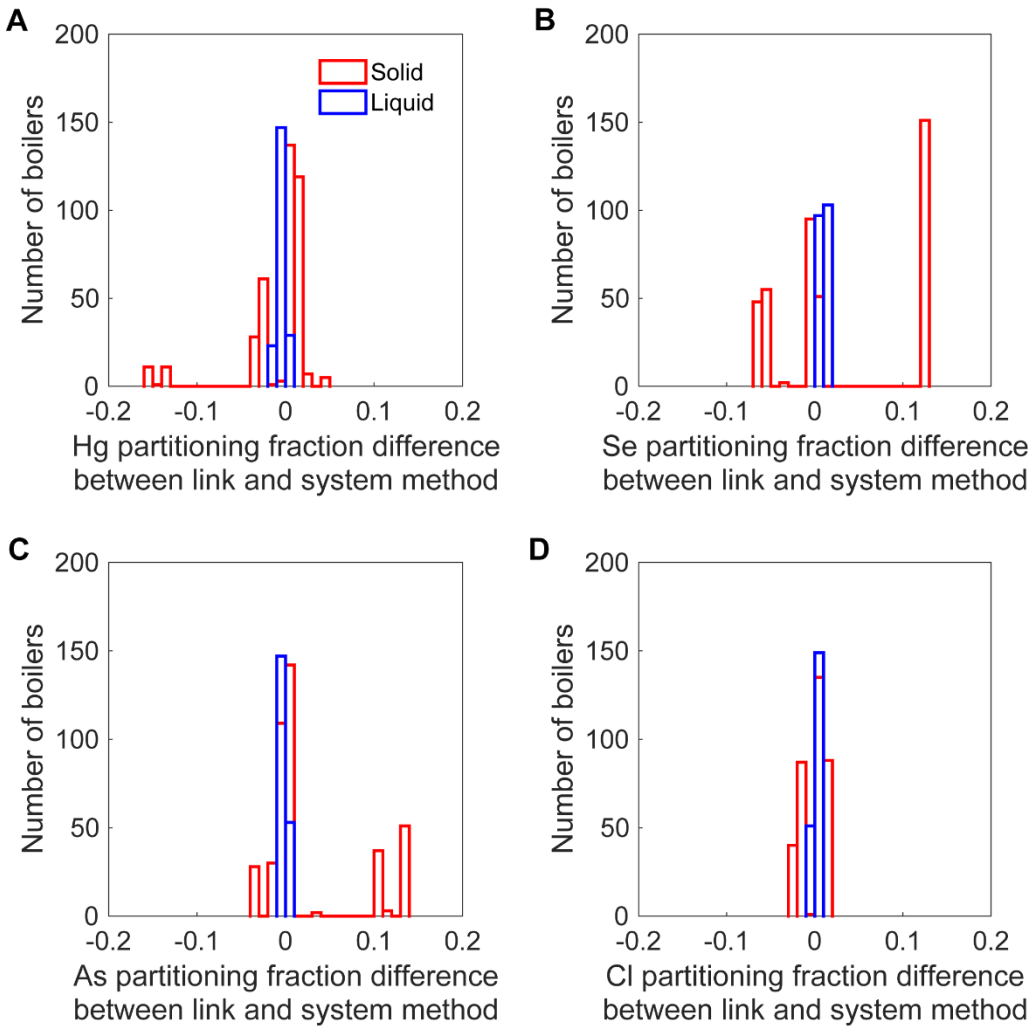

Figure A10: Histograms illustrating differences of boiler-level estimates of trace element partitioning fractions derived from literature by matching literature data with individual air pollution control devices and matching literature data wish combinations of air pollution control devices for the trace elements A) Hg, B) Se, C) As, and D) Cl.

Appendix A.11: Generation treated by different air pollution controls and control combinations

In Table A4 we show the amount of coal generation and the percent of total coal generation in 2015 for each of the post-combustion control options installed to treat Hg, NO_X, particulate matter, and SO_2. We use data from EIA-860, Schedule 6 and electricity generation at the boiler level from EIA-923, Schedule 3.[87,88] EIA-923, Schedule 3 reports 1330 TWh generated from coal in 2015.[88]

The most widely used air emissions control devices for Hg, NO_x, PM, and SO_2 are activated carbon injection systems, selective catalytic reactors, cold-side electrostatic precipitators, and wet flue gas desulfurization systems, respectively. These systems respectively treat 33%, 45%, 58%, and 57% of total coal generation. About 57% of coal generation is not treated by primary Hg controls in 2015, 38% is not treated by NO_x controls, and 18% is not treated by SO_2 controls. All generation is treated by a PM control. As explained in greater detail in Appendix A.3, we do not account for roughly 10% of coal generation from boilers due to data limitations in our datasets. Although a large portion of the generation fleet does not use activated carbon injection to remove mercury, other air emission controls, such as cold-side electrostatic precipitator, hot-side electrostatic precipitator, fabric filters, and wet flue gas desulfurizer, which are not listed by the EIA as mercury pollution controls, remove some mercury.[94]

Table A4: Coal electricity generation treated by different post-combustion air pollution controls (in TWh) and as a percent of total coal generation in 2015.

	Air pollution control	Generation treated (TWh)	Generation treated / total coal generation (%)
Hg	None	755	57%
	Activated carbon injection	435	33%
NO_X	Selective catalytic reactor	603	45%
	None	510	38%
	Selective non-catalytic reactor	77	6%
	Other / Unnamed	0	0%
Particulate matter	Cold-side electrostatic precipitator	770	58%
	Fabric filter	382	29%
	Wet flue gas desulfurizer	178	13%
	Hot-side electrostatic precipitator	108	8%
	Cyclone	14	1%
	Other / Unnamed	26	2%
SO_2	Wet flue gas desulfurizer	753	56%
	None	259	19%
	Dry flue gas desulfurizer	146	11%
	Dry sorbent injection	59	4%

Note: Table produced by the authors using data from EIA-860, Schedule 6 and EIA-923, Schedule 3.[87,88]

Appendix A.12: Comparing partitioning to gas from MATS against literature data

The MATS ICR reports concentrations of trace elements in coal, the heating value of coal, and the heat input normalized trace element mass flow rate exiting the stacks of 278 coal boilers. From that we can estimate the partitioning of trace elements to gas by air pollution control devices and compare those to our bootstrapped estimates.

The MATS ICR sampled 278 coal boilers for trace element concentration in coal and trace element mass flows at the stack. For each boiler in the MATS ICR, we estimate total trace element solid and liquid removal by taking the difference between the mass of trace elements entering the boiler and the mass of trace elements exiting the stacks. After we merge all boilers from the mass flow rate analysis to boilers in the MATS ICR, we compare Hg, Se, As, and Cl removal for 107, 80, 66, and 61 boilers, respectively. Boilers are excluded because the MATS ICR does not sample all four trace elements at every boiler. The unique boilers in this analysis represent 22% of total coal generation in 2015.

We compare our estimated partitioning of trace elements to gas from the literature against the partitioning of trace elements calculated from the 2010 MATS ICR. The MATS ICR reports mass flow rates to gas but not solids or liquids. We estimate a partition fraction *x* to gas for each boiler in the MATS ICR dataset using the median trace element concentrations, median heat input normalized mass flow rate, and median heating values reported at the unit level as shown in Equation A3.

$$x_{gas}^{MATS} = \frac{heat\ input\ normalized\ mass\ flow\ rate\ [\frac{lb}{BTU}]}{concentration\ of\ trace\ elements\ [ppm]*10^{-6}[ppm^{-1}]*higher\ heating\ value\ [\frac{BTU}{lb}]} \quad \text{(A3)}$$

Between our dataset and the MATS ICR dataset, there are 107, 80, 66, and 61 boilers with Hg, Se, As, and Cl removals, respectively. These boilers account for roughly 25% of total coal generation in 2010.

We find that our partitioning estimates trace elements are comparable to those reported in the MATS ICR, with arsenic and chlorine showing better agreement than mercury and selenium. In Figure A11.A, we show the partitioning of trace elements to gas calculated from the MATS ICR dataset. We find that the median partitioning of trace elements to solids and liquids in the MATS ICR are 0.11 for Hg, 0.03 for Se, 0.01 for As, and 0.02 for Cl. For context, the median partitioning to gas estimated from the literature is 0.35 for Hg, 0.21 for Se, 0.05 for As, and 0.03 for Cl.

In Figure A11.B, we show the difference between partitioning into solids and liquids from our dataset versus the MATS ICR dataset. The difference between median gas partitioning estimates from the literature and the MATS ICR is 30% for Hg, 0.18% for Se, 0.074% for As, and 2.9% for Cl. However, at some boilers we find significant errors in estimates of partitioning fraction for all trace elements. Therefore, the mean difference between the partitioning fraction to solids and liquids between the literature versus the MATS ICR is 24% for Hg, 8.5% for Se, 1.9% for As, and 11% for Cl.

We expect the differences in trace element concentrations to contribute more to the overall total estimate differences than differences in partitioning, because the partitioning estimates from the literature are in reasonable agreement with the partitioning from the MATS ICR.

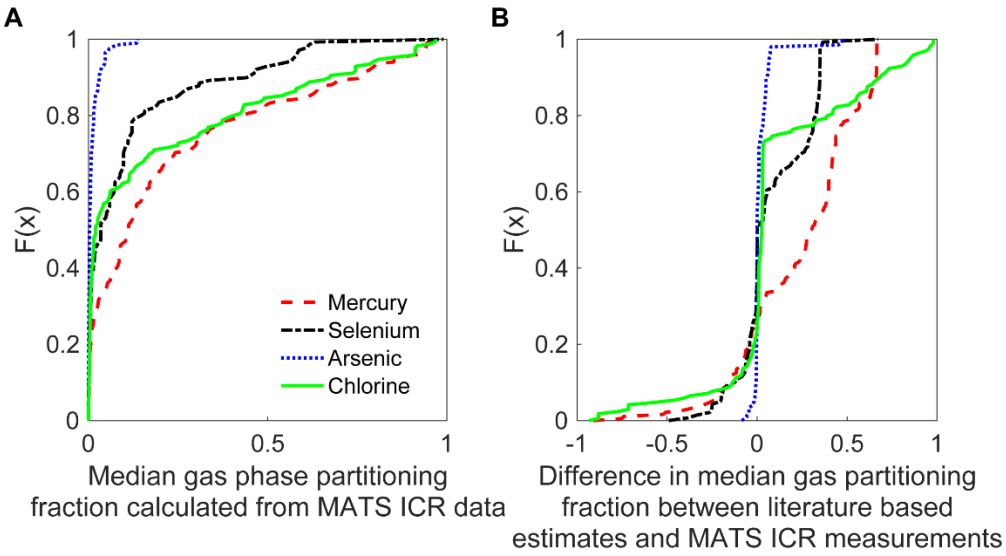

Figure A11: A) Cumulative distribution functions of median trace element partitioning to gas calculated from the reported MATS ICR data. B) Cumulative distribution functions of differences between median removal of trace elements from bootstrapping the literature and median gas partitioning of trace elements calculated from reported MATS ICR data. Figure produced by the authors using data from Table A3, EIA-860, EIA-923 Schedule 5, and MATS ICR. [84,87,88]

Appendix A.13: Generation normalized mass flow rates of trace elements at the boiler level in the U.S. and in different eGRID sub-regions

In Figure A12, we show the median generation normalized mass flow rate of each trace element from coal boilers across the fleet.

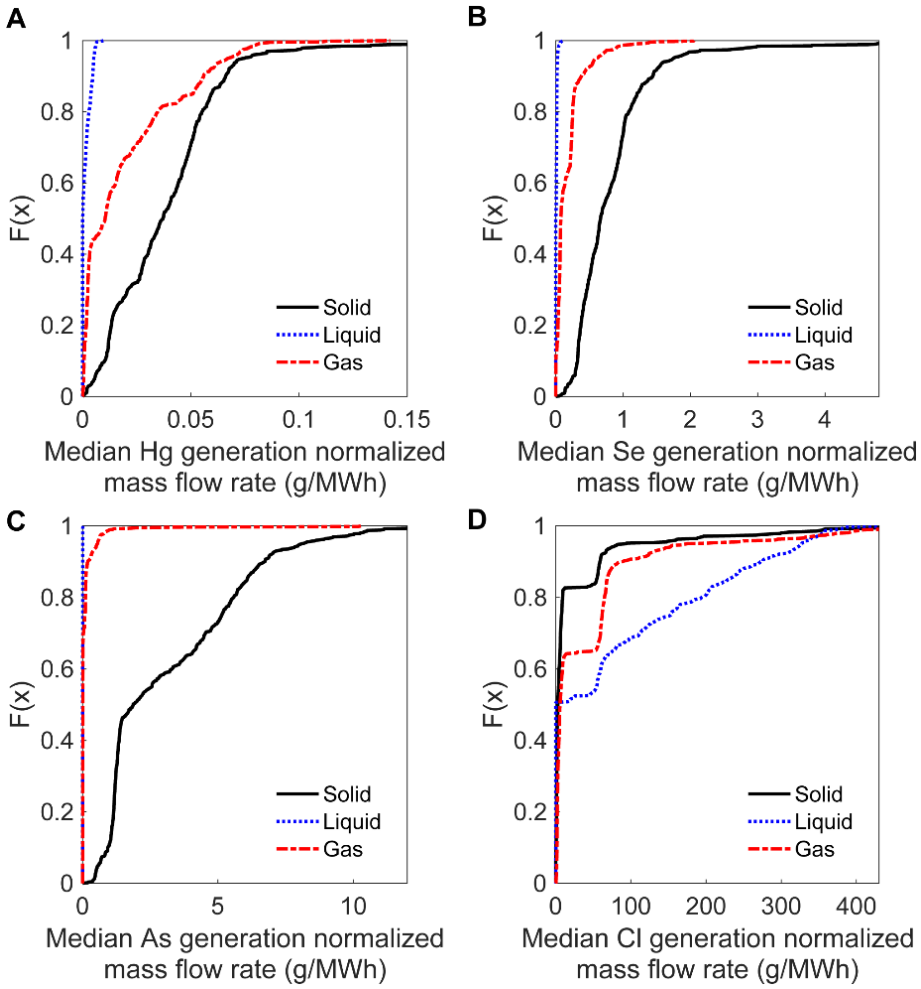

Figure A12: Cumulative distribution functions of median generation normalized mass flow rate into solid, liquid, and gas phases from bootstrapped coal concentrations in coal at each plant and trace element partitioning fractions for air pollution controls at each boiler across the coal fleet for A) Hg, B) Se, C) As, and D) Cl. The x-axis on all figures is cut-off at the 99th percentile (0.14 g/MWh for Hg, 4.6 g/MWh for Se, 11 g/MWh for As, and 406 g/MWh for Cl) for readability. Figure produced by the author using data from COALQUAL, Table A3, EIA-860, and EIA-923.[86–88]

We have included eGRID subregion figures in our data repository here: https://github.com/xdansun/trace_elem_cfpp_model/tree/master/Figures/subrgn_emfs. We encourage the reader to explore the repository and perform their own additional analysis.

Appendix A.14: Temporal variability of trace element concentrations in coal

Coal plants purchase coal in different amounts across different counties from month to month. In Figure A13 we show the 2015 monthly median of the bootstrapped concentration of trace elements in coal at five example power plants. We estimate the concentration of trace elements for each month employing the same bootstrapping approach mentioned in the methods using data from COALQUAL and coal purchase data at that month from EIA 923/5.[86,88]

The five plants we chose are the Monroe plant in Michigan (ORISPL: 1733), the Gavin plant in OH (ORISPL: 8102), the John E Amos plant in WV (ORISPL: 3935), the Roxboro plant in NC (ORISPL 2712), and the Columbia plant in WI (ORISPL: 8023). These 5 plants generated 16 TWh, 16 TWh, 15 TWh, 4.9 TWh, and 4.9 TWh respectively.

We find that the concentration of trace elements varies temporally for a fraction of plants. In Figure A13, the concentration varies from month to month for four plants (ORISPL: 1733, 8102, 3935, and 2712). Concentrations in the coal blend can vary significantly for all four trace elements, such as the coal blend at Roxboro (2712). In other cases, the concentration varies only for one trace element, which is seen for the coal blend at Gavin (8102).

Lastly, the concentration will not vary across time for plants that purchase coal from a single county, such as the coal blend of Columbia (8023). There are 111 out of 276 plants that purchase from a single county. Those plants generated 370 TWh in 2015, which makes up 28% of total coal generation in 2015.

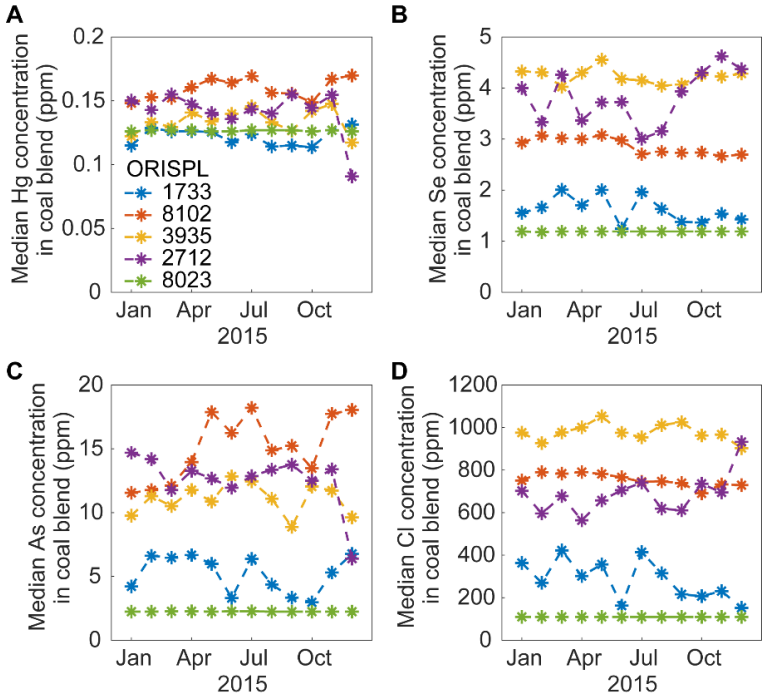

Figure A13: Monthly median bootstrapped concentrations of trace elements for five example plants. Data is produced from COALQUAL and EIA-923/5.[86,88]

Appendix A.15: Comparison of concentrations of trace elements in coal using COALQUAL and EIA against MATS ICR reporting

The 2010 Mercury Air Toxic Standards Information Collection Request (MATS ICR) is a data set resulting from an EPA program that sampled concentrations of trace elements in coal prior to combustion and sampled trace element emission rates from the stacks of coal plants.[84] This dataset is useful for comparing our estimates of trace element concentrations in coal, since the MATS ICR samples coal after any coal cleaning processes might have taken place. The MATS ICR contains coal concentration data for 210 coal plants, with anywhere from 3-54 samples per trace element per plant, but not every coal plant sampled every trace element. Of those 210 CFPPs, 167 plants have coal data for Hg, 161 for Se, 164 for As, and 201 for Cl. The total generation of the coal plants sampled in the MATS ICR was 573 TWh, or roughly 43% of total U.S. coal generation in 2010. After we merge all plants from the coal concentration analysis to the plants in MATS ICR, only 129 plants remain in the analysis.

Although the MATS ICR is a recent database, sampling by MATS ICR may not be representative of trace element concentrations combusted at plants year-round because sampling took place over a few weeks in 2010, and it will not capture changes in the mix of coal purchased by power plants over the course of a year (see the Appendix A.14 for additional information on the temporal variability of coal purchases from power plants).

Also, MATS ICR data was collected in 2010. Thus, to produce a viable comparison between our method and MATS ICR observations, we estimate concentrations of trace elements in coal using our method, but using coal purchase data from for the same months in 2010 as those in which MATS ICR data was collected.[88] Figure A14.A shows the cumulative distribution functions of the median trace element concentrations from sampled coal concentrations in MATS ICR and Figure A14.B provides the difference between bootstrapped median trace element concentrations and the median concentrations from sampled coal concentrations in MATS ICR. Our median estimates for trace element concentrations are 0.13 ppm for Hg, 1.4 for Se, 3.3 ppm for As, and 122 ppm for Cl and we find the median concentrations of coal in MATS ICR are 0.08 ppm for Hg, 1.0 ppm for Se, 2.0 ppm for As, and 200 ppm for Cl.

Of the 260 CFPPs in our dataset, there are 46 coal plants that purchase coal from states without Cl coal samples. These plants represent 13% of all plants and 22% of coal generation. For those states, we approximate Cl concentrations using COALQUAL samples at the basin level. The other trace elements have enough data at the state level and do not require basin level data. In Figure A14.C, we re-create Figure A14.B but only for plants that purchase coal from counties and states with Cl coal data. The median Cl concentration in the coal blend for plants with county and state data is 113 ppm and the median Cl concentration for the same plants listed in the MATS ICR is 108 ppm. The Cl coal concentration estimates improve when we use this smaller dataset, because we interpolate the concentration from a more location specific area.

Our estimates are on the same order of magnitude as the concentrations reported in the MATS ICR, where we get the best agreement with Se and the least agreement with As. We note that our estimates tend to overestimate the concentrations of trace elements reported by the MATS ICR, which means that we are also likely to overestimate mass flow rates from power plants.

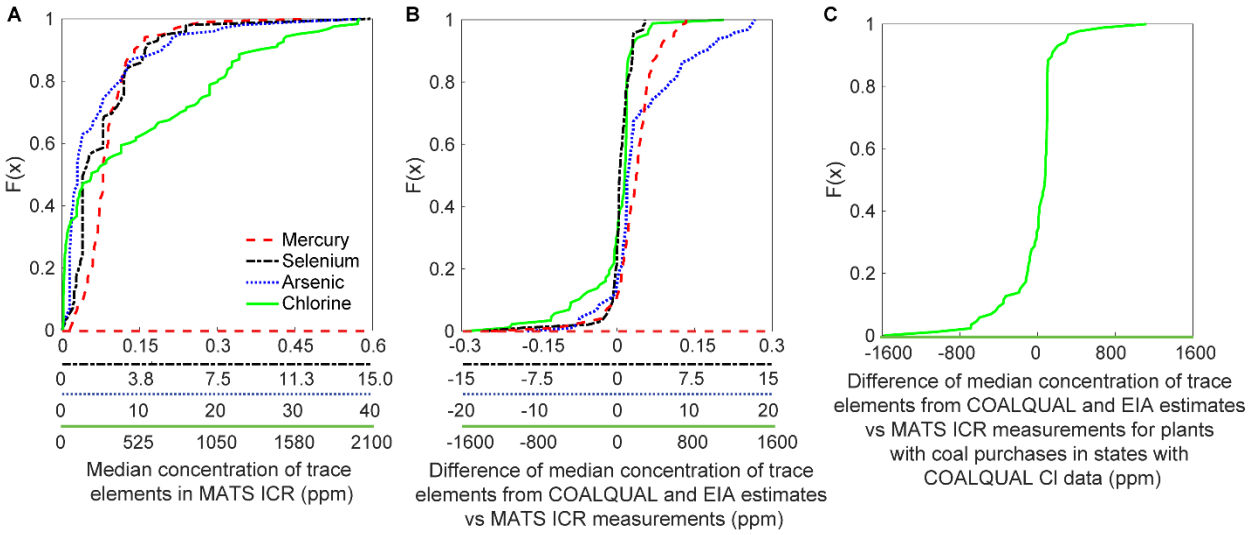

Figure A14: A) Cumulative distribution functions of A) median concentrations in coal combusted at the plant reported from the MATS ICR B) differences of median concentrations in coal combusted at the plant level estimated using COALQUAL and EIA and reported from the MATS ICR. C) median Cl concentrations in coal combusted at the plant level estimated using COALQUAL and EIA and reported from the MATS ICR only for plants with coal purchases from states with Cl COALQUAL data. Figure produced by the authors using data from COALQUAL, EIA-923 Schedule 5, and MATS ICR.[84,86,88]

Appendix A.16: Comparison of minimum model estimates of gas phase Hg mass flows against CEMS

Figure A15 plots the CDF of the difference between Hg CEMS emissions and modeled boiler-level calculated emissions using the median Hg concentration in coal and Hg partitioning to air and the minimum Hg concentration in coal and Hg partitioning to gas phase. In Figure A15, we find we overestimate Hg emissions for 58% of 224 boilers in our Hg CEMS validation. When we select the minimum Hg concentrations and minimum gas-phase Hg partitioning coefficient, we still overestimate Hg CEMS emissions for 15% of boilers in our Hg CEMS validation. This suggests that there are fundamental issues with the quality of published data on the concentration of Hg in the coal and/or the partitioning coefficients for gas-phase Hg. For example, it is possible that COALQUAL has yet to sample low Hg concentration coals or that the coal mining and coal purchasing process can select for coal with lower ash content, which may lead to lower mercury content. We posit that our model would more closely match CEMS data if our input data quality more accurately reflected the Hg concentrations in coal that is combusted in plant boilers and/or removed in APCDs. In short, the inaccuracies should not be viewed as grounds to dismiss the model, but rather highlight the need for greater data fidelity.

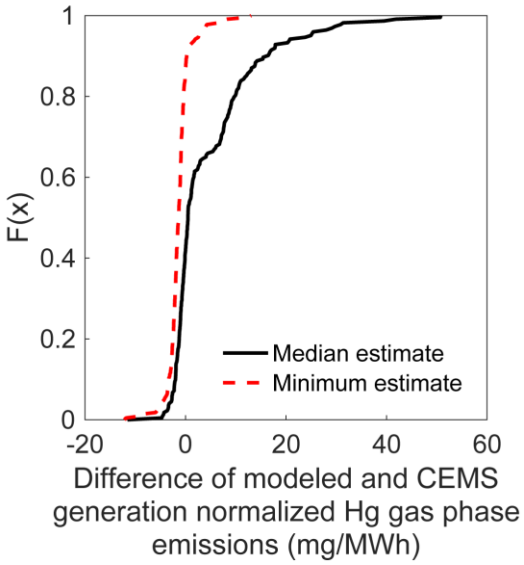

Figure A15: Difference of modeled and CEMS Hg gas phase emissions where the modeled emissions are either the median result from the manuscript (Median estimate) or utilize the lowest reported Hg concentration in coal and the lowest gas phase Hg partitioning fraction (Minimum estimate).

Appendix A.17: Benchmarking estimates of gas-phase, generation-normalized mass flow rates against separate model results

In 2018, the Electric Power Research Institute (EPRI) estimated the hazardous air pollutant emissions from U.S. coal-fired electric generating units for the baseline year 2017, but they do not perform a separate validation analysis.[95] Here we validate their results for Hg emissions and compare their results with our results for As, Se, and Cl emissions to evaluate the relative strengths and weaknesses of the two emissions models. We validate against 2015 Hg emissions from CEMS, because EPRI used coal consumption and fuel purchase data from 2015.[95]

In Figure A16, we show the difference of modeled Hg gas phase emissions and CEMS reported Hg gas phase emissions, where the modeled emissions are generated by either our median bootstrapping analysis or EPRI's emissions model, provided in Appendix G of the EPRI report.[95] We note that the EPRI model estimates Hg emissions for 216 plants, which generated 66% of coal-fired electricity in 2015. There are 84 plants in common between EPRI's 216 plants and the 113 plants in our Hg validation analysis. Because EPRI's emission numbers are at the plant level, we assume that each boiler at the plant has the same generation normalized emissions as the plant. We find that EPRI's emissions model is generally a closer match with the CEMS emission data, but can still differ from CEMS emissions by up to 20 mg Hg/MWh. We find that the error of 68 of the 84 boilers in the EPRI analysis are within 2 mg Hg/MWh of CEMS emissions while 49 of the same 84 boilers are within 2 mg Hg/MWh.

We hypothesize that EPRI's model better fits the CEMS emissions data for three reasons. First, EPRI uses the CEMS data to develop their mercury emission estimates, utilizing the boiler measurement data when available and the average CEMS heat-input normalized emissions (lb/trillion BTU) when the measurement data was not available. Second, EPRI has access to more datasets for estimating coal concentration and partitioning fractions. Because EPRI is only estimating trace element mass flows to the gaseous phase, they can use the MATS ICR dataset. Second, EPRI also has access to additional coal concentration and plant partitioning data obtained from their own sampling efforts. Between MATS ICR and EPRI's internally held datasets, EPRI reports that they have access to at least 524 Hg, 250 Se, 263 As, and 280 Cl sampling events.[95] Third, the larger dataset enables EPRI to use regression based approaches to derive heat-input normalized emissions for each APCD combination as a function of coal trace element content, ash content (for arsenic), and sulfur content (for selenium).

EPRI also modeled gas phase emissions for Se, As, and Cl from the same 216 plants they used to model Hg emissions. We benchmark our model's median bootstrapped gas phase emissions against EPRI's gas phase emissions. We find 184 coal plants in common between our data sets, which generated 65% of 2015 coal generation, that are used in the benchmarking.

In Figure A17, we show the results of our benchmarking. The median difference between our results and EPRI's is 5.8 mg Se/MWh, -2.9 mg As/MWh, and 980 mg Cl/MWh. Based on these results, we tend to overestimate gaseous emissions at the plant level for Hg, Se, and Cl compared to EPRI's estimates. We find our Se, As, and Cl estimates are within ±30% of EPRI's estimates for 56%, 63%, and 44% of 184 plants, respectively. For Se and As, more than half of our plants show comparable estimates to EPRI's model. We find these results encouraging, as it suggests that if input data quality improves, then the bootstrap model that might be comparable or even more accurate to other plant level estimates.

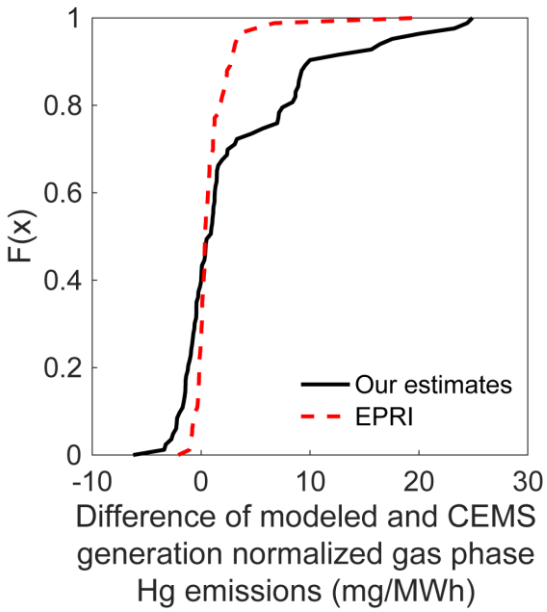

Figure A16: Difference of CEMS reported versus modeled generation normalized gas phase Hg emissions, where the modeled emissions are either the median bootstrapping result from the manuscript (our estimates) or the reported result from EPRI's modeling analysis.

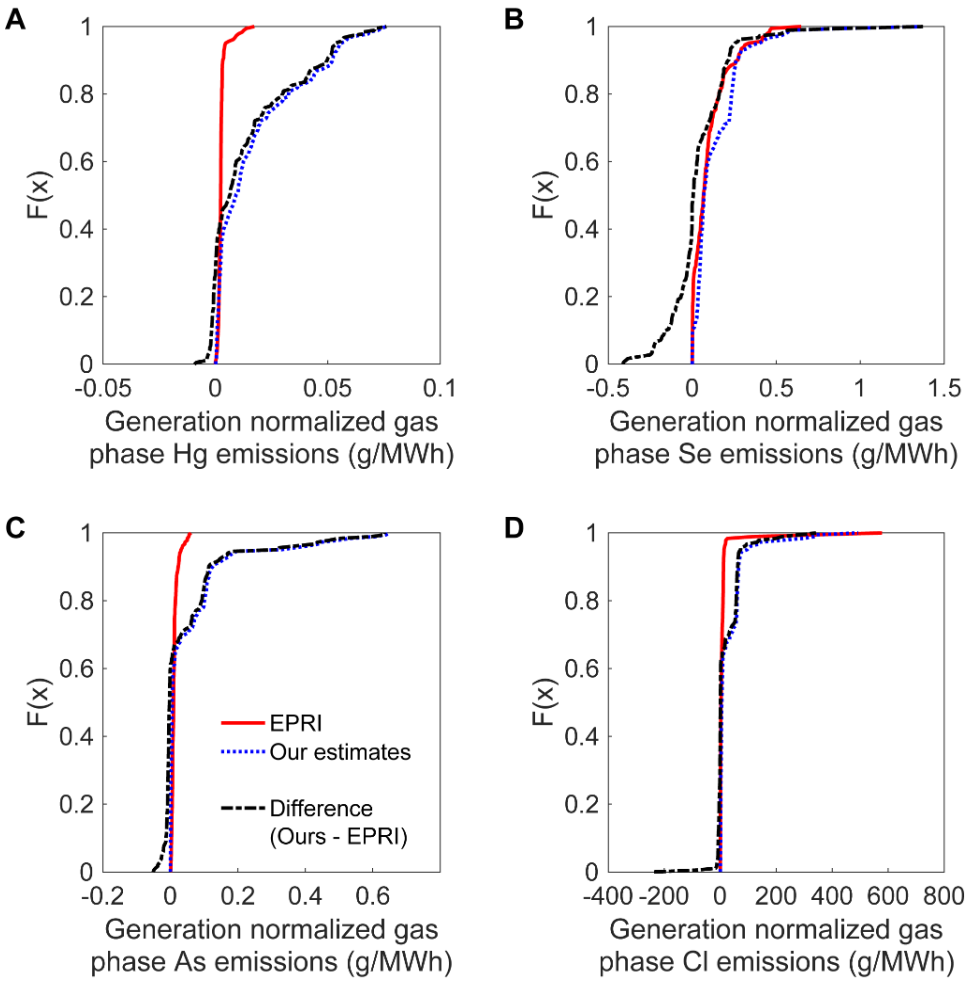

Figure A17: Generation normalized gas phase emissions estimated by the EPRI model and by our model alongside the difference between our model and EPRI's for the trace elements A) Hg, B) Se, C) As, and D) Cl.

Appendix B: Supplemental Information for Chapter 2

Appendix B.1: Sensitivity analysis of air pollution control device efficiencies

According to the Environmental Protection Agency (EPA), a review of air pollution control removal efficiencies states that selective catalytic reaction (SCR) removes 70-90% of NOx emissions and wet flue gas desulfurization (wFGD) removes 80-98% of SO_2 emissions.[109,110] In one of our scenarios, we estimate the SO_2, and NOx emissions when coal plants turn off SCR and wFGD devices. In our modeling, we assumed SCR devices remove 80% of NOx emissions and wFGD removes 90% of SO_2 emissions. In that scenario we estimate the U.S. electricity sector emits 2.2 million metric tons of NO_x and 3.9 million metric tons of SO_2.

In Figure B1, we perform a sensitivity analysis on NO_x and SO_2 emitted by from the U.S. electricity sector when coal plants turn off SCR and wFGD devices as a function of the SCR and wFGD removal efficiencies. NO_x emissions ranged from 1.6 – 3.7 million metric tons and SO_2 emissions varied 2.4 – 15.9 million tons. The relationship between emissions and removal efficiency is nonlinear and inversely proportional, so assuming higher removal efficiencies will lead to significantly higher emissions. However, despite this nonlinearity, emissions when SCR and wFGD devices are turned off are higher than the 1.4 million metric tons NO_x and 1.7 million metric tons SO_2 emitted when coal displaces natural gas regardless of the removal efficiency of the air pollution control devices. Therefore, turning off wFGD and SCR devices at coal plants will lead to greater NO_x and SO_2 emissions.

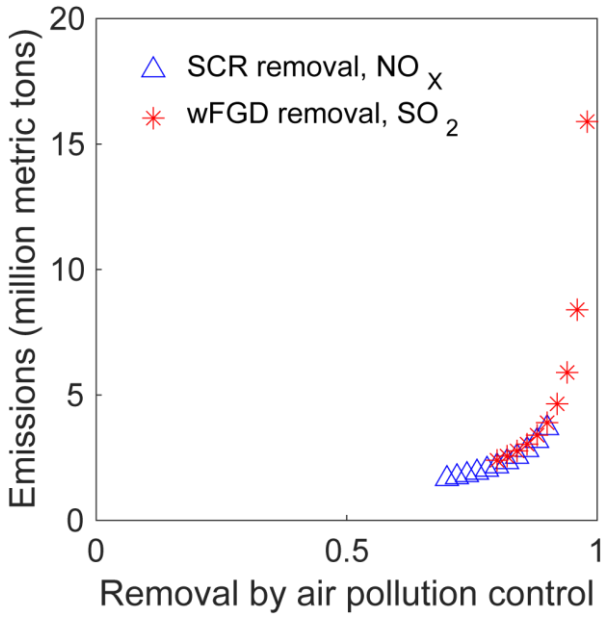

Figure B1: NO_x and SO_2 emissions as a function of selective catalytic reactor removal efficiency and wet flue gas desulfurizer removal efficiency.

Appendix B.2: Temporal variation of the emission factors from coal and natural gas boilers

In Figure B2, we show the hourly emission factors of a sample of coal and natural gas boilers with some of the highest and lowest average emission factors. These emission factors are normalized by the gross generation, which is the hourly generation data provided by CEMS. In each subfigure, we show 25 boilers out of a total of 3009 coal and natural gas boilers. We find that regardless of the pollutant and the magnitude of the emission factor, there are significant hourly variations (up to a factor of 10) for every boiler shown in Figure B2. Therefore, when changing the generation of a coal or natural gas boiler, it is important to use the hourly emission factor to accurately estimate the emissions. When coal boilers are not operating at an hour we want to bring the boiler online, we use the average emission factor at a lower temporal resolution to best approximate the hourly emission factor.

We note that many natural gas boilers appear with the highest emission factors even though they typically emit less SO_2 and CO_2 than coal boilers. For example, in Figure BA, 2 of the 25 featured boilers are natural gas boilers. We find that these high emission intensity boilers operate a secondary fuel like diesel oil or coal and operate for a fraction of the year, so that their emission intensity profile more closely resembles a coal plant.

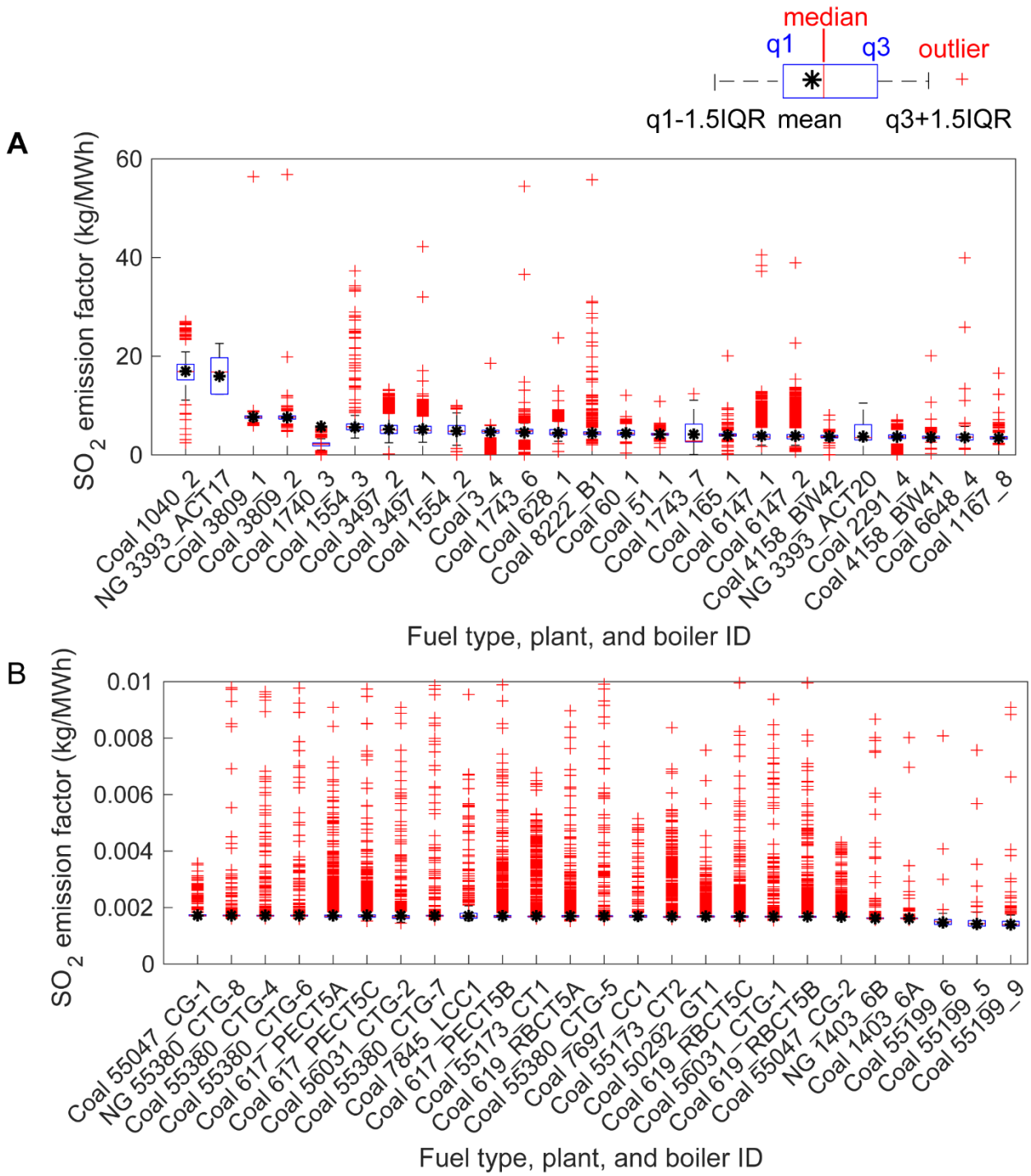
median
q1
q3
outlier
q1-1.5IQR
mean
q3+1.5IQR
A
SO2 emission factor (kg/MWh)
60
40
20
0
Coal 1040_2
NG 3393_ACT17
Coal 3809_1
Coal 3809_2
Coal 1740_3
Coal 1554_3
Coal 3497_2
Coal 3497_1
Coal 1554_2
Coal 3_4
Coal 1743_6
Coal 628_1
Coal 8222_B1
Coal 60_1
Coal 51_1
Coal 1743_7
Coal 165_1
Coal 6147_1
Coal 6147_2
Coal 4158_BW42
NG 3393_ACT20
Coal 2291_4
Coal 4158_BW41
Coal 6648_4
Coal 1167_8
Fuel type, plant, and boiler ID
B
SO2 emission factor (kg/MWh)
0.01
0.008
0.006
0.004
0.002
0
Coal 55047_CG-1
NG 55380_CTG-8
Coal 55380_CTG-4
Coal 55380_CTG-6
Coal 617_PECT5A
Coal 617_PECT5C
Coal 56031_CTG-2
Coal 55380_CTG-7
Coal 7845_LCC1
Coal 617_PECT5B
Coal 55173_CT1
Coal 619_RBCT5A
Coal 55380_CTG-5
Coal 7697_CC1
Coal 55173_CT2
Coal 50292_GT1
Coal 619_RBCT5C
Coal 56031_CTG-1
Coal 619_RBCT5B
Coal 55047_CG-2
NG 1403_6B
Coal 1403_6A
Coal 55199_6
Coal 55199_5
Coal 55199_9
Fuel type, plant, and boiler ID

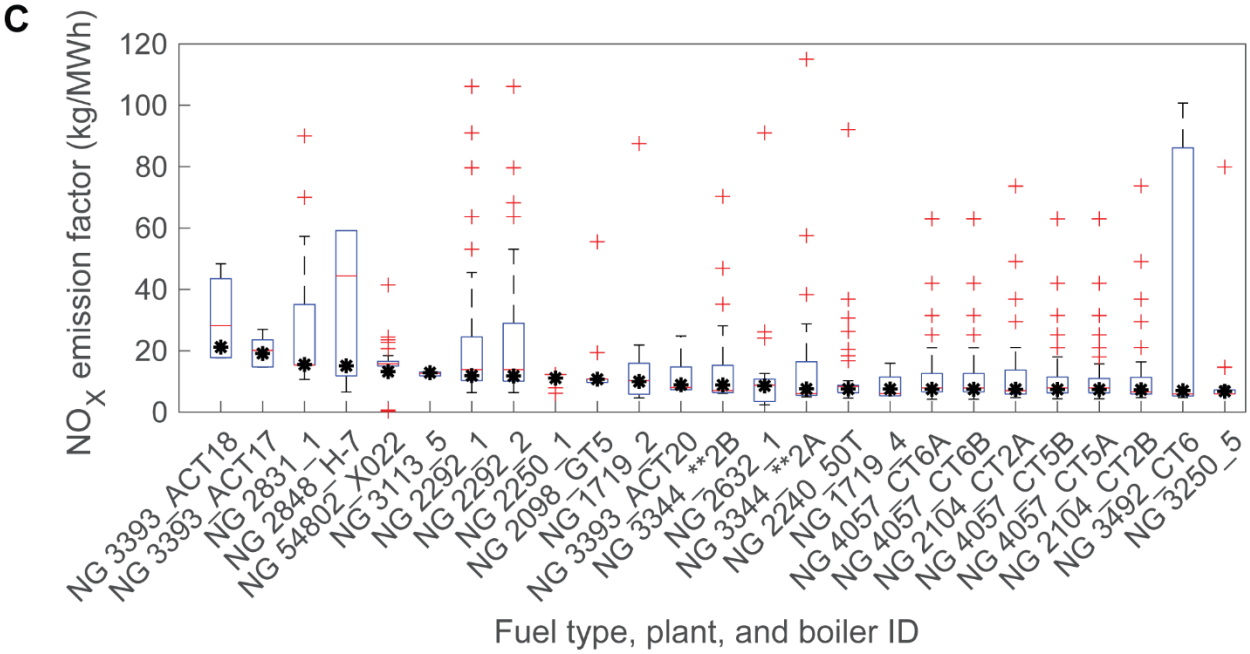
C
NOX emission factor (kg/MWh)
120
100
80
60
40
20
0
NG 3393_ACT18
NG 3393_ACT17
NG 2831_1
NG 2848_H-7
NG 54802_X022
NG 3113_5
NG 2292_1
NG 2292_2
NG 2250_1
NG 2098_GT5
NG 1719_2
NG 3393_ACT20
NG 3344_**2B
NG 2632_1
NG 3344_**2A
NG 2240_50T
NG 1719_4
NG 4057_CT6A
NG 4057_CT6B
NG 2104_CT2A
NG 4057_CT5B
NG 4057_CT5A
NG 2104_CT2B
NG 3492_CT6
NG 3250_5
Fuel type, plant, and boiler ID

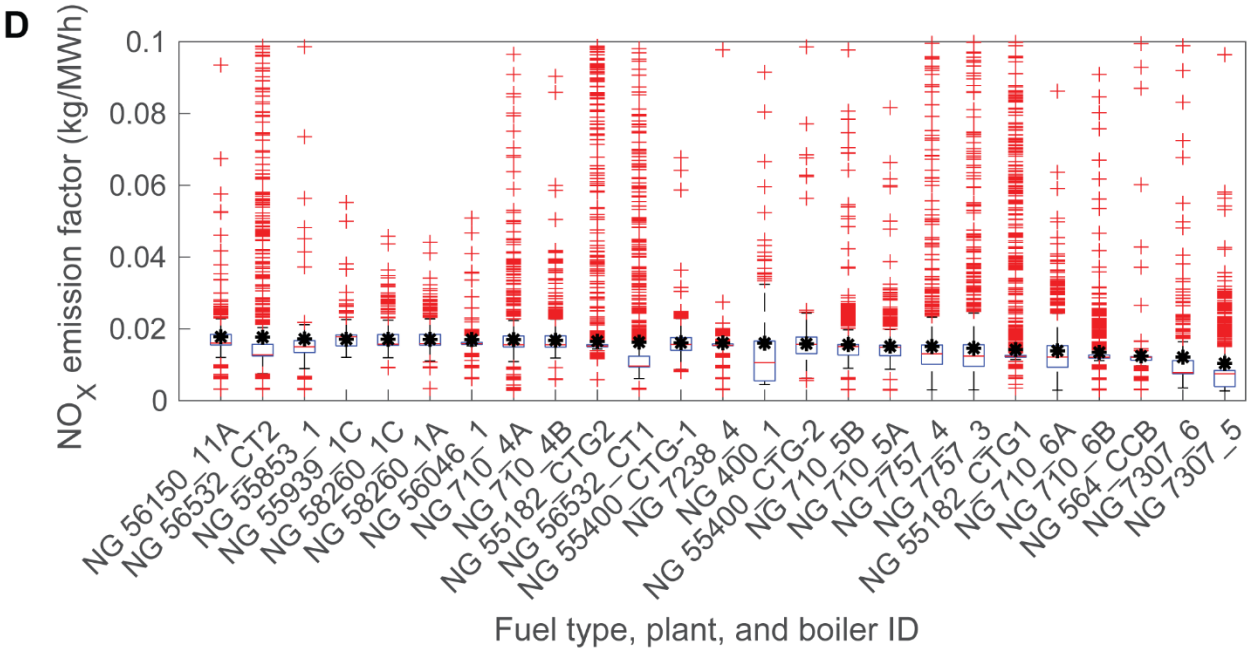
D
NOX emission factor (kg/MWh)
0.1
0.08
0.06
0.04
0.02
0
NG 56150_11A
NG 56532_CT2
NG 55853_1
NG 55939_1C
NG 58260_1C
NG 58260_1A
NG 56046_1
NG 710_4A
NG 710_4B
NG 55182_CTG2
NG 56532_CT1
NG 55400_CTG-1
NG 7238_4
NG 400_1
NG 55400_CTG-2
NG 710_5B
NG 710_5A
NG 7757_4
NG 7757_3
NG 55182_CTG1
NG 710_6A
NG 710_6B
NG 564_CCB
NG 7307_6
NG 7307_5
Fuel type, plant, and boiler ID

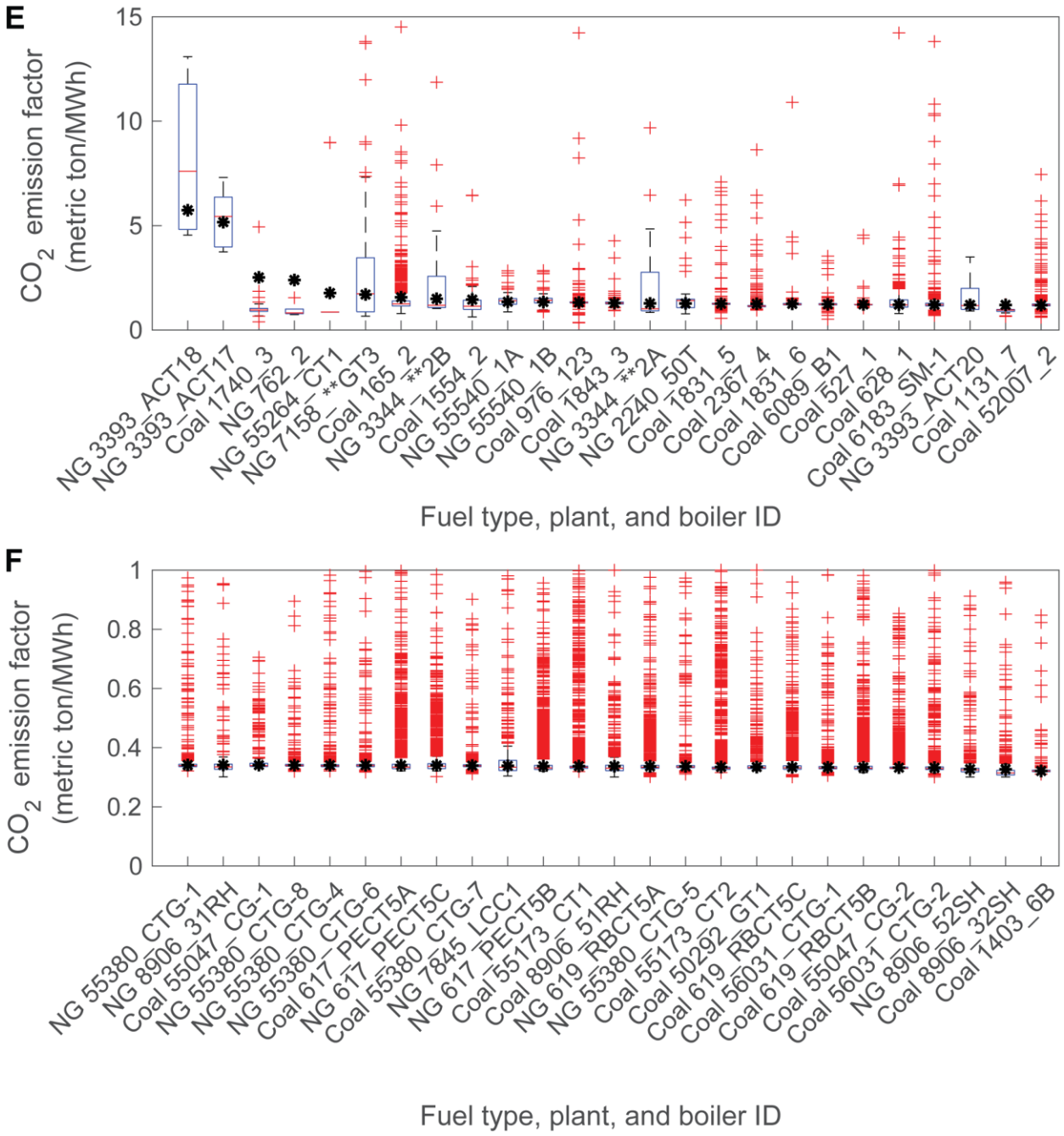

Figure B2: Boxplots showing the hourly emission factors of A) and B) SO_2, C) and D) NO_x, and E) and F) CO_2 of 25 coal and natural gas boilers that have the highest (A, C, and E) and lowest (B, D, and F) average emission factors in our modeled dataset for every hour they generated electricity. In the boxplot, the red line is the median, the blue lines are the first and third quartiles, the lower whisker is the first quartile minus 1.5 times the interquartile range, the upper whisker is the third quartile plus 1.5 times the interquartile range, the red crosses are outliers, and the black asterisk is the average emission factor, which is equal to the annual emission divided by the total gross generation.

Appendix B.3: Map of eGRID sub-regions

Figure B3 shows the 26 Emissions and Generation Resource Integrated Database (eGRID) sub-regions in the U.S. The EPA designed the eGRID sub-regions to mimic regional transmission organizations and independent system operators within North American Electric Reliability Corporation regions. In our study, we focus on the contiguous U.S.

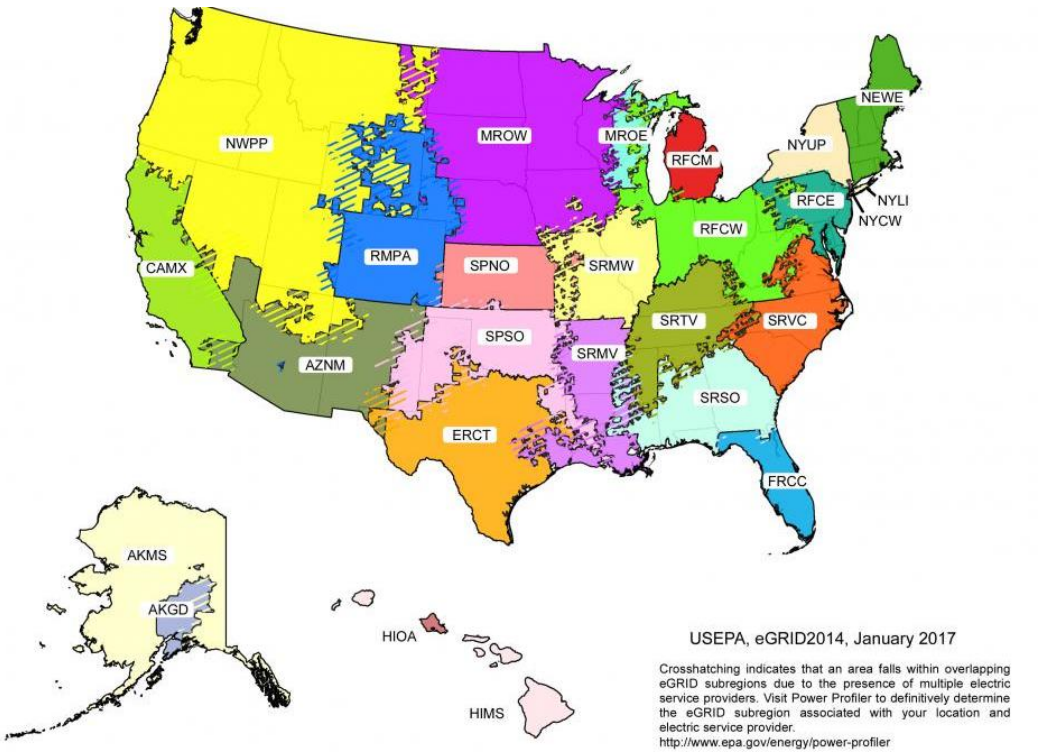

Figure B3: Map of eGRID sub-regions (source: https://www.epa.gov/energy/egrid-sub-region-representational-map)

Appendix B.4: Amount of natural gas generation displaced by coal electricity by eGRID subregion

In one of our scenarios, we displace natural gas generation in each eGRID sub-region by coal electricity. We displace natural gas generation equal to 90% of the total coal spare capacity available (the total coal capacity minus the total coal generation). If there is less natural gas generation than 90% of the spare coal capacity, then we displace all the natural gas in the sub-region. In Figure B4A we show the baseline coal generation, baseline natural gas generation, the total coal capacity, and the total coal and natural gas capacity for each eGRID sub-region. In Figure B4B we show the coal generation and natural gas generation alongside the capacity after coal displaces natural gas. In Figure B4C, we show the change in coal and natural gas generation between coal displacing natural gas and the baseline.

The amount of natural gas generation displaced ranges from 16-100% across the sub-regions, with a median of 77%. Sub-region SRMW is the only eGRID sub-regions with 100 of its natural gas generation displaced. Meanwhile, coal generation increases from 9-110% with a median increase of 56%. Sub-regions ERCT, FRCC, SRSO and SRMC have coal generation equal to 90% of the total coal capacity. We find that even if the eGRID sub-region has sufficient coal capacity to displace all natural gas generation, that does not mean there will be sufficient coal capacity at each hour to displace all natural gas generation. For example, in the summer, natural gas is less likely to be displaced because coal capacity factors tend to be higher and less coal capacity is available to displace gas.

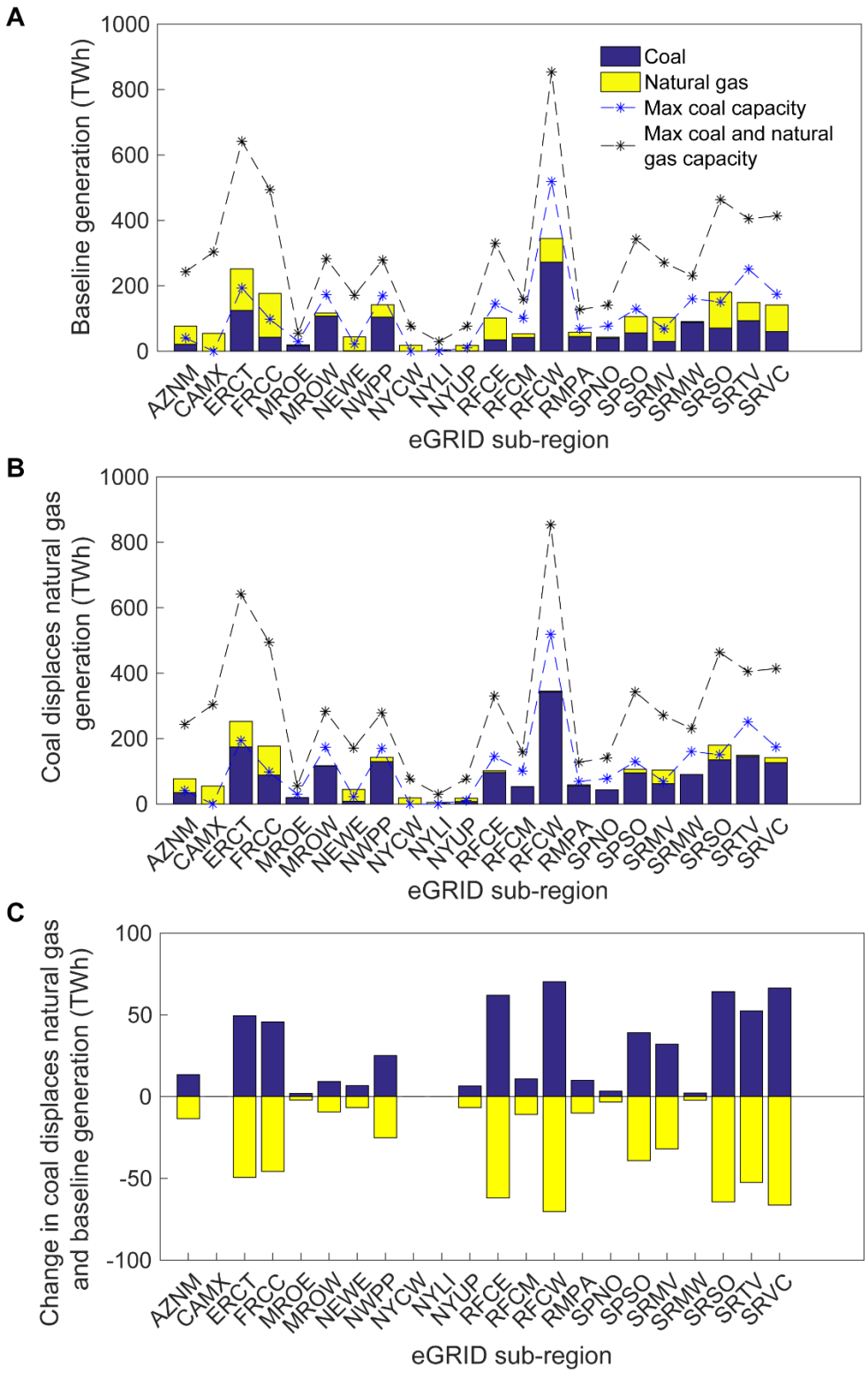

Figure B4: Coal and natural gas generation in 2017 at each eGRID subregion for the A) baseline and B) when coal displaces natural gas, and C) the amount of increased coal generation and decreased natural gas generation.

Appendix B.5: Emissions from coal displacing natural gas using average SO_2 emission factors

When coal displaces natural gas, coal plants increase generation by order of ascending SO_2 emission factors. This order was selected to produce a more conservative estimate of emissions. In this SI Section, we perform a back-of-envelop estimate of annual emission increases if each coal plant emitted the average emission factor in their eGRID sub-region to estimate what emissions might be if we selected a different dispatch order. We estimate emission increases from the baseline at each eGRID sub-region by multiplying the annual increase in coal generation by the difference of the average annual coal emission factor and average annual natural gas emission factor.

In Figure B5, we show the emission increases from the baseline using the above methodology and the method in the manuscript, where we dispatch coal plants by lowest hourly SO_2 emission factor first. The emissions increase when the coal plants with lowest SO_2 emission factor are selected first are 0.50 million metric tons of SO_2, 0.43 million metric tons of NO_x, and 350 billion metric tons of CO_2. When we use the average annual SO_2 emission factors, the emissions are 0.51 million metric tons of SO_2, 0.32 million metric tons of NO_x, and 300 billion metric tons of CO_2. Comparing the emission increases against each other, estimating emissions using the average emission factor increases SO_2 emissions by 3% and decreases NO_x and CO_2 emissions by 26% and 15%, respectively. Compared to the 40%, 40%, and 20% emission increases from the baseline in SO_2, NO_x, and CO_2, respectively, the back-of-envelop estimates an additional 1% increase in SO2 emissions and a 12% and 3% decrease in NO_x and CO_2 emissions. These results suggest that even if coal plants with the lowest SO_2 emission factors are selected first, enough generation is displaced so that plants with above average SO_2 emission factors are dispatched. Additionally, because NO_x and CO_2 emission increases are less in the back-of-envelop analysis, coal plants with low SO_2 emission factors do not necessarily have low NO_x and CO_2 emission factors.

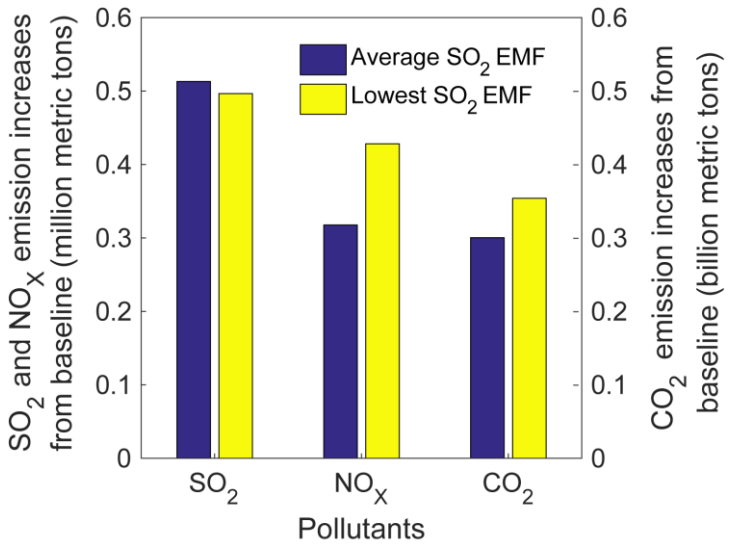

Figure B5: SO_2, NO_x and CO_2 emissions increases from the baseline when coal displaces natural gas in the U.S. electricity sector. The blue bar corresponds to an emission increase estimated by multiplying coal generation increases by the average coal and natural gas emission factors by eGRID sub-region. EMF stands for emission factors. The yellow bar corresponds emission increases used in the manuscript where coal plants with the lowest SO_2 emission factors are picked hourly.

Appendix B.6: Emission factors of pollutants by eGRID subregion

In Figure B6, S7, and S8, we show plant-level emission factors for SO_2, NO_x, and CO_2, respectively, as a function of generation for all coal and natural gas plants in the U.S. and in each eGRID sub-region. Generally, we find that the SO_2 emission factors of coal plants are an order of magnitude greater than natural gas plants. NO_x emission factors and CO2 emission factors of coal plants are about 5 times and 2 times greater than natural gas plants, respectively. Additionally, qualitatively, we find that the emission factors of the pollutants are not correlated with the generation of the plants, except for some plants with extremely high emission factors due to near-zero generation. These emission factors are likely due to plants being less efficient at low capacity factors.

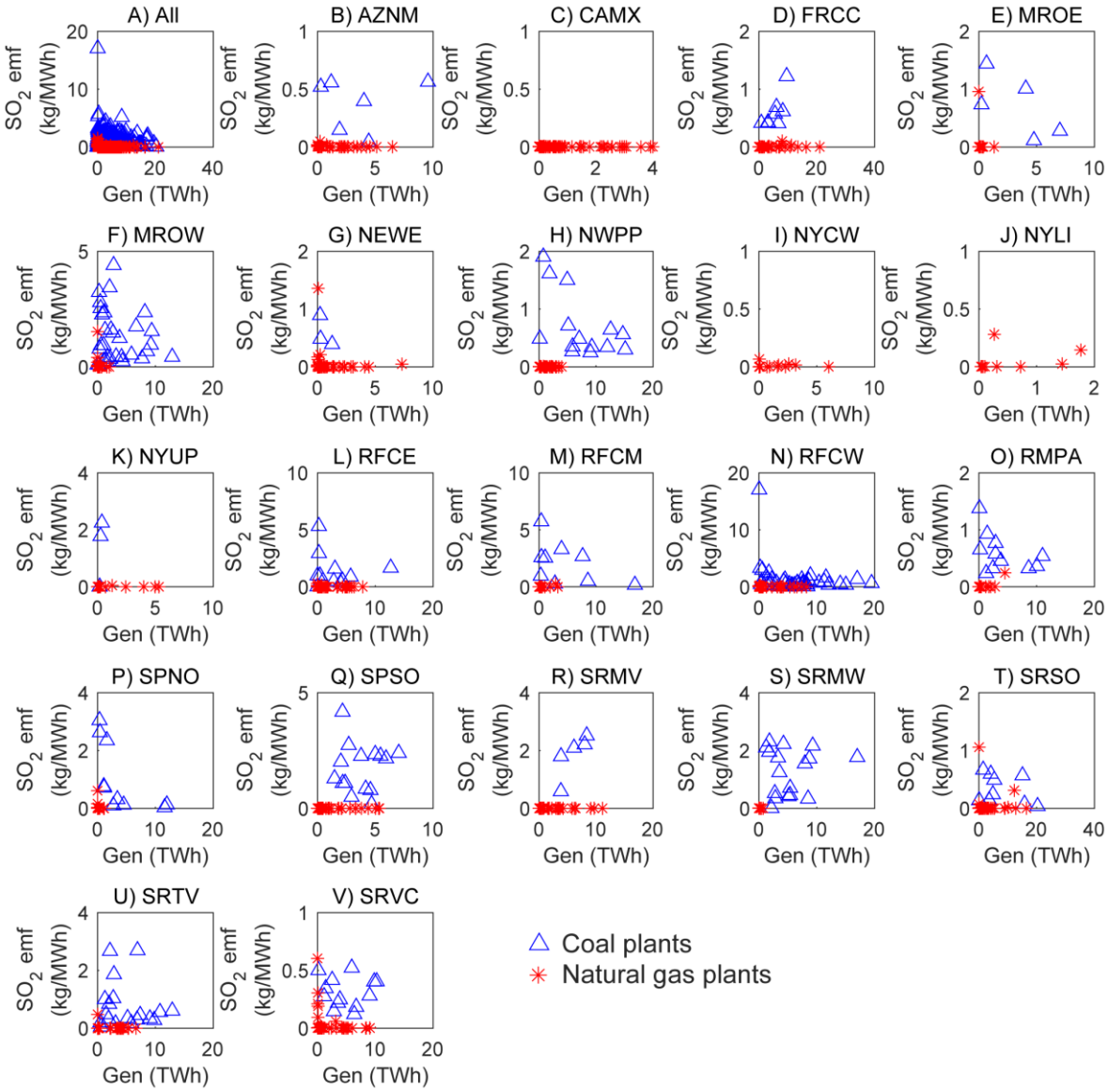

Figure B6: Annual SO_2 emission factors calculated from 2017 CEMS emissions and generation data of natural gas (red) and coal plants (blue) in the A) contiguous U.S. and in eGRID subregions B) AZNM, C) CAMX, D) FRCC, E) MORE, F) MROW, G) NEWE, H) NWPP, I) NYCW, J) NYI, K) NYUP, L) RFCE, M) RFCM, N) RFCW, O) RMPA, P) SPNO, Q) SPSO, R) SRMV, S) SRMW, T) SRSO, U) SRTV, and V) SRVC. Each point represents a single plant.

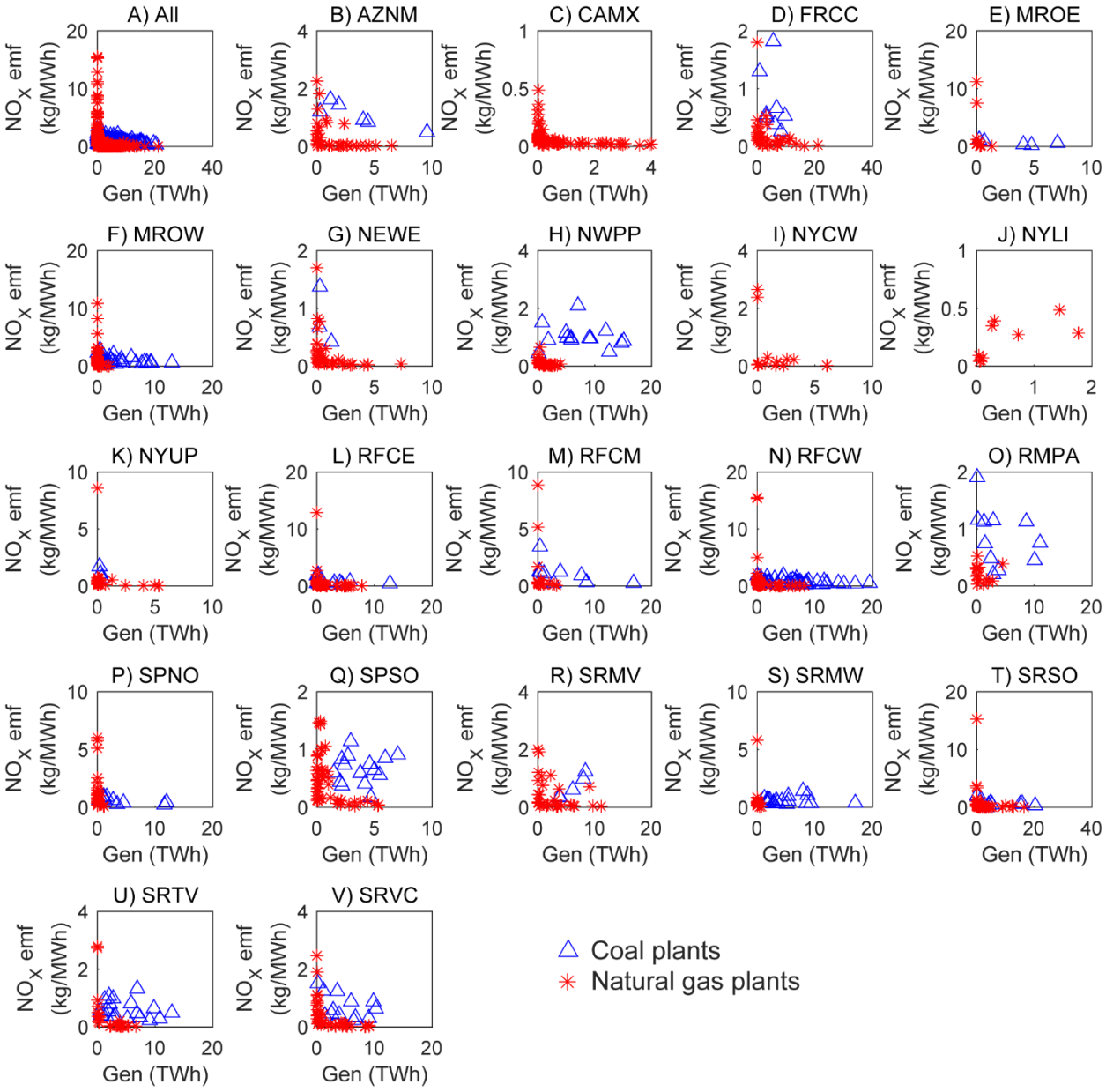

Figure B7: Annual NOx emission factors calculated from 2017 CEMS emissions and generation data of natural gas (red) and coal plants (blue) across the the A) contiguous U.S. and in eGRID subregions B) AZNM, C) CAMX, D) FRCC, E) MORE, F) MROW, G) NEWE, H) NWPP, I) NYCW, J) NYI, K) NYUP, L) RFCE, M) RFCM, N) RFCW, O) RMPA, P) SPNO, Q) SPSO, R) SRMV, S) SRMW, T) SRSO, U) SRTV, and V) SRVC. Each point represents a single plant.

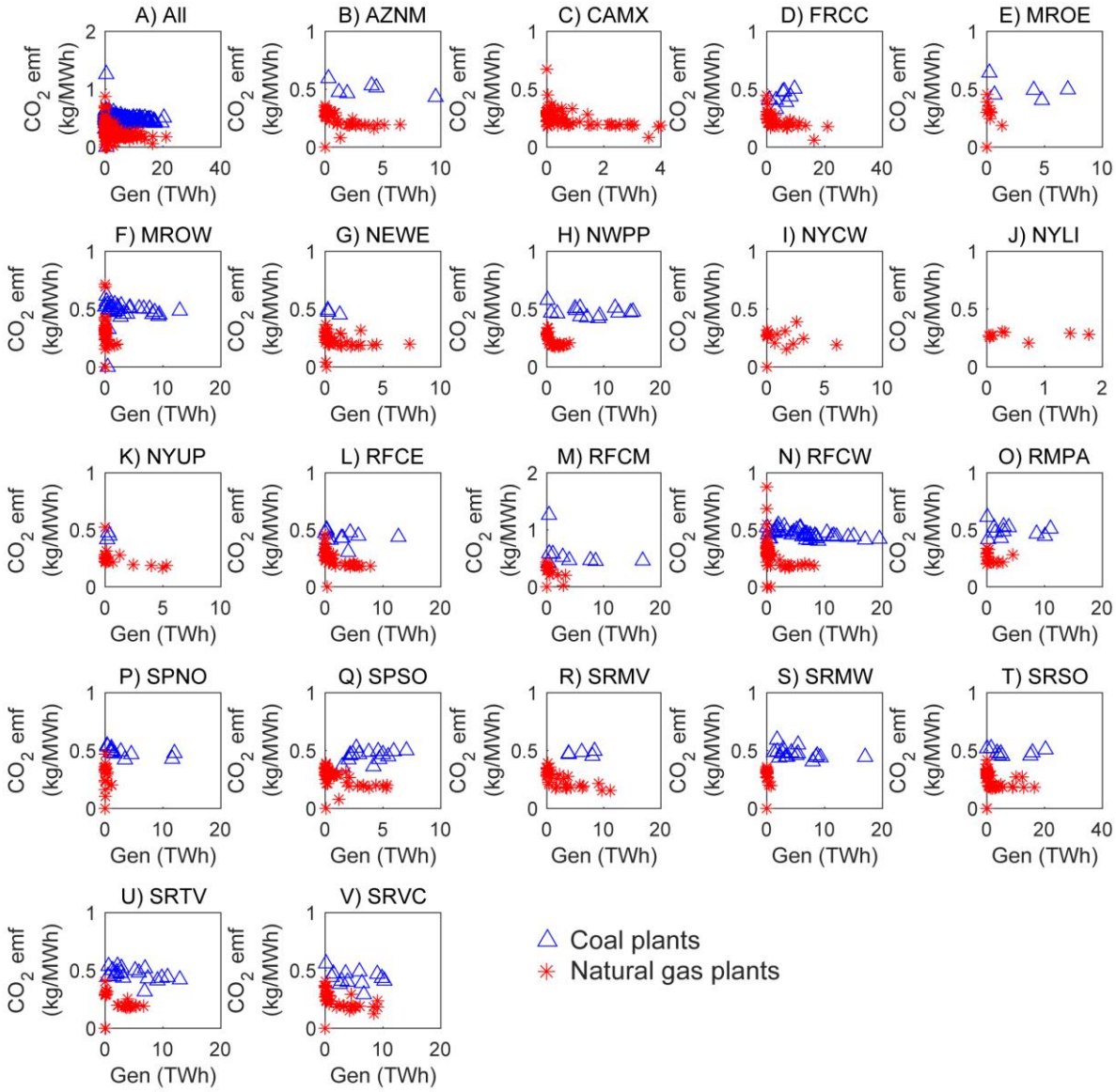

Figure B8: Annual CO2 emission factors calculated from 2017 CEMS emissions and generation data of natural gas (red) and coal plants (blue) across the A) contiguous U.S. and in eGRID subregions B) AZNM, C) CAMX, D) FRCC, E) MORE, F) MROW, G) NEWE, H) NWPP, I) NYCW, J) NYI, K) NYUP, L) RFCE, M) RFCM, N) RFCW, O) RMPA, P) SPNO, Q) SPSO, R) SRMV, S) SRMW, T) SRSO, U) SRTV, and V) SRVC. Each point represents a single plant.

Appendix B.7: Increase in emissions at the state level

In Figure B9, we show the increase in SO_2, NOx, and CO_2 emissions at the state level between the baseline and when wFGD and SCR devices are turned off at coal plants and the baseline and when coal displaces natural gas at the eGRID subregions. When wFGD and SCR devices are turned off, emissions can increase by up to 500 thousand tons of SO_2 (Texas) and 120 thousand tons of NOx (Indiana). When coal displaces natural gas, emissions can increase by up to 140 thousand tons of SO_2 (Texas), 60 thousand tons of NO_x (Maryland), and 47 million tons of CO_2 (Maryland).

Similar to the results at the eGRID sub-region level, we find that for most states, turning off wFGD and SCR devices leads to greater NO_x and SO_2 emissions at the state level than coal displacing natural gas. The states where that is not true are Arizona, Connecticut, Louisiana, Maryland, New Hampshire, New York, Oklahoma, South Carolina, Utah, and Virginia. Additionally, when coal displaces natural gas, some states may decrease their emissions from the baseline, because natural gas electricity displaced in one state may be displaced by coal electricity in a different state. The states that can benefit from an increase in coal use are California, Indiana, Illinois, Massachusetts, Maine, Mississippi, New Jersey, Nevada, Oregon, Pennsylvania, Rhode Island, and Virginia. These states have a greater fuel share in natural gas than in coal, and in some cases, they do not have any coal-fired electricity. Although these states may benefit from an increase in coal use by decreasing emissions in their state, the decreases are relatively minor and could be outweighed by downwind emissions from other states.

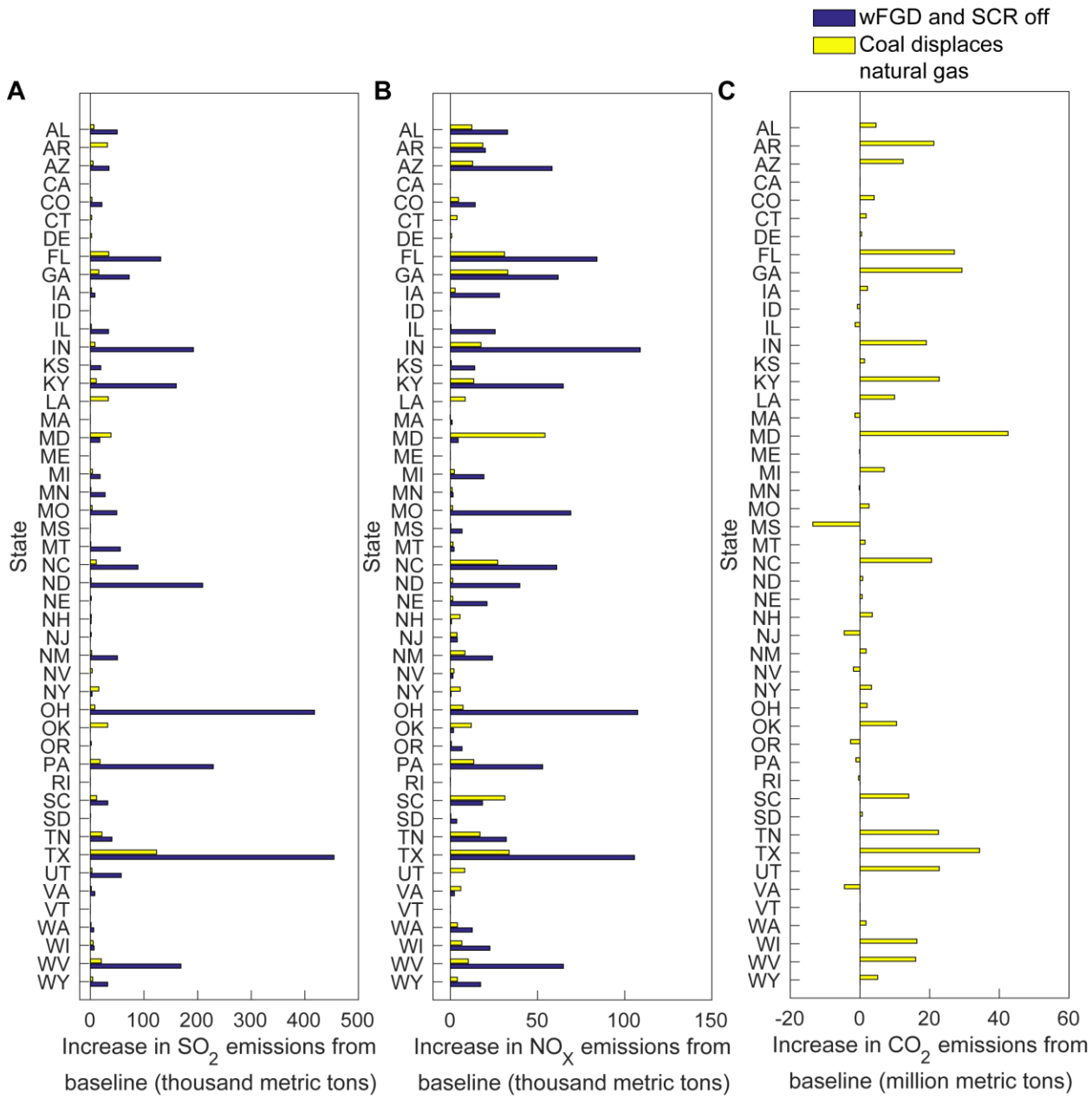

Figure B9: Increases in pollutant emissions at the state level when air emission controls are turned off and when coal displaces natural gas compared to the baseline emissions for A) SO_2, B) NOx, and C) CO_2. Note that CO_2 emissions are not affected when air emission controls are turned off.

Appendix C: Supplemental Information for Chapter 3.

Appendix C.1: Electricity demand since 2001.

In Figure C1, we show the electricity demand in Pennsylvania from 2001-2016. We estimate electricity demand as the difference of total electricity consumed in the residential, industrial, and commercial sectors and the total electricity consumed by the electricity sector. All data is provided by the Energy Information Administration (EIA) and their estimates of total consumption by end-use sector.[153] We find in Figure C1 that there are no significant changes to demand in the last 15 years and so we assume this trend holds until 2050 in our assumptions.

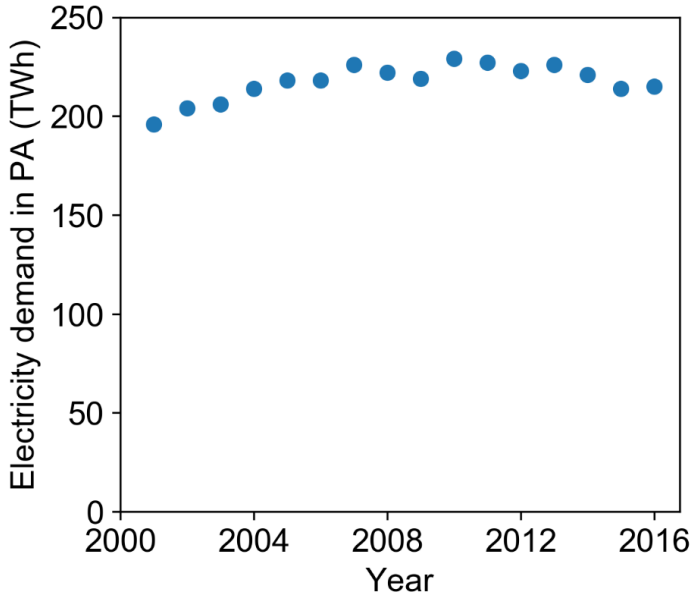

Figure C1: Electricity demand in Pennsylvania (TWh) from 2001-2016. Data is provided by Energy Information Administration (EIA).[153]

Appendix C.2: Data sources used in land use analysis and exclusion criteria

We identified forested areas in Pennsylvania using the 2011 National Land Cover Database.[154] In the dataset, we identify land types 41, 42, and 43, which are deciduous forest, evergreen forest, and mixed forest, as forested areas and assumed all other land types are non-forested areas.[155]

In Table C1, we provide the exclusion criteria and the sources of those criteria.

In Figure C2, we provide the map used in the baseline analysis, with all manmade areas excluded. The total area and total forested area in the baseline analysis is 64,000 sq km and 47,000 sq km, respectively.

Table C1: Exclusion criteria applied for the solar PV and wind land use and fragmentation analysis. Excluded areas, except for elevation, slope, and area excluded at farm site, include a 100 m buffer zone to account for edge effects. Exclusion criteria that are considered "manmade" are excluded from all analysis including the fragmentation analysis. Area excluded at farm site is a way to ensure there is sufficient contiguous land area to build renewables capacity.

Criteria	Solar PV	Wind	Manmade	Source
Elevation	>1500 m	>1500 m		USGS: Earth Explorer, SRTM dataset https://lta.cr.usgs.gov/SRTM1Arc
Slope	>10%	>3%		Slope estimated from elevation data using "slope" feature on ArcMap
Area excluded at farm site	>15%	>50%		Available area at the farm site is calculated with Python.
Protected areas	X	X		U.S. Geological Survey, Gap Analysis Program (GAP). May 2016. Protected Areas Database of the United States (PAD-US), version 1.4 Combined Feature Class: https://gapanalysis.usgs.gov/padus/data/download/
Water bodies and rivers	X	X		USA Detailed Water Bodies from UTC Geodata Portal: http://geodata.utc.edu/datasets/48c77cbde9a0470fb371f8c8a8a7421a_0
Census urban zones	X	X	X	2017 Urban Areas from U.S. Tiger Dataset: https://www.census.gov/cgi-bin/geo/shapefiles/index.php
Surface mines	X	X	X	U.S. Geological Survey: Active mines and mineral plants in the U.S.:

				https://mrdata.usgs.gov/mineplant/
Airports, Roads, and Rails	X	X	X	PA Transportation files in the Staged Products Directory from the U.S. Geological Survey National Map: https://prd-tnm.s3.amazonaws.com/index.html?prefix=StagedProducts/Tran/Shape/
Existing solar plants	X		X	EIA-860, Schedule 3: https://www.eia.gov/electricity/data/eia860/
Existing wind plants		X	X	EIA-860, Schedule 3: https://www.eia.gov/electricity/data/eia860/

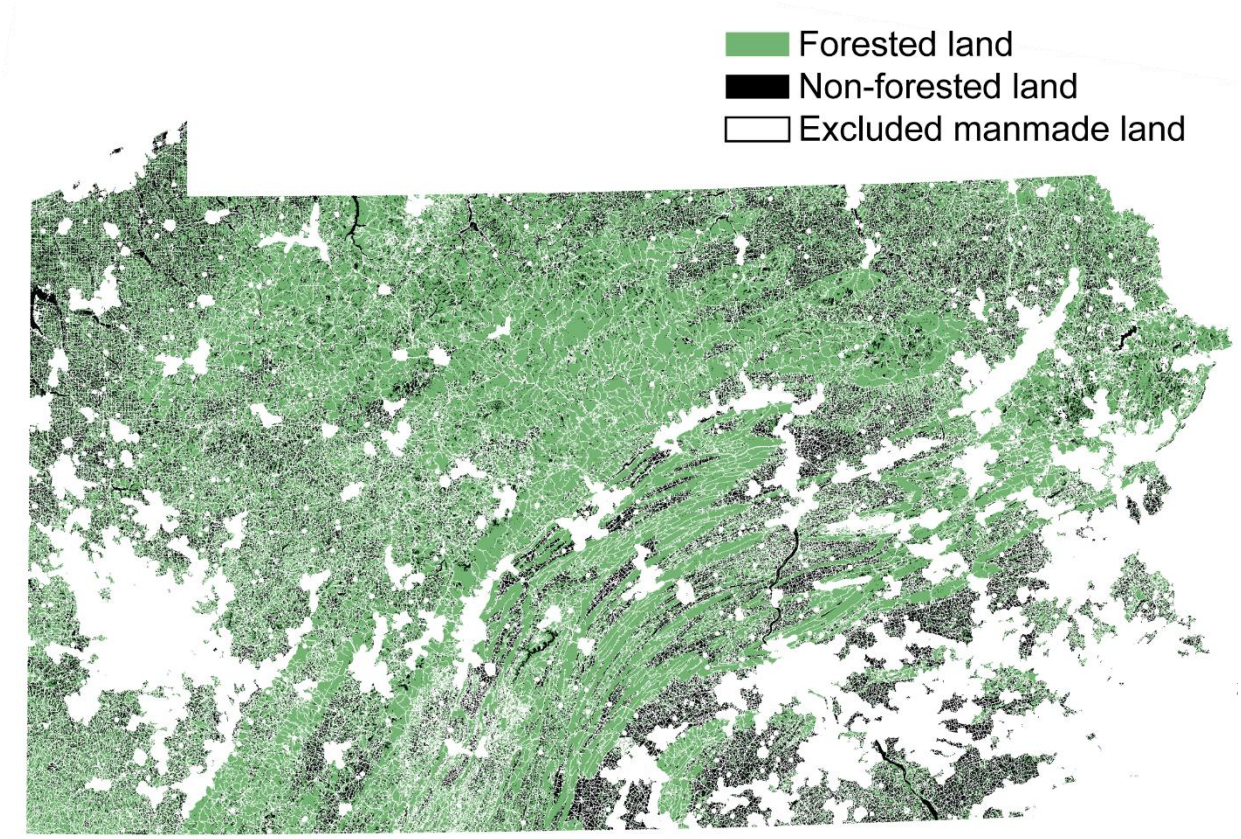

Figure C2: Map used for baseline analysis, with forested land, non-forested land, and excluded manmade land. Excluded manmade land is all land excluded due to the criteria listed in Table C1 that is considered manmade, suggesting that those lands do not contribute meaningfully to habitats and ecology in Pennsylvania.

Appendix C.3: Distribution of solar and wind farm capacities in the U.S.

In Figure C3, we show the capacities of wind farms in the U.S. using data from EIA-860, Schedule 2.[87] We find that the mean and median wind farm capacities are 84 MW and 59 MW, respectively. The maximum wind farm capacity is 735 MW. In our model assumptions, wind farms can have a capacity up to 128 MW. We find 282 wind farms out of 1050 wind farms have a capacity greater than 128 MW.

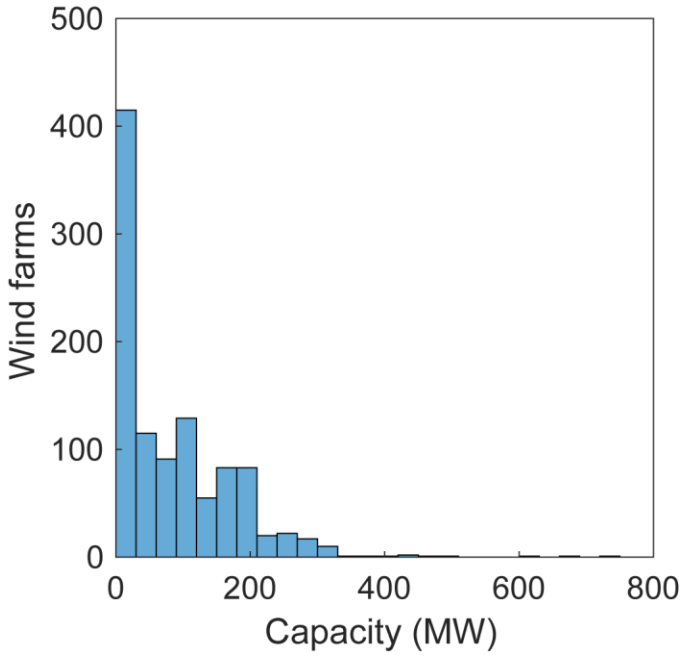

Figure C3: Histograms of capacity in MW of wind farms in the U.S. Data is from EIA-860, Schedule 2.[87]

Appendix C.4: Wind generation

We estimate the capacity of wind farms from wind speeds using Equation S1, which are methods similar to the ones provided in Wu et al.[37]

$$P_{avg} = R * \frac{1}{2} \rho A_{blade} v_{avg}^3 \qquad \text{(S1)}$$

Where P_{avg} is the average power output of a turbine in Watts; ρ is the air density, which is 1.225 kg/m^3 at 15 degrees Celsius and 1 atm; R is the Rayleigh's correction factor for average wind speeds, A_{blade} is the swept area of the turbine blades in m^2, which we estimate assuming 100 m turbine blades; $v_{avg}$is the average wind velocity in m/s, provided by National Renewable Energy Laboratory's mid-Atlantic wind resource maps, which gives wind speeds at 50 m.[130] We assume turbines of 100 m and extrapolate the wind speed using the 1/7 rule of thumb, which is the ratio of the unknown wind speed to the known wind speeds is equal to the ratio of the two heights raised to the 1/7th power.[37]

Based on this power output, we then constrain the capacity of the wind farm based on land impact factor and the area used to site farms. Since wind farms are constructed on 16 sq km land and the land impact factor we assume is 8 MW/sq km, the maximum wind farm capacity is 128 MW. Therefore, any land with wind speeds high enough that can site wind farms higher than 128 MW instead site wind farms with 128 MW.

To estimate generation, we assume each wind farm operates annually at an average capacity factor of 0.3, which we believe is a reasonable assumption based on the performance of existing wind farms.[156]

Appendix C.5: CCS and coal and natural gas plants

In Table C2, we list every coal and natural gas plant in Pennsylvania and whether the plant is cited above a saline formation. Natural gas plants that are above a saline formation generated 18.9 TWh in 2016, which is 28% of natural gas generation. Coal plants cited above a saline formation generated 44 TWh in 2016, which is 93% of coal generation. All coal plants except for plant 3140 is cited above a saline formation.

Table C2: Coal and natural gas plants in Pennsylvania by plant code, fuel type, net generation, latitude, longitude, and whether they are cited above a saline reservoir. Saline reservoir data is provided by NETL Carbon Storage Atlas.[127] All other data is provided by EIA.[87]

Plant Code (ORISPL)	Fuel Type	Net Generation (TWh)	Latitude	Longitude	Above saline reservoir
3096	natural gas	0.1	40.465	-80.044	yes
3110	natural gas	0	39.866	-77.165	no
3118	coal	9.2	40.384	-79.061	yes
3120	natural gas	0	41.706	-77.082	yes
3122	coal	6.6	40.513	-79.196	yes
3131	natural gas	0.2	41.068	-78.366	yes
3136	coal	10.2	40.660	-79.341	yes
3138	natural gas	0.8	40.938	-80.369	yes
3140	coal	3.3	40.096	-76.696	yes
3148	natural gas	4.4	40.798	-75.105	yes
3149	coal	4.4	41.071	-76.667	no
3161	natural gas	0.1	39.858	-75.323	no
3176	natural gas	0.7	41.201	-76.070	yes
6094	coal	11.6	40.635	-80.416	yes
7397	natural gas	0	39.939	-77.658	no
8226	coal	2	40.538	-79.791	yes
10129	natural gas	0	40.614	-79.159	yes
10870	natural gas	0	40.928	-76.041	no
50074	natural gas	0	39.810	-75.428	no
50284	coal	0	40.680	-78.233	yes
50373	natural gas	0	40.265	-76.877	no
50463	natural gas	0.9	41.574	-76.043	yes
52149	natural gas	0.3	40.220	-75.302	no
54250	natural gas	0	40.014	-75.053	no
54333	natural gas	0	40.955	-76.879	yes
54693	natural gas	0	39.986	-76.676	no
54785	natural gas	1	39.942	-75.188	no
55193	natural gas	4.2	40.422	-75.936	no

55196	natural gas	0.1	40.547	-79.768	no
55231	natural gas	4.1	39.861	-75.336	no
55233	natural gas	0.2	41.291	-79.806	yes
55298	natural gas	8.6	40.148	-74.741	no
55337	natural gas	5.4	40.351	-76.366	no
55347	natural gas	1.2	40.638	-79.352	yes
55377	natural gas	0	39.748	-79.839	yes
55516	natural gas	4.6	39.859	-79.918	yes
55524	natural gas	1.6	39.738	-76.307	no
55654	natural gas	0.2	39.867	-77.686	no
55667	natural gas	3.9	40.802	-75.108	no
55690	natural gas	5.3	40.618	-75.315	no
55710	natural gas	4.4	40.545	-79.769	yes
55801	natural gas	5	39.807	-75.422	no
55976	natural gas	4.6	39.873	-77.167	no
55997	natural gas	0	39.911	-77.667	no
56397	natural gas	0	41.203	-76.068	yes
56513	natural gas	0	40.098	-75.243	no
58195	natural gas	0.1	40.809	-77.848	yes
58420	natural gas	2.6	41.768	-76.390	yes
58426	natural gas	2.9	41.181	-76.839	yes
58715	natural gas	0.1	41.658	-76.049	yes
58811	natural gas	0.1	41.611	-76.843	yes
58897	natural gas	0	39.980	-75.151	no
59056	natural gas	0	40.184	-75.234	no